

## **Appendix G**

### **Sediment Transport Modeling Study**

**Note: The Section 508 amendment of the Rehabilitation Act of 1973 requires that the information in Federal documents be accessible to individuals with disabilities. The USACE has made every effort to ensure that the information in this appendix is accessible.**

**However, this appendix is not fully compliant with Section 508, and readers with disabilities are encouraged to contact Mr. Jayson Hudson at the USACE at (409) 766-3108 or at [SWG201900067@usace.army.mil](mailto:SWG201900067@usace.army.mil) if they would like access to the information.**



# Environmental Impact Assessment for Channel Deepening, Port of Corpus Christi

Sediment Transport Modelling Study

April 1, 2022 | 13242.102

# Baird.

Innovation Engineered.

[baird.com](http://baird.com)

# Environmental Impact Assessment for Channel Deepening, Port of Corpus Christi

## Sediment Transport Modelling Study

Prepared for:

Prepared by:



Freese & Nichols, Inc.  
10431 Morado Circle  
Suite 300  
Austin, Texas 78759



W.F. Baird & Associates Coastal Engineers Ltd

For further information, please contact  
Larry Wise  
lwise@baird.com  
www.baird.com

13242.102

Z:\Shared With Me\QMS\2022\Reports\_2022\13242.102.R5.RevA\_PCCA\_EIS\_Sediment\_Modelling.docx

Revision	Date	Status	Comments	Prepared	Reviewed	Approved
RevA	2022-04-01	Draft	For Client Review	YT/RQ	MD/LAW	LAW

© 2022 W.F. Baird & Associates Coastal Engineers Ltd (Baird) All Rights Reserved. Copyright in the whole and every part of this document, including any data sets or outputs that accompany this report, belongs to Baird and may not be used, sold, transferred, copied or reproduced in whole or in part in any manner or form or in or on any media to any person without the prior written consent of Baird.

This document was prepared by W.F. Baird & Associates Coastal Engineers Ltd for Freese & Nichols, Inc.. The outputs from this document are designated only for application to the intended purpose, as specified in the document, and should not be used for any other site or project. The material in it reflects the judgment of Baird in light of the information available to them at the time of preparation. Any use that a Third Party makes of this document, or any reliance on decisions to be made based on it, are the responsibility of such Third Parties. Baird accepts no responsibility for damages, if any, suffered by any Third Party as a result of decisions made or actions based on this document.



## Executive Summary

---

W.F. Baird & Associates Ltd. (Baird) was retained by Freese & Nichols, Inc. (FNI) to provide modeling studies in support of the third-party environmental impact study (EIS) for the Corpus Christi Ship Channel Deepening Project (CDP). The project is the proposed deepening of the offshore channel, entrance channel, and seaward most portion of the Corpus Christi Ship Channel to a nominal depth of 75 ft. Baird has provided consulting services for the past 11 months on the project to FNI as part of the 3<sup>rd</sup> Party EIS contract with the Port of Corpus Christi Authority (PCCA). The work has been coordinated with the US Army Corps of Engineers (USACE) Galveston District Regulatory Branch. The main purpose of this sediment transport modeling study is to provide a direct response to the data gaps identified in the PCCA CDP Recommended Actions Plan developed by FNI on 30 September 2020 (Freese and Nichols, Inc., 2020).

Corpus Christi Bay connects to several subtropical bays, such as Nueces Bay to northwest, Aransas Bay and Copano Bay on the northeast side, and Baffin Bay on the southwest side. It is separated from the GOM by the longshore barrier islands, such as Mustang Island, Padre Island, and San Jose Island. These bays are connected to the GOM by a narrow entrance channel, Aransas Pass, where the navigation channel will be deepened in the CDP. There is a secondary pass, Packery Channel.

MIKE21 and MIKE3 models were used to develop a model to predict the sedimentation in the channel. The model was calibrated and validated against the shoaling rates obtained from the Corps Shoaling Analysis Tool (CSAT) for the periods of 2011-2015 and 2016-2020, respectively. The impact of sedimentation in the channel was evaluated using three scenarios: existing, Future Without Project (FWOP) and Future With Project (FWP). Additional features such as the offshore berms, beach nourishment and Berms and Offshore Dredged Material Disposal Area (ODMS) were also evaluated.

Predicted FWOP and FWP shoaling rates were comparable to the existing condition. Overall, both 2D and 3D model results indicate that the project impact on sedimentation rates in the inner channels is limited to less than 10%. The model predicted that sedimentation in the outer channel increases from approximately 95,000 yd<sup>3</sup>/year (73,000 m<sup>3</sup>/year) for the FWOP to approximately 214,000 yd<sup>3</sup>/year (164,000 m<sup>3</sup>/year) for the FWP scenario, approximately 2.25 times higher. This is primarily due to that fact that the FWP has a deeper and longer channel compared to FWOP. The beach nourishment and offshore berms make small contributions to channel sedimentation with less than 600 yd<sup>3</sup> (459 m<sup>3</sup>) of total sedimentation predicted by the model. On the other hand, the model predicted that sedimentation in the outer channel under FWP conditions increases from approximately 214,000 yd<sup>3</sup>/year (164,000 m<sup>3</sup>/year) in the absence of the ODMS mound to approximately 342,000 yd<sup>3</sup>/year (262,000 m<sup>3</sup>) (approximately 1.6 times greater) when the ODMS mound is present. Individual hurricane events could result in sedimentation volumes in the outer channel that are several times higher than the average annual sedimentation. In contrast, the impact of hurricanes on the inner channel sedimentation is small.

The stability of the designed offshore berm and beach nourishment was assessed using two 1D cross-shore transport numerical models: XBeach by Deltares and CSHORE by the USACE. Assessment of the cross-shore profile response to long-term wave conditions and short-term storm conditions found it is unlikely that significant sediment movement will occur at the designed placement depth of -25 to -30 ft NAVD88 as it is placed beyond the depth of closure. As for the beach nourishment, XBeach predicted significant overtopping of the dune during stronger storms (e.g., Hurricane Allen and Hurricane Harvey). XBeach storm response predictions were validated using pre- and post-Hurricane Harvey imagery and surveys. Model results indicated that the offshore berm does not provide meaningful protection for beach nourishment, except during smaller storms with longer wave periods.

A sediment budget model to assess the fate of the placed beach nourishment was developed by Baird. Cross-shore and longshore transport processes were incorporated in the model using XBeach (cross-shore) and Baird's COSMOS model (longshore). In the Mustang Island domain, the average nourishment loss rate is approximately 29k to 112k yd<sup>3</sup> (22k to 86k m<sup>3</sup>) per year (1 to 5% of the total volume per year); the lost sediment is generally transported to the northeast towards the jetties. In the San Jose Island domain, the average nourishment erosion rate is approximately 0 to 80k yd<sup>3</sup> (0 to 62k m<sup>3</sup>) per year (0 to 2% of the total volume per year); the lost sediment is generally redistributed over the model domain.

# Table of Contents

---

<b>1. Introduction .....</b>	<b>8</b>
<b>2. Data Collection and Analysis .....</b>	<b>9</b>
2.1 Relevant Data Collection	9
2.1.1 Geospatial Data	9
2.1.1.1 Elevation Data	9
2.1.1.2 Navigation Channel Data	11
2.1.2 Forcing Data	11
2.1.2.1 Water Levels	11
2.1.2.2 River Flows	13
2.1.2.3 HYCOM Model	14
2.1.2.4 Offshore Wave Data	14
2.1.2.5 Wind Data	16
2.1.3 Sediment Data	17
2.1.3.1 Sediment Fraction Distribution	17
2.1.3.2 River Sediment Rating Curves	22
2.1.3.3 CSAT Dredging Data	23
<b>3. Sedimentation Model Description .....</b>	<b>27</b>
3.1 Model Development	27
3.1.1 Model Setup	29
3.1.2 Spectral wave model	29
<b>4. Model Calibration and Validation.....</b>	<b>30</b>
4.1 Scaling Factor due to Wind	30
4.2 Erosion in the Inner Harbor	31
4.3 Two-dimensional model	33

4.4	Comparison of Two-dimensional and Three-dimensional models	35
<b>5.</b>	<b>Modeling Assessment of Potential Project Impacts .....</b>	<b>36</b>
5.1	Model Scenarios	36
5.2	Impact Assessment	37
5.2.1	Shoaling Rates in the Inner Channel	37
5.2.2	Sedimentation Volumes in the Outer Channel	39
<b>6.</b>	<b>Modeling Assessment of Beach Nourishment, Offshore Berms and Offshore Dredged Material Disposal Area (ODMDS) .....</b>	<b>41</b>
6.1	Model Scenarios	41
6.2	Impact Assessment	43
6.2.1	Contribution of Beach Nourishment and Offshore berms to Channel Sedimentation	43
6.2.2	Contribution of the ODMDS Sediment to Channel Sedimentation	44
6.2.3	Impact of the ODMDS Mound on Channel Sedimentation	45
6.2.4	Impact of Hurricanes on Sedimentation in the Outer Channel	48
<b>7.</b>	<b>Stability of Offshore Berms and Beach Nourishment.....</b>	<b>51</b>
7.1	Numerical Models	51
7.2	Beach Profile	51
7.3	Modeling Assessment	53
7.3.1	Profile Response to Long Term Wave Conditions	53
7.3.2	Short-term Profile Response to Individual Storm Conditions	55
<b>8.</b>	<b>Fate of Beach Nourishment.....</b>	<b>62</b>
8.1	Development and Setup of the Sediment Budget Model	62
8.1.1	Representative Profiles and Model Domain	62
8.1.2	Model Equations	64
8.1.3	Cross Shore Transport	66
8.1.3.1	Beach Erosion (Offshore Transport)	66

8.1.3.2 Beach Recovery (Onshore Transport)	69
8.1.4 Longshore Transport	70
8.1.5 Scaling Factors	72
8.2 Model Calibration	73
8.3 Beach Nourishment Assessment Runs	75
<b>9. Conclusions</b> .....	<b>82</b>
<b>10. References</b> .....	<b>84</b>

## Tables

---

Table 2.1: Summary of hourly data available from NOAA stations .....	11
Table 2.2: Summary of river flow gages from USGS .....	13
Table 2.3: Summary of suspended sediment data available from USGS .....	22
Table 2.4: Average annual shoaling rates from CSAT .....	26
Table 4.1: Erosion area in the inner harbor .....	32
Table 5.1: Predicted sedimentation volumes .....	40
Table 6.1: Sedimentation in the channel due to beach nourishment and offshore berms .....	43
Table 6.2: Sedimentation in the channel with and without ODMDS .....	44
Table 6.3: Sedimentation in the channel due to the presence of the ODMDS.....	45
Table 6.4: Sedimentation in the outer channel due to hurricane .....	49
Table 6.5: Sedimentation in the inner channel due to hurricane .....	49
Table 7.1: Storm conditions for offshore berm and beach nourishment stability assessment .....	55
Table 8.1: Sediment budget model parameters.....	75

# Figures

---

Figure 2.1: Bathymetry data collected for this modeling study .....	10
Figure 2.2: Water level stations on Corpus Christi Bay .....	12
Figure 2.3: Location of USGS gages .....	13
Figure 2.4: HYCOM model nodes and boundary of the computational mesh.....	14
Figure 2.5: Location of WIS data point .....	15
Figure 2.6: Wave Height Rose at WIS Station 73040 (1980 to 2019) .....	16
Figure 2.7: Wind Speed at Bob Hall Pier.....	17
Figure 2.8: Sediment fraction distribution along the channel.....	18
Figure 2.9: Sediment fraction distribution along the Corpus Christi channel .....	19
Figure 2.10: Sediment fraction distribution in the Corpus Christi Bay and adjacent water bodies (TGLO)..	20
Figure 2.11: Silt content in the Corpus Christi Bay .....	21
Figure 2.12: Sediment rating curve at 8211500 (Nueces River at Calallen) .....	22
Figure 2.13: Sediment rating curve at 8189700 (Aransas River near Skidmore) .....	23
Figure 2.14: Sediment rating curve at 8189500 (Mission River at Refugio).....	23
Figure 2.15: National channel network reach numbers for Corpus Christi channel.....	25
Figure 3.1: Computational mesh for the MIKE sedimentation model.....	28
Figure 3.2: Computational mesh for the MIKE sedimentation model showing the grid cells in the channel	28
Figure 4.1: Wind rose and schematics of channel sedimentation processes inside Corpus Christi Bay .....	31
Figure 4.2: Variation of wind energy between April and July from 2006 to 2020 .....	31
Figure 4.3: Erosion in the Inner Harbor (Reach 12) between 1995 and 2004.....	32
Figure 4.4: Erosion in the Inner Harbor (Reach 12) between 2004 and 2020.....	33
Figure 4.5: Comparison of CSAT shoaling rates (2011-2015) and model predictions (2011) .....	34
Figure 4.6: Comparison of CSAT shoaling rates (2016-2020) and model predictions (2020) .....	34

Figure 4.7: Comparison of CSAT shoaling rates (average) and model results (average)..... 35

Figure 4.8: Comparison of CSAT shoaling rates and model results (2D and 3D) ..... 35

Figure 5.1: Model bathymetry around the jetties for (a) FWOP, and (b) FWP scenarios ..... 36

Figure 5.2: Model Bathymetry for FWP scenario showing the terminals ..... 37

Figure 5.3: Comparison of CSAT shoaling rate (2011-2015) and the 2D model results for existing conditions, FWOP and FWP scenarios ..... 38

Figure 5.4: Average annual shoaling rates predicted by the 2D model in the channel including the terminals for FWOP and FWP scenarios ..... 38

Figure 5.5: Comparison of CSAT shoaling rate (2011-2015) and the 3D model results for existing conditions, FWOP and FWP scenarios ..... 39

Figure 5.6: Average annual shoaling rates predicted by the 3D model in the channel including the terminals for FWOP and FWP scenarios ..... 39

Figure 5.7: Segments for sediment volume calculation ..... 40

Figure 6.1: Location of the beach nourishment, offshore berms and the extend of data received from Freese and Nichol’s for the ODMDS. .... 42

Figure 6.2: Distribution of settled sediment thickness from the beach nourishment and offshore berms over the fixed bed at the beginning of the model run ..... 43

Figure 6.3: Distribution of settled sediment thickness from the beach nourishment and offshore berms over the fixed bed at the end of the model run ..... 44

Figure 6.4: Locations used to investigate the change in hydrodynamics due to the ODMDS ..... 46

Figure 6.5: Current rose plots at point 1 for scenario (a) without ODMDS and (b) with ODMDS ..... 46

Figure 6.6: Current rose plots at point 2 for scenario (a) without ODMDS and (b) with ODMDS ..... 47

Figure 6.7: Current rose plots at point 3 for scenario (a) without ODMDS and (b) with ODMDS ..... 47

Figure 6.8: Velocity field during typical ebb tide for scenario (a) without the ODMDS and (b) with the ODMDS mound ..... 48

Figure 6.9: Segments for sediment volume calculation in the Corpus Christi Bay..... 50

Figure 7.1: Location of design profile ..... 52

Figure 7.2: Design profile used for the modeling assessment typical on San Jose Island and Mustang Island ..... 52

Figure 7.3: Annual wave energy density from WIS Station 73040 from 1980-2019 ..... 53

Figure 7.4: Modeled profile response to 2016 wave conditions from WIS Station 73040 ..... 54

Figure 7.5: Modeled profile response to 2017 wave conditions from WIS Station 73040 ..... 55

Figure 7.6: Modeled profile response to Hurricane Allen ..... 56

Figure 7.7: Modeled profile response to Hurricane Harvey ..... 57

Figure 7.8: Transect location (pink) across the dune crest (satellite image dated July 6, 2020) ..... 58

Figure 7.9: Satellite image from August 28, 2017 (post-Hurricane Harvey) from Google Earth ..... 59

Figure 7.10: Pre- (2016) and post-Hurricane Harvey (2018) dune crest elevations ..... 59

Figure 7.11: Modeled profile response to Hurricane Hanna ..... 60

Figure 7.12: Modeled profile response to Hurricane Delta ..... 61

Figure 8.1: Cross-shore sections of the representative beach profile; profile with beach nourishment and offshore berm shown ..... 63

Figure 8.2: Sediment budget model domains ..... 64

Figure 8.3: Matrix of XBeach wave conditions (red points) and all wave conditions measured at WIS Station 73040 from 1980 to 2019 (blue points)..... 67

Figure 8.4: Example of XBeach results for one wave condition {3.2 ft NAVD88 (1 m NAVD88) water level, 26.2 ft (8 m) wave height, 10 s wave period, 90-degree wave direction} and summarized cross-shore volume change rates (in yd<sup>3</sup>/ft/hr)..... 68

Figure 8.5: Summary of cross-shore volume change over Cell 5 (nourished beach with offshore berm) under all wave conditions with a water level of 3.2 ft NAVD88 (1 m NAVD88) ..... 69

Figure 8.6: Schematic of onshore sediment movement process applied in the sediment budget model .... 70

Figure 8.7: Potential annual longshore transport rates from 1980 to 2019 for a nourished profile with offshore berm ..... 71

Figure 8.8: Summary of potential longshore transport rates at Cell 5 (nourished beach with offshore berm) under all wave conditions with a water level of 3.2 ft NAVD88 (1 m NAVD88)..... 72

Figure 8.9: Longshore scaling factors for incoming wave from the south (164 degrees from north)..... 73

Figure 8.10: Sediment budget model results for the 1992-2002 calibration period (FWOP, average thicknesses shown are for presentation purposes only and should not be taken literally) ..... 75

Figure 8.11: Beach nourishment (orange) and offshore berm (green) placement cells within the Mustang Island and San Jose Island domains ..... 76

Figure 8.12: Sediment budget model results for 2011 (FWP, thicknesses shown are for presentation purposes only and should not be taken literally)..... 77

Figure 8.13: Sediment budget model results for the 1992-2002 model period (FWP, thicknesses shown are for presentation purposes only and should not be taken literally)..... 78

Figure 8.14: Sediment budget model results for the 2000-2019 model period (FWP, thicknesses shown are for presentation purposes only and should not be taken literally)..... 79

Figure 8.15: Change in beach nourishment volume and potential channel infilling volumes for the Mustang Island (left) and San Jose Island (right) domains for the period from 1992-2002 ..... 80

Figure 8.16: Change in beach nourishment volume and potential channel infilling volumes for the Mustang Island (left) and San Jose Island (right) domains for the period from 2000-2019 ..... 81

# 1. Introduction

---

W.F. Baird & Associates Ltd. (Baird) was retained by Freese & Nichols, Inc. (FNI) to provide modeling studies in support of the third-party environmental impact study (EIS) for the Corpus Christi Ship Channel Deepening Project (CDP). The project is the proposed deepening of the offshore channel, entrance channel, and seaward most portion of the Corpus Christi Ship Channel to a nominal depth of 75 ft. Baird has provided consulting services on the project to FNI as part of the 3<sup>rd</sup> Party EIS contract with the Port of Corpus Christi Authority (PCCA). The work has been coordinated with the US Army Corps of Engineers (USACE) Galveston District Regulatory Branch. The main purpose of this sediment transport modeling study is to provide a direct response to the data gaps identified in the PCCA CDP Recommended Actions Plan developed by FNI on 30 September 2020 (Freese and Nichols, Inc., 2020).

The objectives for this modeling study are:

- To address Data Gap Analysis Section 2.20.5 with Recommended Action “Option 2 for 408/TPC to perform sediment transport modeling to assess channel shoaling rates. For both options sedimentation analysis to cover full extents of project including areas within Corpus Christi Bay and the Jetty Channel. For both options consider CSAT data to provide historic shoaling analysis validation.”
- To address Data Gap Analysis Section 2.20.7 with Recommended Action “USACE408/TPC Team to support EPA in performing FATE (DELFT 3D) modeling for the proposed expanded ODMDS.”
- To better understand sedimentation processes in turning basin and Inshore Channel using a physics-based modeling approach
- To better understand sedimentation processes in channel outside of jetties using a physics-based modeling approach
- To assess potential impacts of channel deepening on sedimentation rates using a physics-based modeling approach

This report documents the data collected and used for the study, the model development, and the assessment on the impacts of CDP on sediment transport. The report consists of:

- Section 1. Introduction (this section)
- Section 2. Data collection and analysis – to document all data used in this study, including data sources, data gaps, data processing, and the understandings of physical processes from the data analysis
- Section 3. Sedimentation Model Description: - to describe the model development and set up
- Section 4. Model Calibration and Validation: - to describe the process of calibrating and validating the model against CSAT data
- Section 5. Modeling Assessment of Potential Project Impacts: - to present and compare model results and assess potential project impacts on channel sedimentation rates
- Section 6. Modeling Assessment of Beach Nourishment, Offshore Berms and Offshore Dredged Material Disposal Area (ODMDS): - to present simulation results with beach nourishment, offshore berms and ODMDS in place and assess their potential impacts on channel sedimentation
- Section 7. Stability of Offshore Berms and Beach Nourishment – to present simulation results of profile response to short-term storm events and long-term annual wave climate and assess the stability of the placed sediment using cross-shore profile change models
- Section 8. Fate of Beach Nourishment – to assess beach nourishment longevity using a sediment budget approach
- Section 9. Conclusion, Uncertainties, and Recommendation: - to document the conclusions made from this study

## 2. Data Collection and Analysis

---

### 2.1 Relevant Data Collection

#### 2.1.1 Geospatial Data

Several geospatial datasets were acquired in support of the numerical modelling of the Port of Corpus Christi. Elevation datasets were downloaded to cover the model domain as well as navigation channel boundaries in the study area.

##### 2.1.1.1 Elevation Data

Four elevation datasets were acquired for use in the model grid, listed in hierarchical order within the model domain below. Figure 1 shows the spatial coverage within the model domain of each elevation source.

- United States Army Corps of Engineers (USACE), Galveston District, Sea Bar Channel Survey, 2018/07/17
- Continuously Updated Digital Elevation Model (CUDEM) - 1/3 Arc-Second Resolution Bathymetric-Topographic Tiles (v2020)
- Corpus Christi, Texas 1/3 arc-second MHW Coastal Digital Elevation Model
- U.S. Coastal Relief Model Vol.5 - Western Gulf of Mexico

Elevation data in Nueces Bay was estimated based on discussions with a surveyor familiar with the bay and interpretation of aerial images from Google Earth.

All elevations were converted to the North American Vertical Datum of 1988 (NAVD 88) at Port Aransas. The horizontal coordinate system of Universal Transverse Mercator 14-North (UTM-14N) was used for all bathymetry data.

The model was validated against the Corps Shoaling Analysis Tool CSAT data for the period of 2016 to 2020 and therefore the use of the channel bathymetry in 2018 is appropriate for this study.

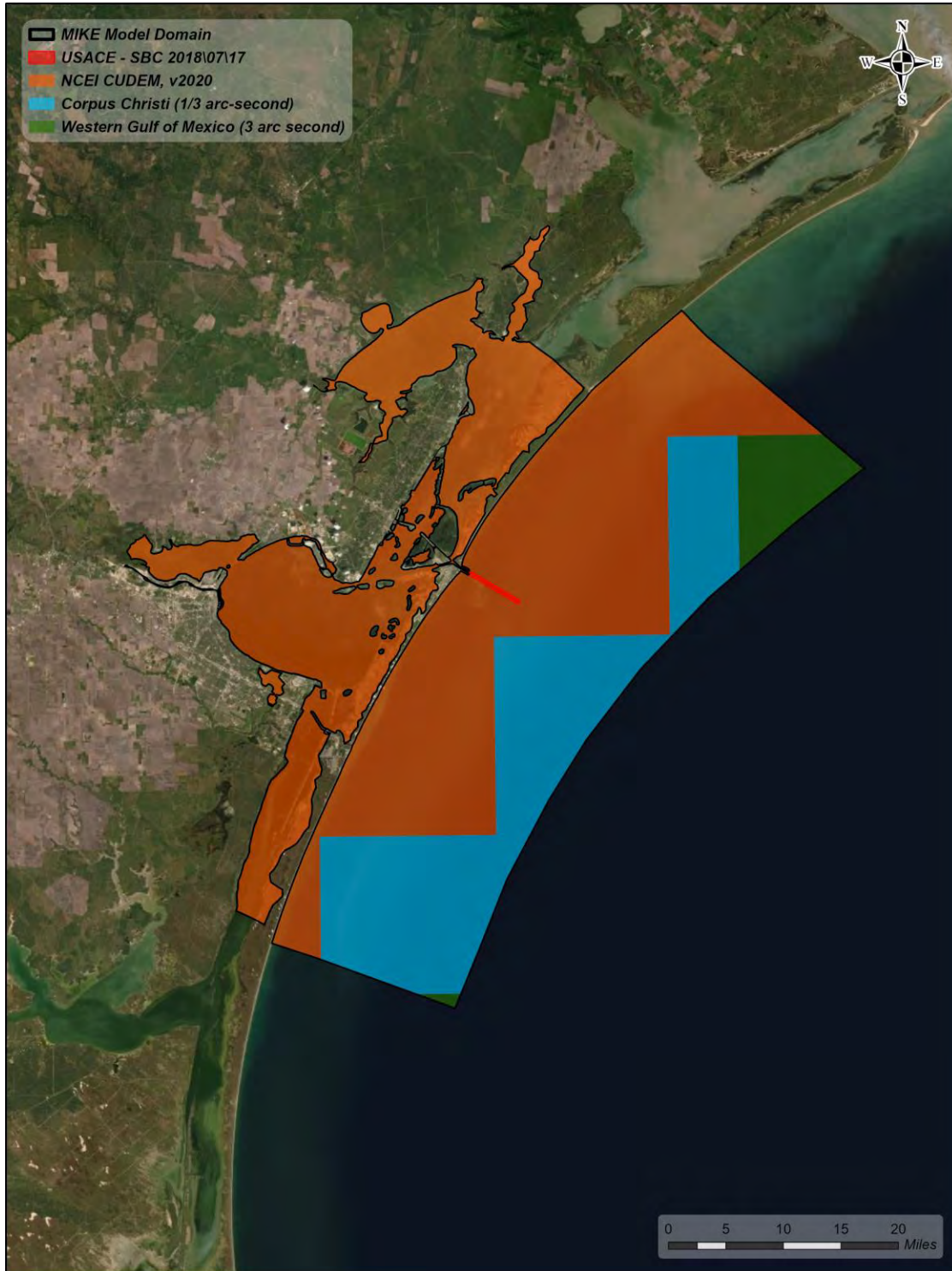


Figure 2.1: Bathymetry data collected for this modeling study

**2.1.1.2 Navigation Channel Data**

The extents of the navigation channels within the study area were downloaded from the USACE Geospatial National Channel Framework (NCF) portal (USACE, 2017). These data included channel areas, reaches and lines.

**2.1.2 Forcing Data**

**2.1.2.1 Water Levels**

Water levels from 10 stations was obtained in Corpus Christi’s Bay and in Aransas Bay from the National Oceanic and Atmospheric Administration’s Tides & Currents database (NOAA, <https://tidesandcurrents.noaa.gov/map/index.html> ). Data availability at the stations is summarized in Table 2.1, and the locations are illustrated in Figure 2.7. Data gaps exist for four stations during the period of interest: Aransas Wildlife Refuge, Rockport, USS Lexington, and South Bird Island. Of these stations, Rockport has the greatest number of data gaps, representing approximately 14% of the available data. The other three stations have data gaps representing less than 2% of the available data for the period of interest. Some stations provide 6-min data instead of hourly data for certain time period. In these cases, the data was interpolated to hourly data.

**Table 2.1: Summary of hourly data available from NOAA stations**

Name	Station ID	Start Date	End Date
Aransas Wildlife Refuge	8774230	2012-11-01	Present
Rockport	8774770	1937-03-01	Present
Aransas Pass	8775241	2016-12-20	Present
Port Aransas	8775237	2002-06-26	Present
Nueces Bay	8775244	2012-01-01	2012-12-31
USS Lexington	8775296	2012-01-01	Present
Packery Channel	8775792	1996-01-01	Present
Bob Hall Pier	8775870	1983-11-30	Present
South Bird Island	8776139	2012-10-01	Present
Baffin Bay	8776604	2012-10-01	Present



Figure 2.2: Water level stations on Corpus Christi Bay

### 2.1.2.2 River Flows

River flows draining into Corpus Christi Bay and Aransas Bay were retrieved from seven USGS gages (<https://maps.waterdata.usgs.gov/mapper/index.html>). Four of the gages drain into Corpus Christi Bay, three of which are located along the Nueces River, and one along Oso Creek. The remaining gage stations drain into Copano Bay. The data availability for each gage is summarized in Table 2.2. Figure 2.3 shows the location for each gage.

**Table 2.2: Summary of river flow gages from USGS**

Name	Gage ID	Start Date	End Date
Nueces Rv nr Mathis	08211000	1987-09-01	Present
Nueces Rv at Bluntzer	08211200	1992-04-01	Present
Nueces Rv at Calallen	08211500	1989-10-02	Present
Oso Ck at Corpus Christi	08211520	1995-10-01	Present
Aransas Rv nr Skidmore	08189700	1964-03-27	Present
Mission Rv at Refugio	08189500	1939-07-01	Present
Copano Ck nr Refugio	08189200	1970-06-17	Present

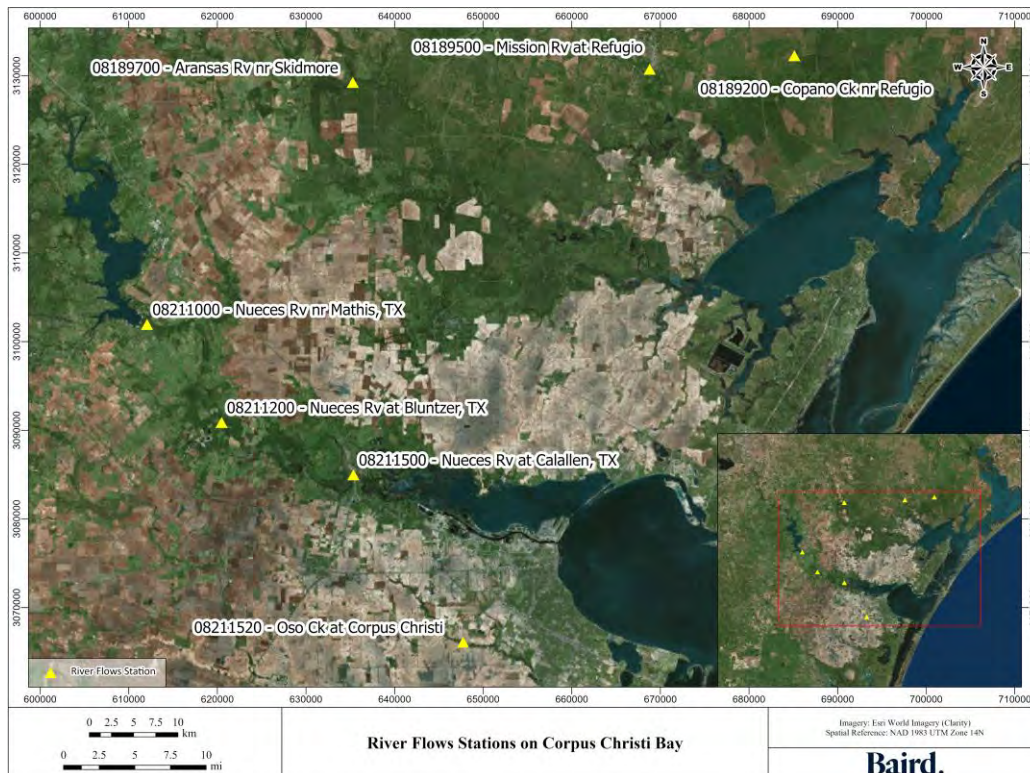


**Figure 2.3: Location of USGS gages**

More details about the river inflows to the Corpus Christi Bay can be found in the hydrodynamic and salinity study conducted by Baird (Baird, 2020).

### 2.1.2.3 HYCOM Model

The HYCOM (Hybrid Coordinate Ocean Model) ocean circulation model results were used to obtain surface elevation and fluxes at the model boundary (<https://www.hycom.org/>). Figure 2.4 shows in black dots the HYCOM model nodes, in yellow dots the offshore boundary of the mesh, in purple dots the northeast offshore boundary, in orange dots the southwest offshore boundary and in blue lines the mesh elements used. At the offshore boundary (yellow) the interpolated surface elevation was extracted from the HYCOM nodes, while velocities were extracted at the northeast and southwest offshore boundary.

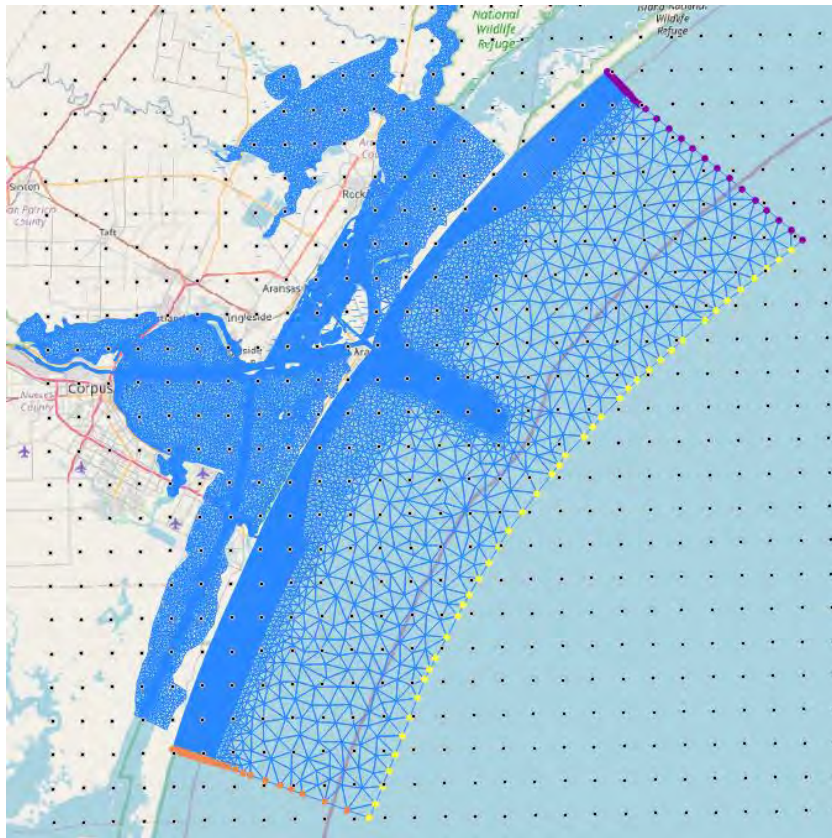


**Figure 2.4: HYCOM model nodes and boundary of the computational mesh.**

### 2.1.2.4 Offshore Wave Data

Offshore wave conditions in the Corpus Christi Bay and Gulf of Mexico were extracted from the U.S. Army Corps of Engineers (USACE) Wave Information Studies (WIS) hindcast station ST73040 for 2011 and 2019. The station is located approximately 25 km offshore of Port Aransas, where the water depth is approximately 30 m. The WIS hindcast data was not available for 2020 therefore wave data from NOAA buoy 42020 (see Figure 2.5) was used in this case. The wave rose in Figure 2.6 presents offshore wave heights by direction at the WIS station from 1980 to 2019; the waves at this location are predominately from the southeast direction.



Figure 2.5: Location of WIS data point

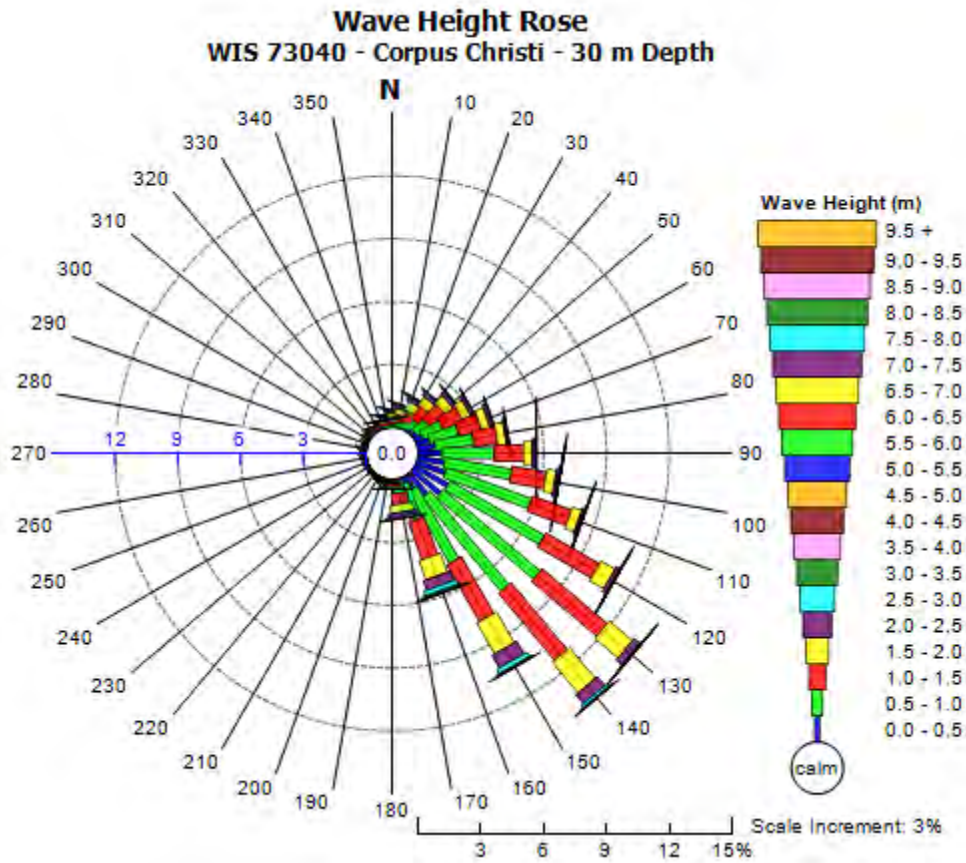


**Figure 2.6: Wave Height Rose at WIS Station 73040 (1980 to 2019)**

**2.1.2.5 Wind Data**

Wind data used in the sediment transport model was obtained from the Bob Hall Pier in-situ observation station operated by the National Oceanic and Atmospheric Administration (NOAA) with hourly data available online: <https://tidesandcurrents.noaa.gov>. Wind speed and direction was collected in hourly increments for 2011, 2017 and 2020. The wind sensor is 46.87 ft (14.29 m) above MSL. Observed wind speeds were converted to 33 ft (10 m) wind speeds using the log law shown below:

$$u_2 = u_1 * \left( \frac{\ln \frac{z_2}{z_0}}{\ln \frac{z_1}{z_0}} \right)$$

Where  $u_2$  is the wind speed at the desired elevation,  $u_1$  is the observed wind speed at the station elevation,  $z_2$  is the desired elevation (33 ft/10 m),  $z_1$  is the station instrument elevation and  $z_0$  is the roughness length coefficient. Figure 2.7 displays an example 33 ft (10 m) wind speed plot for Bob Hall Pier.

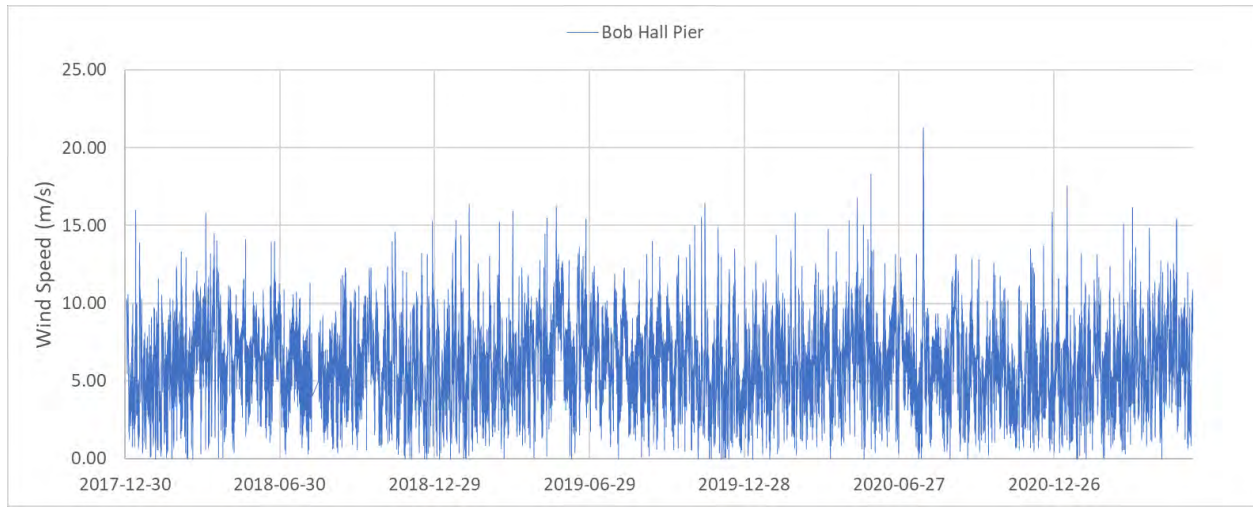


**Figure 2.7: Wind Speed at Bob Hall Pier**

Wind data from Bob Hall Pier was usable with small data gaps. However, larger data gaps of up to 1 month were present in 2011. Thus, for the year 2011, the wind data obtained from the WIS data station mentioned in section 2.1.2.4 was used.

## 2.1.3 Sediment Data

### 2.1.3.1 Sediment Fraction Distribution

Baird received from the USACE Galveston District historical sediment grain size and fraction distribution data along the Corpus Christi channel collected between 1977 and 2015. An example figure showing the spatial and temporal distribution of the sediment data is provided in Figure 2.8. The data is plotted with respect to the station numbers going from the Jetty Channel to the Viola Turning Basin, as shown in Figure 2.9, featuring a wide scatter. The trend lines in this figure indicate that, on average, the sediment composition is made up of higher sand content (~60%) in the Jetty Channel in the Gulf of Mexico. The fraction of sand decreases in the Corpus Christi Bay (~20%) and increases again slightly (~30%) toward the Viola Turning Basin in the inner harbor. Silt and clay content is higher in the Corpus Christi Bay (~80%). While silt was generally present everywhere along the channel, clay content was down to 10% in the jetty channel.



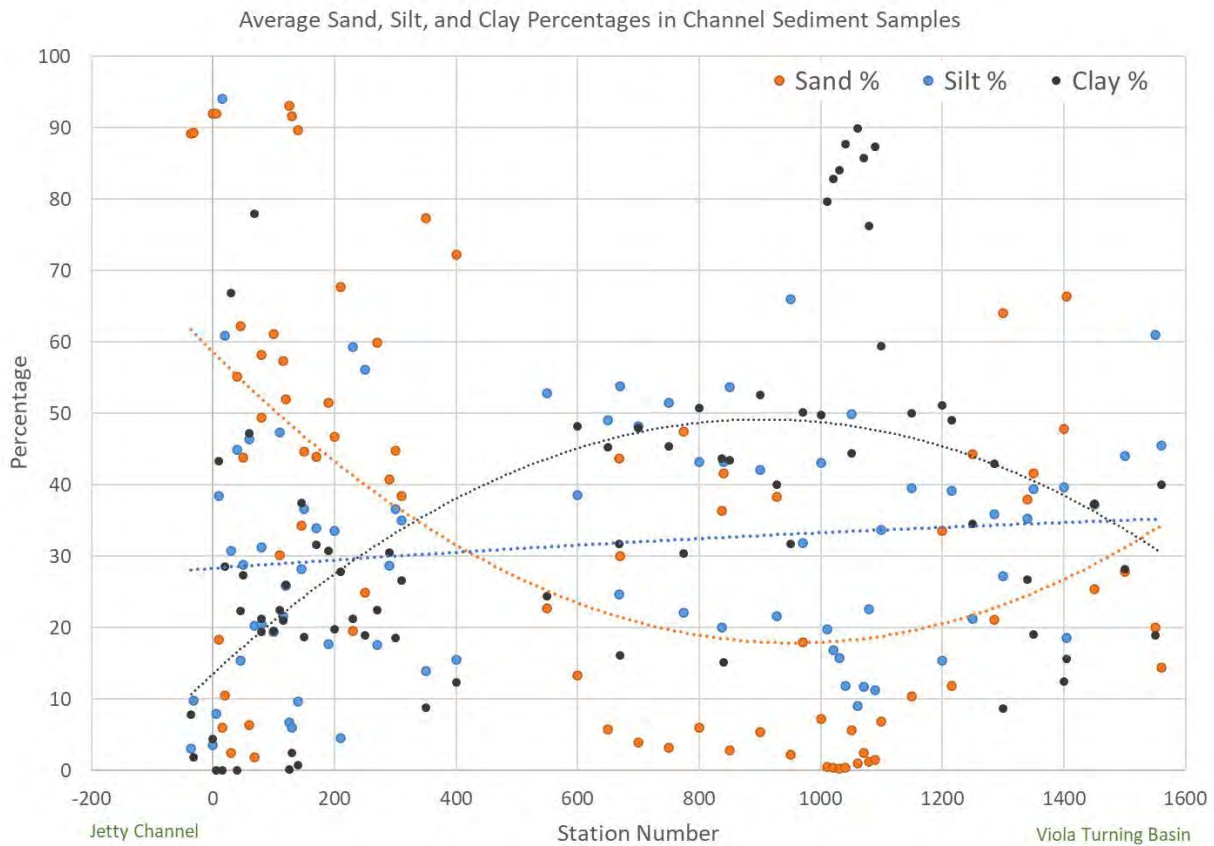


**Figure 2.9: Sediment fraction distribution along the Corpus Christi channel**

Sediment fraction data on the seabed outside of the Corpus Christi channel was acquired from the Texas Sediment Geodatabase by the Texas General Land Office (<https://cgis.glo.texas.gov/txsed/index.html>). The data comes from surface grab samples taken at different times ranging from 1976 to 2006. Figure 2.10 shows the sample locations and the sediment fraction distribution from each sample. Based on this data, interpolated maps of sediment type and grain size were developed for model input. The interpolation for silt is shown in Figure 2.11.

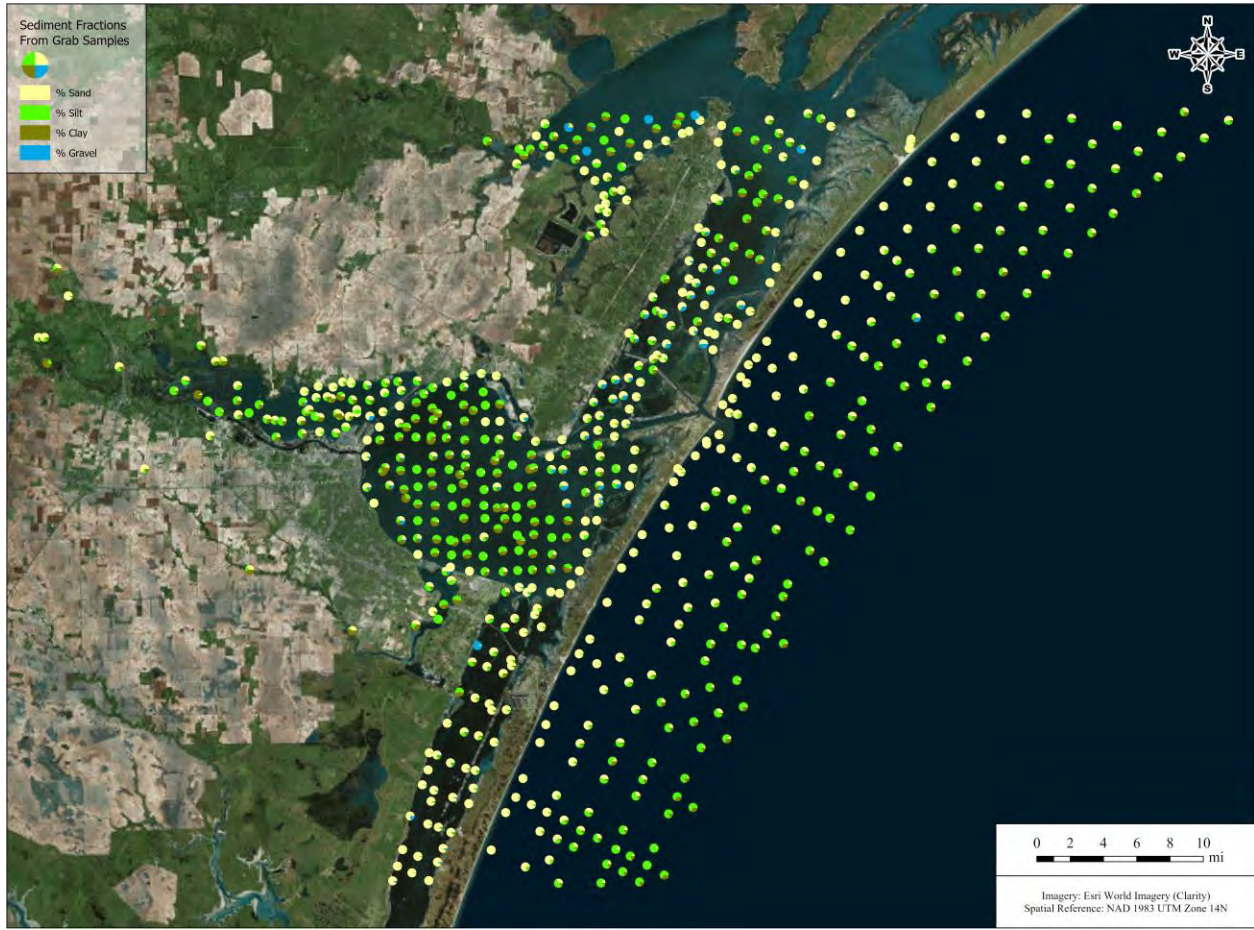


Figure 2.10: Sediment fraction distribution in the Corpus Christi Bay and adjacent water bodies (TGLO)

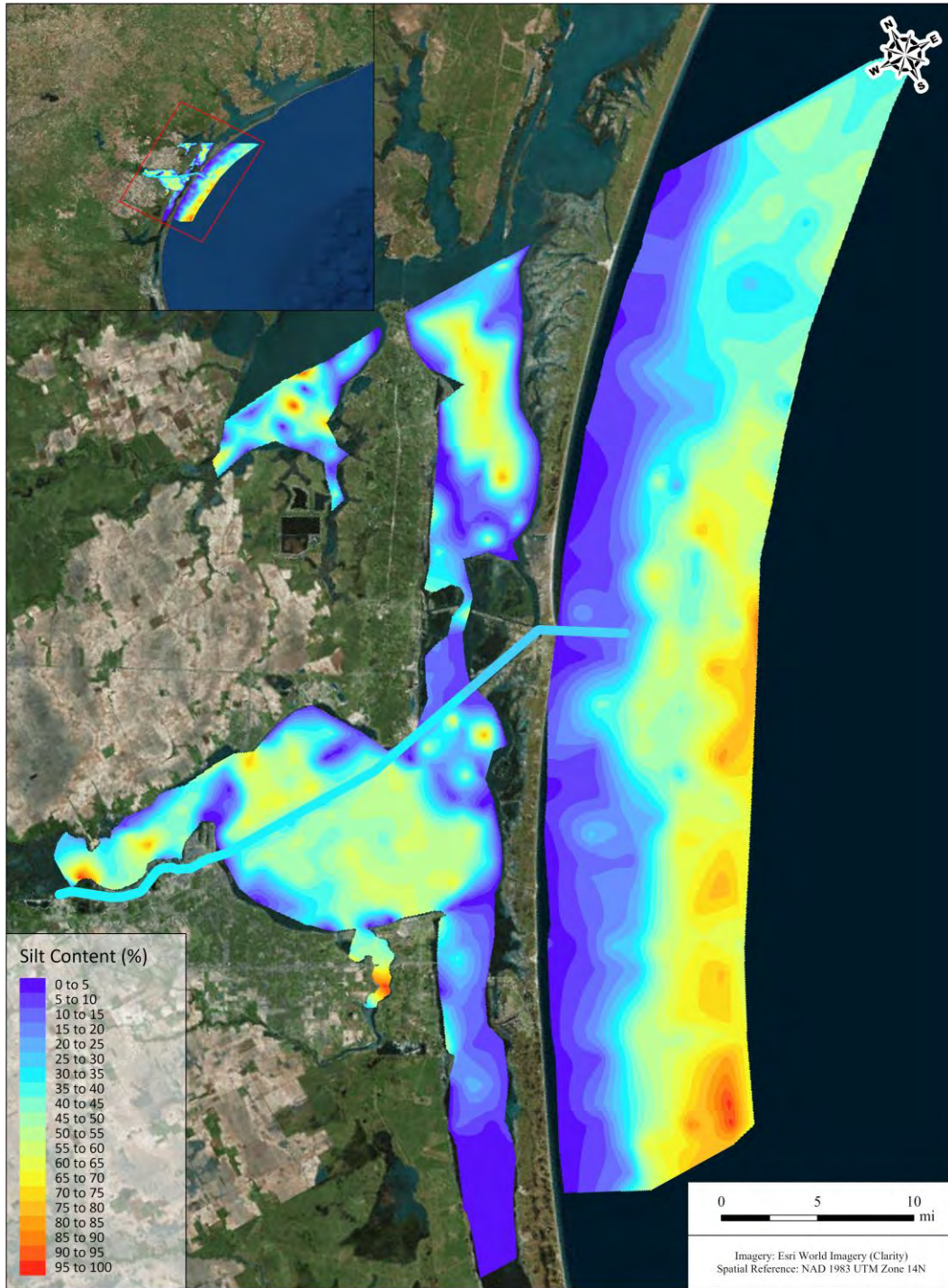


Figure 2.11: Silt content in the Corpus Christi Bay

### 2.1.3.2 River Sediment Rating Curves

To evaluate the sediment concentration coming in from the rivers, sediment rating curves were developed. Suspended sediment concentration data was available at three USGS stations. The summary of the available suspended sediment data is shown in Table 2.3.

**Table 2.3: Summary of suspended sediment data available from USGS**

Name	Station ID	Start Date	End Date	Number of Data Points
Nueces River at Calallen	08211500	2006-05-16	2018-04-11	12
Aransas River near Skidmore	08189700	1966-02-15	1975-05-23	36
Mission River at Refugio	08189500	1973-08-09	1993-08-17	89

The sediment concentration data and the corresponding flow rate was used to develop the sediment rating curves. The rating curves are plotted on the log scale and is shown in Figure 2.12, Figure 2.13, and Figure 2.14.

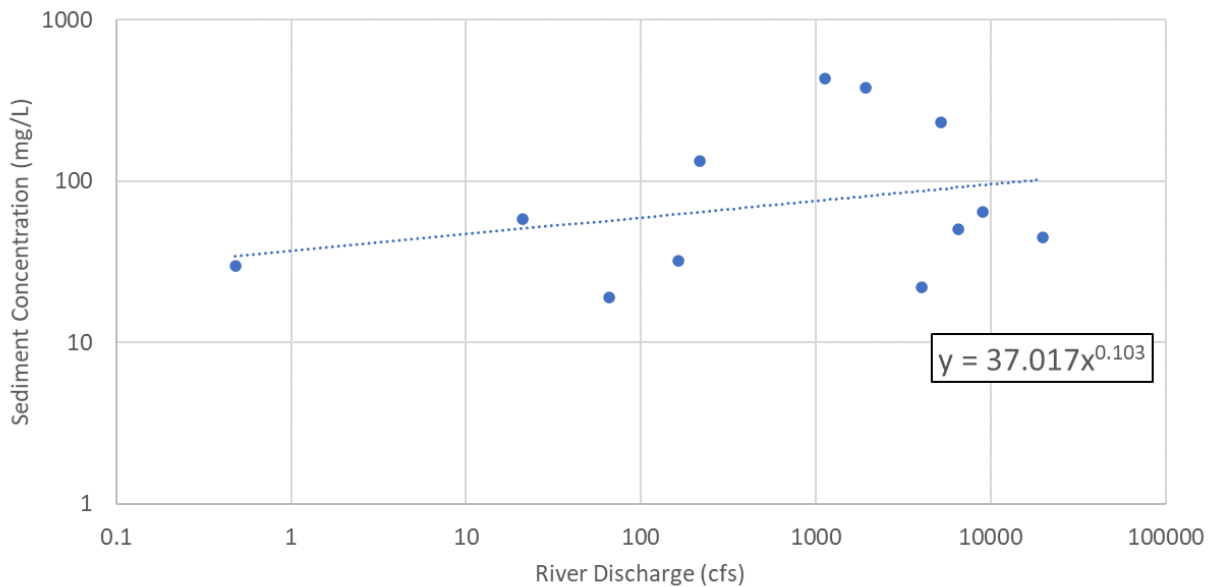


**Figure 2.12: Sediment rating curve at 8211500 (Nueces River at Calallen)**

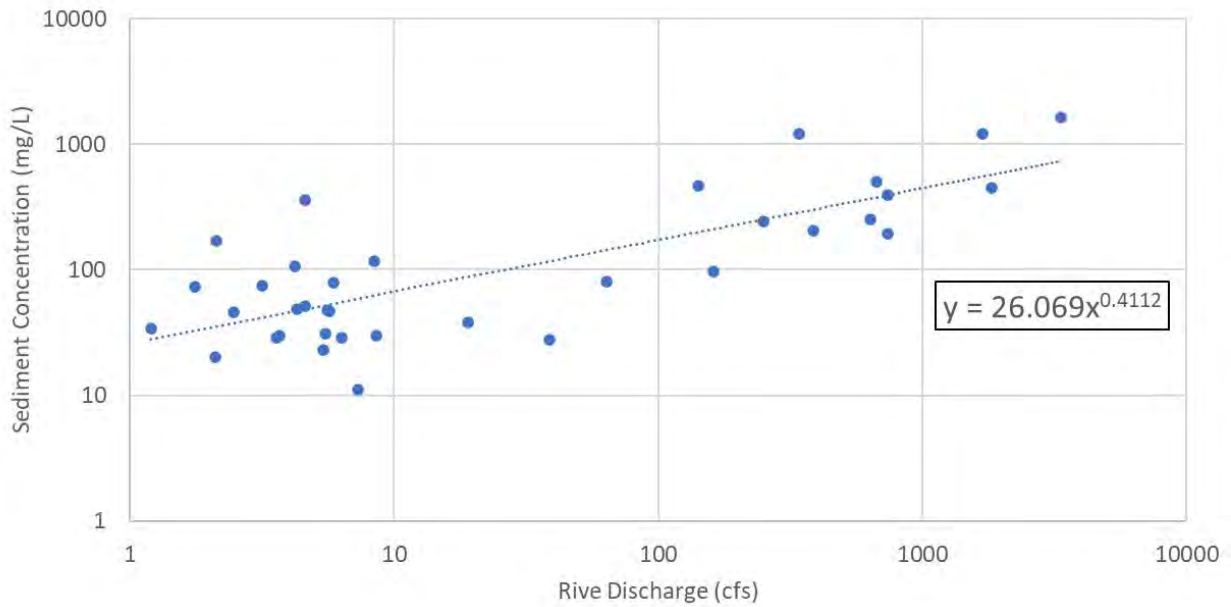


Figure 2.13: Sediment rating curve at 8189700 (Aransas River near Skidmore)

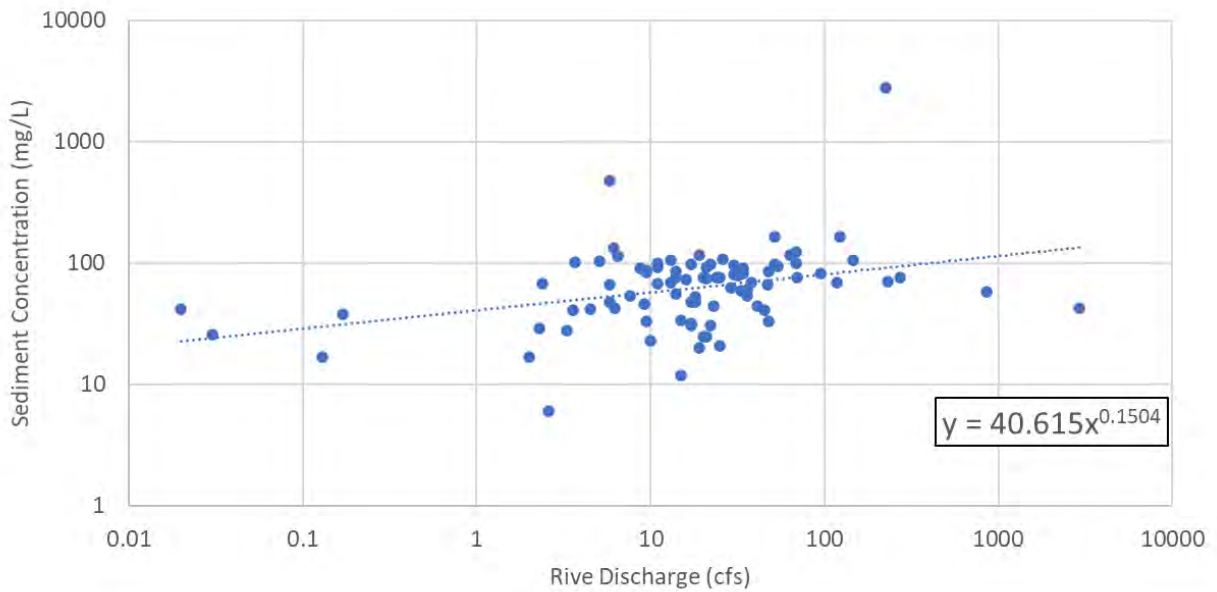


Figure 2.14: Sediment rating curve at 8189500 (Mission River at Refugio)

### 2.1.3.3 CSAT Dredging Data

The Corps Shoaling Analysis Tool (CSAT) is a tool developed by USACE that calculates channel shoaling volumes using historical channel survey. CSAT can predict future dredging volumes base on the shoaling rates. CSAT can also generate shoaling rate maps to identify hotspots or areas of increased sedimentation.

The data for CSAT tool at Corpus Christi can be divided into two periods based on the vertical datum used in the surveys. The period from 2011 to 2015 is based on the mean low tide datum and the period from 2016 to 2020 is based on the mean lower low water datum. CSAT uses the reaches defined by the natural channel network, according to which, the Corpus Christi shipping channel has 15 reaches (Figure 2.15). The period from 2011-2015 was used for model calibration and the period from 2016-2020 was used for model validation. The average annual shoaling rates calculated by CSAT for the two periods is shown in

Table 2.4. CSAT data indicates that most of the sedimentation occurs in Reach 1, Reach 6, Reach 7, and Reach 8.

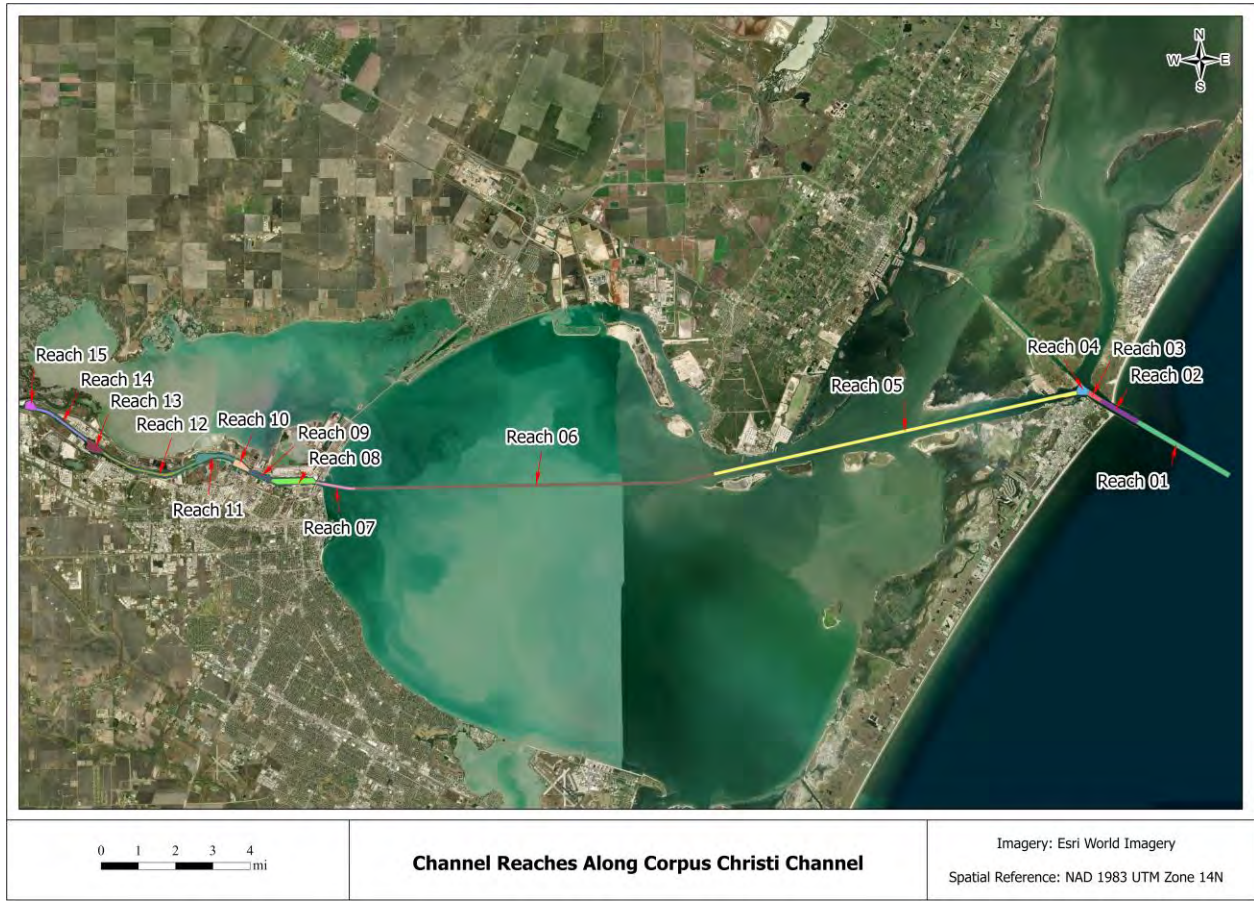


Figure 2.15: National channel network reach numbers for Corpus Christi channel

**Table 2.4: Average annual shoaling rates from CSAT**

Reach Number	Reach ID	Reach Name	Average Annual Shoaling Rate [ ft/yr (m/yr) ]	
			2011-2015	2016-2020
01	CESWG_CC_01_SBC_1	Sea bar channel	0.097 (0.03)	1.029 (0.314)
02	CESWG_CC_02_JEC_2	Jetty channel	0	0
03	CESWG_CC_03_IMC_3	Inner Basin at Main Channel	0	0
04	CESWG_CC_04_IHI_4	Inner Basin at Harbor Island	0.184 (0.056)	0
05	CESWG_CC_05_HLQ_5	Humble Basin to Junction at La Quinta Channel	0.022 (0.007)	0
06	CESWG_CC_06_LQB_6	La Quinta Channel Junction to Bcn. 82	0.782 (0.238)	1.585 (0.483)
07	CESWG_CC_07_BTBT_7	Bcn. 82 to Main Turning Basin	1.419 (0.432)	1.523 (0.464)
08	CESWG_CC_08_MTB_8	Main turning basin	0.945 (0.288)	1.090 (0.332)
09	CESWG_CC_09_INC_9	Industrial canal	0.186 (0.057)	0.246 (0.075)
10	CESWG_CC_10_ATB_10	Avery point turning basin	0.497 (0.151)	0.384 (0.117)
11	CESWG_CC_11_CTB_11	Chemical turning basin	0.432 (0.132)	0
12	CESWG_CC_12_TLC_12	Tule lake channel	0.203 (0.062)	0.026 (0.008)
13	CESWG_CC_13_TTB_13	Tule lake turning basin	0.281 (0.086)	0
14	CESWG_CC_14_VCH_14	Viola channel	0.425 (0.130)	0
15	CESWG_CC_15_VTB_15	Viola turning basin	0.260 (0.079)	0.004 (0.001)

## 3. Sedimentation Model Description

---

### 3.1 Model Development

Baird developed MIKE21 and MIKE3 models to simulate sedimentation/shoaling rates for the Port of Corpus Christi Channel Deepening Project 3rd Party study. Developed by the Danish Hydraulic Institute (DHI), MIKE21 Flow Model FM is a two-dimensional modeling system capable of simulating free surface flows where stratification is not of concern. MIKE3 Flow Model FM is three-dimensional modelling system unlike MIKE21 Flow Model FM, the free surface is taken into account using sigma-coordinate transformation approach or using a combination of a sigma and z-level coordinate system. Both MIKE21 and MIKE3 hydrodynamic models were calibrated and validated under the hydrodynamic and salinity modeling task (Baird, 2022). The sedimentation model is described in this report.

The model domain includes two major inner bays, i.e., Corpus Christi Bay and Nueces Bay,) in which the sediment is mainly clay. The shorelines of Mustang and San José islands in the Gulf of Mexico, on the other hand, are predominantly sandy out to approximately the 15 m depth contour in the Gulf. Therefore, a combination of the Mud Transport module (MT) and the Sand Transport module (ST) was used in the sedimentation. Model Domain and Grid

The model domain includes Nueces Bay, Corpus Christi Bay, and several linked bays on the north and south sides of it separated from the Gulf of Mexico (GOM) by Mustang Island, North Padre Island, and San José Island. These bays are connected to the GOM by a narrow entrance channel, Aransas Pass, and a secondary inlet, Packery Channel. River inflows come from the Nueces River and Oso Creek at the domain's western and southern extensions. The open boundaries for the model were selected sufficiently far from the navigation channel to avoid boundary effects on the study area. Figure 3.1 shows the model domain.

Mesh generation is one of the most important parts of the modeling strategy, since it defines the level of detail included in the model and the computation time required. An unstructured flexible mesh with triangular and quadrangular elements of different sizes was used to provide greater accuracy in and around the channels and nearshore areas.

Model bathymetry was obtained as mentioned in Section 2.1.1. The horizontal coordinates are located at UTM14N, while all bed elevations were adjusted to the datum of NAVD88. This mesh is shown in Figure 3.1. Figure 3.2 shows an example of the finer mesh resolution area around the channel where the different sizes and transitions to smaller elements can be seen. As waves are believed to be an important driving factor in movement of sediments around the outer channel in the GOM, the offshore boundary was set at 98ft (30 m) depth to match with the location of WIS hindcast wave data.



Figure 3.1: Computational mesh for the MIKE sedimentation model



Figure 3.2: Computational mesh for the MIKE sedimentation model showing the grid cells in the channel

### 3.1.1 Model Setup

The boundary conditions used by the model are surface elevation from the HYCOM model along the offshore boundary, and fluxes at the northeastern and southwestern lateral boundaries in the GOM. The open inland boundaries use measurements of water levels from nearby stations (Rockport to the northeast and Baffin Bay to the southwest). At river boundaries, measured discharge from stations upstream of the boundary, such as Nueces River, Aransas River, Mission River, Oso Creek, and Copano Creek were applied. The intake at the Nueces Bay power plant is located in the inner harbour portion of the channel (Reach 9). From the permitting documentation, the intake rate is 500 mgd, which is incorporated into the model as a sink term.

Sensitivity tests were performed with bed roughness to observe changes in surface elevation and current velocity. It was determined to use spatially variable roughness values in the domain to properly reproduce desired flow conditions. For the 2D model, Manning values in the range of 43 to 67 were used, which are equivalent to Manning's "n" values in the range of 0.023 to 0.015. For the 3D model, Nikuradse roughness values of 0.003 to 0.039 were used. These values represent a range of roughness from natural streams to excavated or dredged channels, as occurs in the main channels. See the Hydrodynamic and Salinity modeling report (Baird, 2022) for more details.

Three sediment fractions were included in the model: clay, silt, and sand. The fraction of available sediment in the bed was generated by spatial interpolation of the sediment fraction data mentioned in Section 2.1.3.1. The sediment contribution from the rivers and creeks was calculated using the sediment rating curves mentioned in section 2.1.3.2. Data was not available for Oso Creek and Copano Creek and therefore, the rating curves for Nueces River and Mission River were used respectively since they are close by. Settling velocities for mud fractions were set assuming medium silt and medium clay.

### 3.1.2 Spectral wave model

Baird used the Danish Hydraulic Institute (DHI) MIKE21 Spectral Wave (SW) model to transform the offshore wave climate, from the WIS station to the nearshore region in front of the project shoreline. The same model domain, including the model mesh and bathymetry mentioned above were used for the SW model. The offshore wave data and wind data from the WIS station and NOAA buoy were used as boundary conditions for the spectral wave model. The same model was used to simulate wind generated waves over Corpus Christi Bay and other inland water bodies.

## 4. Model Calibration and Validation

---

The sedimentation model was calibrated and validated against the CSAT data. For the calibration, one-year two-dimensional simulations were completed for 2011 and model results were compared to CSAT data for period of 2011 to 2015. Similarly, the validation runs were conducted for 2020 and compared to CSAT data for 2016 to 2020. The above simulation periods were selected based on availability of HYCOM data for boundary conditions.

### 4.1 Scaling Factor due to Wind

The sedimentation model was calibrated to the CSAT data representing average sedimentation rates for the period of 2011 to 2015. Due to data availability, one year of model runs were done for 2011. However, wind conditions were above average in 2011 resulting in higher-than-average sedimentation in the Northern part of the channel in Corpus Christi Bay. A scaling factor was thus used to adjust the result to represent a typical year.

Most sedimentation in Corpus Christi Bay occurs between the months of April and July. The predominant wind direction in the area is from 130 degrees (or southeast) as shown in the wind rose in Figure 4.1. As shown in this figure, southeasterly winds and associated waves generated within Corpus Christi Bay are in the key contributing factor to sediment resuspension in the northeastern part of Corpus Christi Bay and in Nueces Bay. It is mainly the resuspended sediment from this area that ends up in Reaches 6 and 7 of the channel causing sedimentation. Therefore, the effective wind energy was calculated from the wind speeds projected onto the 130-degree direction (Figure 4.2). A scaling factor was defined as the ratio of the excess wind energy in a certain year to the long-term average annual wind energy. Model results indicated that the critical wind speed for sediment resuspension is around 21.3 ft/s (6.5 m/s), resulting in a threshold wind energy of 35,000 J/kg. The final scaling factor for the calibration runs (2011) was calculated to be 1.39 and that of the validation runs (2020) was 0.55.

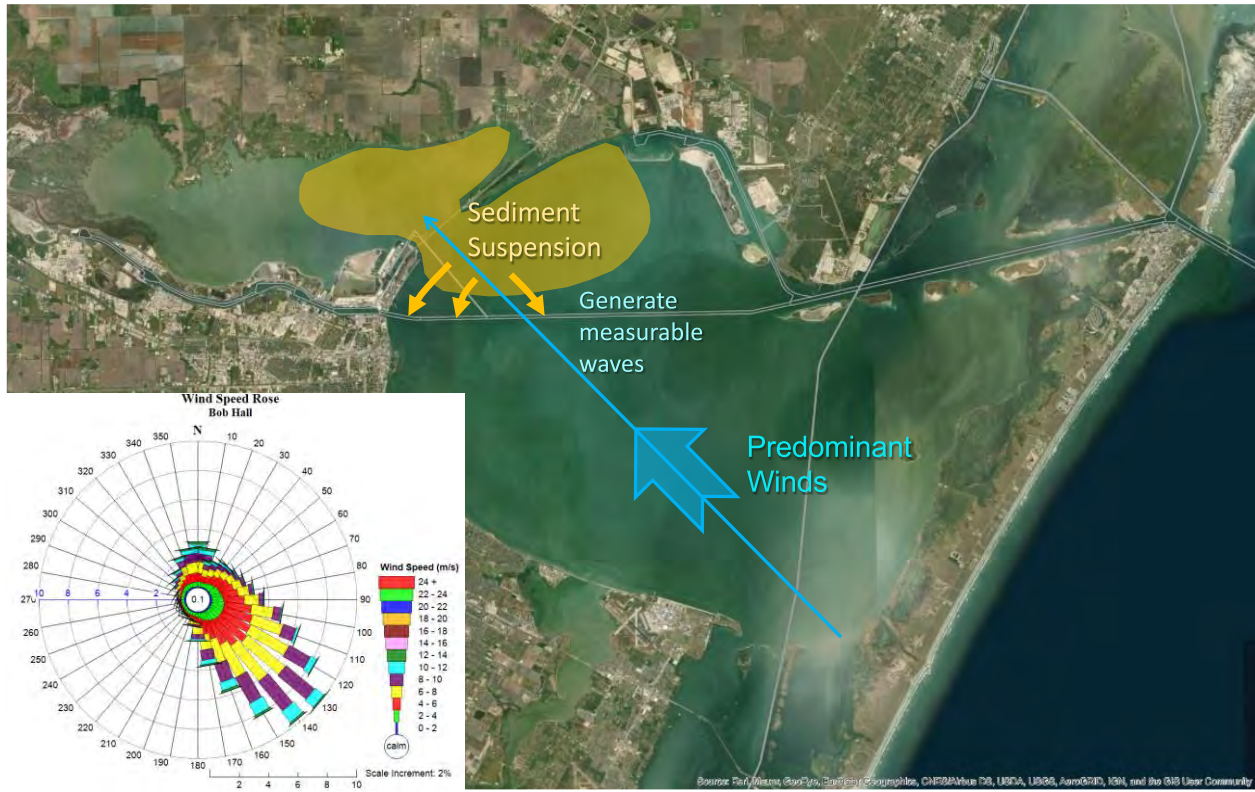


Figure 4.1: Wind rose and schematics of channel sedimentation processes inside Corpus Christi Bay

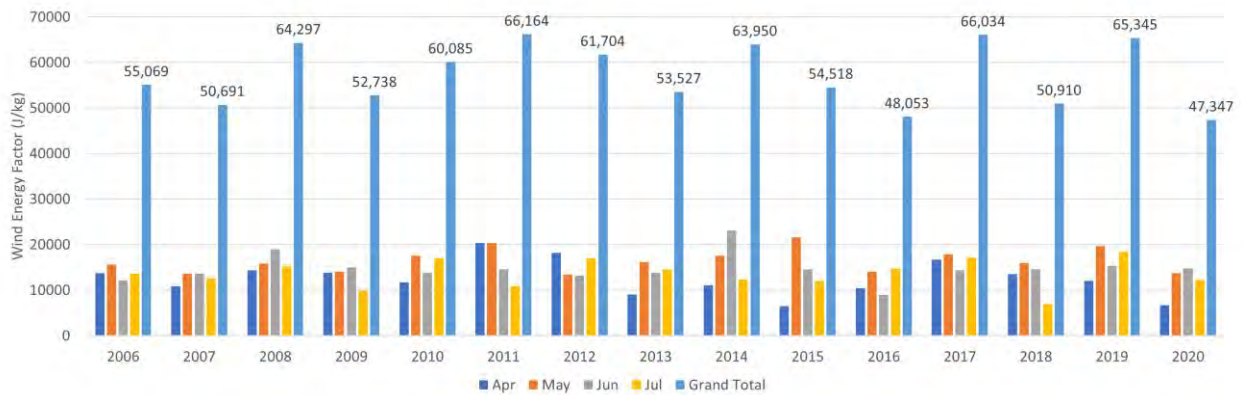


Figure 4.2: Variation of wind energy between April and July from 2006 to 2020

## 4.2 Erosion in the Inner Harbor

Examination of historic shorelines in the Inner Harbor determined shoreline erosion as the source of sediment causing sedimentation in Reaches 9 to 15 of the channel. Bank erosion and sediment transport processes are not included in the sedimentation model. Sedimentation volume was thus calculated using aerial images between 1995 to 2020 (Figure 4.3 and Figure 4.4). Using the areas shown in Table 4.1 and assuming a depth

of 48 ft (15 m), the average shoaling rate in the inner harbor was calculated to be around 0.325 ft/year (0.099 m/year). It is expected that this rate will decrease as/if the shoreline becomes more stable into the future.

**Table 4.1: Erosion area in the inner harbor**

Year	Erosion Area (yd <sup>2</sup> )
2004-2020	152,690
1995-2004	274,710

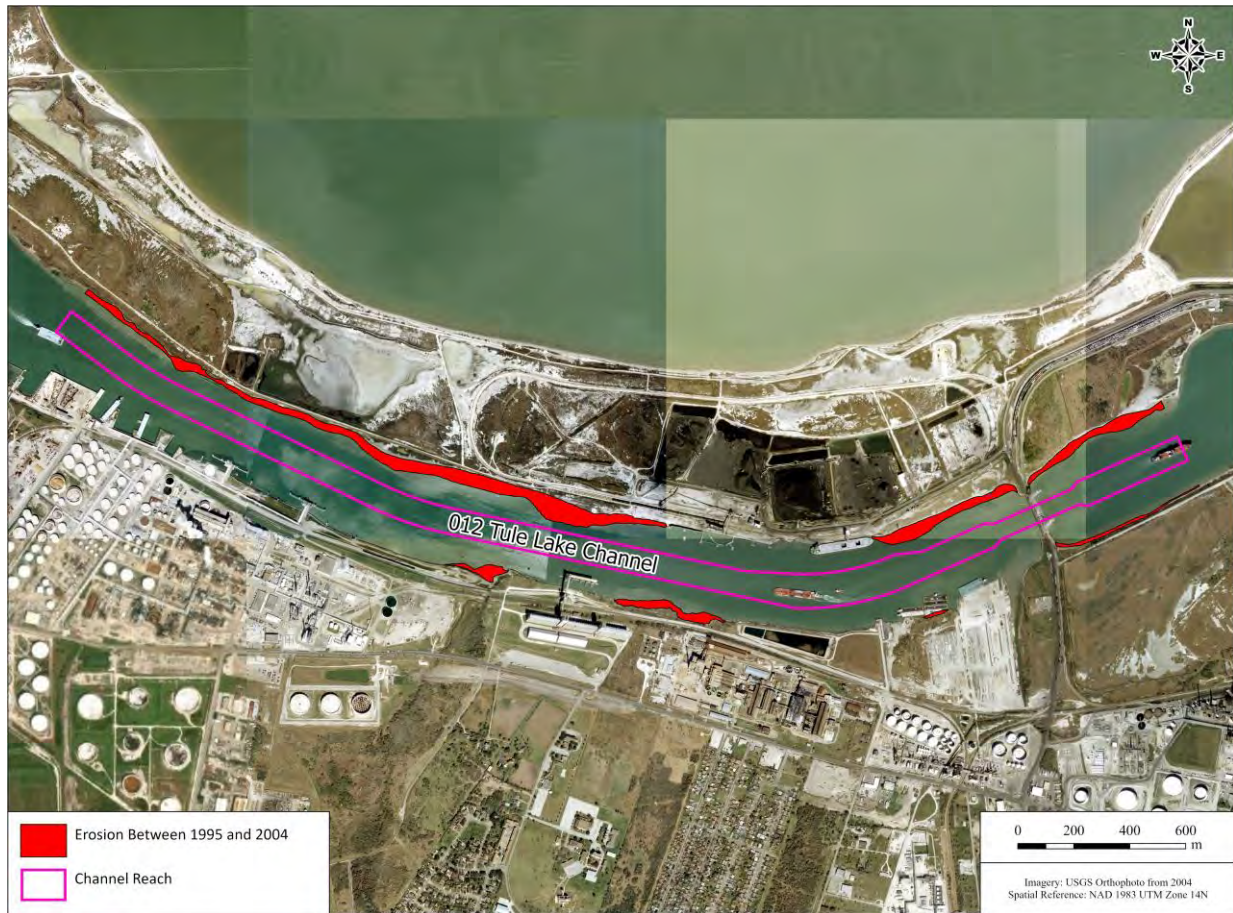


**Figure 4.3: Erosion in the Inner Harbor (Reach 12) between 1995 and 2004**

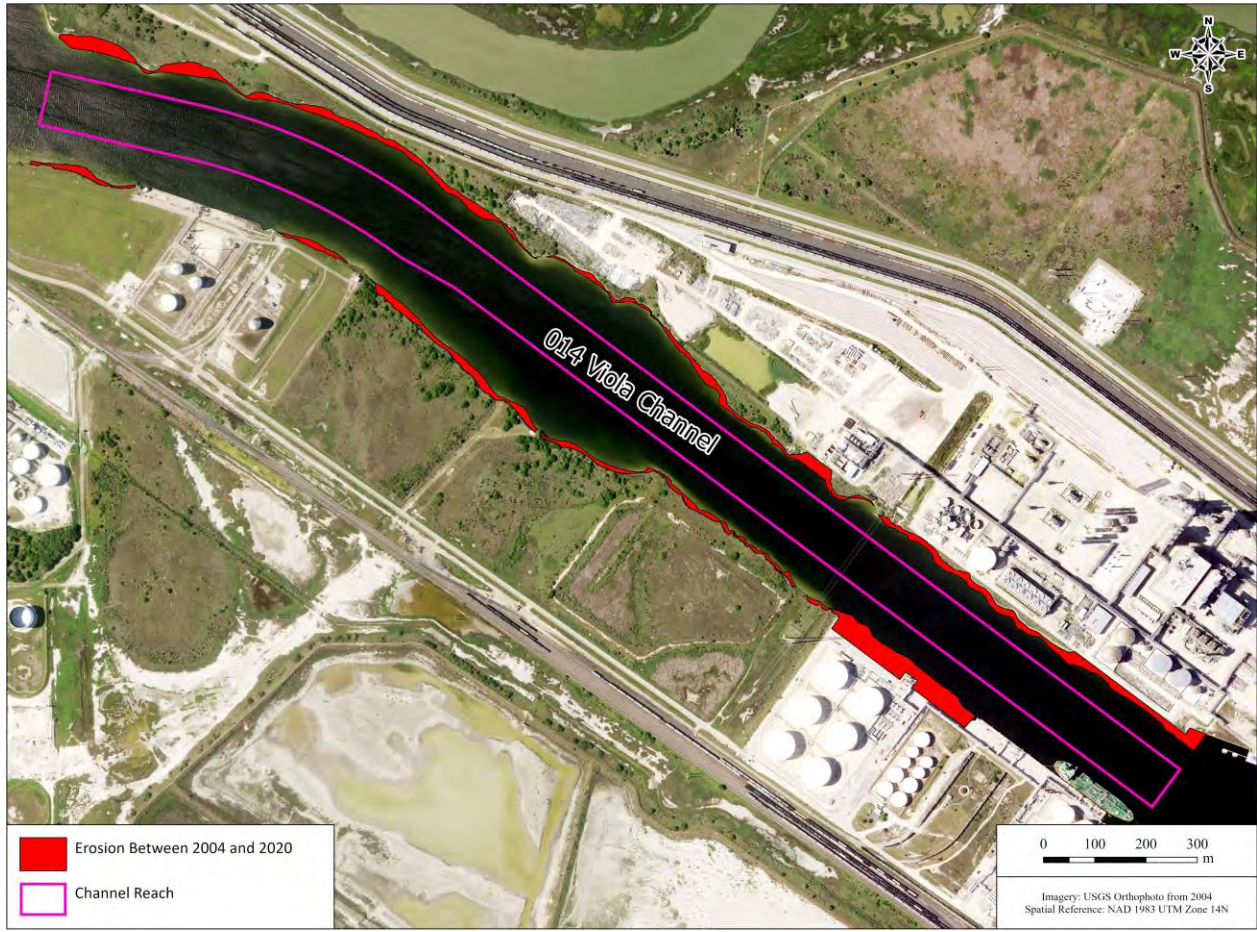


**Figure 4.4: Erosion in the Inner Harbor (Reach 12) between 2004 and 2020**

### 4.3 Two-dimensional model

Shoaling rates were calculated from predicted sedimentation for 2011 using the national channel database polygons which includes the channel bottom and have 15 reaches as described in Section 2.1.3.3. Figure 4.5 shows the predicted average annual shoaling rate in the different reaches of the channel compared to the CSAT data. Most of the sedimentation in the Corpus Christi Bay is predicted to occur at the northern end of the shipping channel (i.e., Reaches 6, 7, and 8) which is consistent with CSAT. Predicted sedimentation rates for Reaches 9 to 15 include average shoreline erosion volumes discussed in the previous section. Predicted sedimentation rates are in reasonable agreement with CSAT data despite some overprediction in Reach 6 and underestimation in Reach 8.

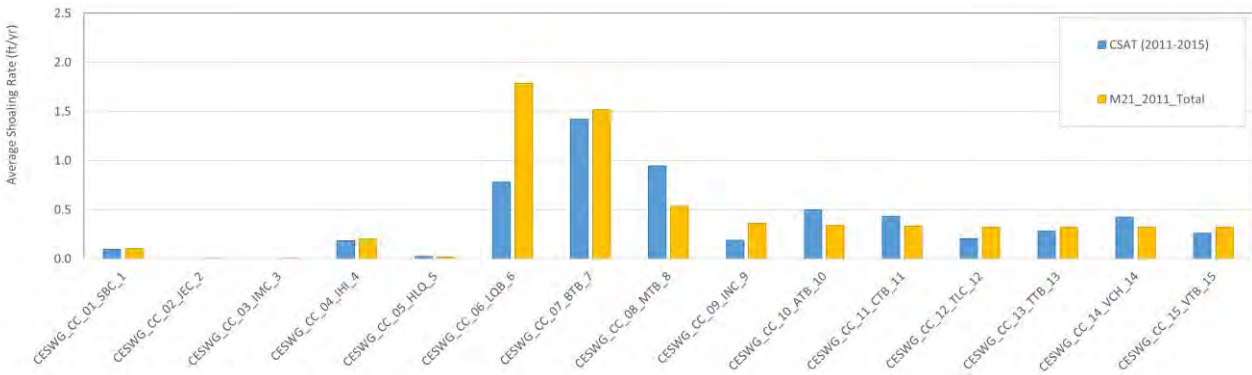


**Figure 4.5: Comparison of CSAT shoaling rates (2011-2015) and model predictions (2011)**

Subsequently, channel sedimentations in 2020 were predicted and compared with the CSAT data to validate the model. The 2020 predicted rates were first normalized by a factor of 0.55 as discussed in the prior section. The 2016-2020 CSAT data shows significantly higher sedimentation in the outer channel (Reach 1) because of Hurricane Harvey which occurred in 2017. Therefore, wind and wave conditions during Hurricane Harvey were incorporated into the input wind and wave time-series files for 2020 for the duration of the storm. The comparison between the CSAT shoaling rates and model predictions is shown in Figure 4.6 and indicates a reasonable agreement.

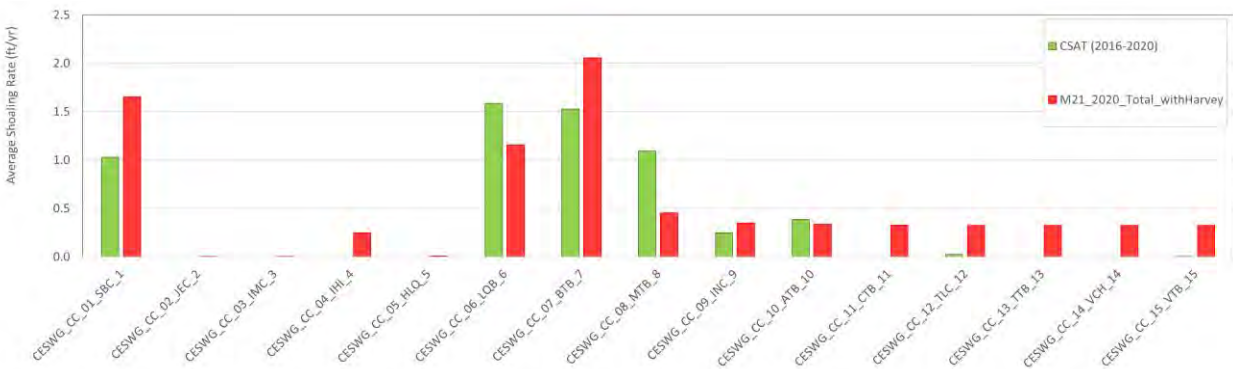


**Figure 4.6: Comparison of CSAT shoaling rates (2016-2020) and model predictions (2020)**

Figure 4.7 shows the comparison of the average shoaling rate between the two periods above from the CSAT data and model predictions. The model predictions were slightly higher than the CSAT with the exception of reaches 8 and 10, which are both in the inner harbor. It is concluded that the model performance is acceptable for assessment of potential project impacts.

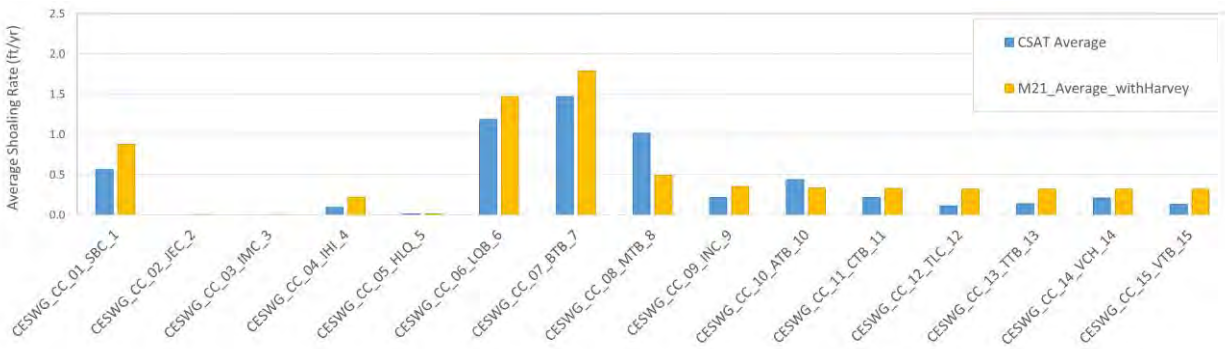


Figure 4.7: Comparison of CSAT shoaling rates (average) and model results (average)

#### 4.4 Comparison of Two-dimensional and Three-dimensional models

Three-dimensional model runs require extensive computer resources and run at relatively slow speeds and thus are not practical for year-round simulations. As noted earlier, model results indicated that most of the sedimentation in the inner channels occur during months of April to July when predominant winds are from the 130 deg direction. Preliminary model runs and analysis of wind data indicated that June 2020, once properly scaled, may be used as a representative month to predict sedimentation in the inland portion of the Corpus Christi channel where mud transport is predominant. The outer channel or Reach 1 is subject to sand transport by waves and currents requiring full year 3D simulations that are not computationally practical. Therefore, only the 2D model was used for Reach 1 simulations. Figure 4.8 shows the comparison between the CSAT shoaling rates and the model results (both 2D and 3D). The 3D run was scaled for the time period (assuming similar sedimentation occurs per month between April and July) and also scaled to be comparable to a typical year (scale factor of 0.55 for 2020) as mentioned in section 4.1. The 3D model results are comparable with the 2D model results.

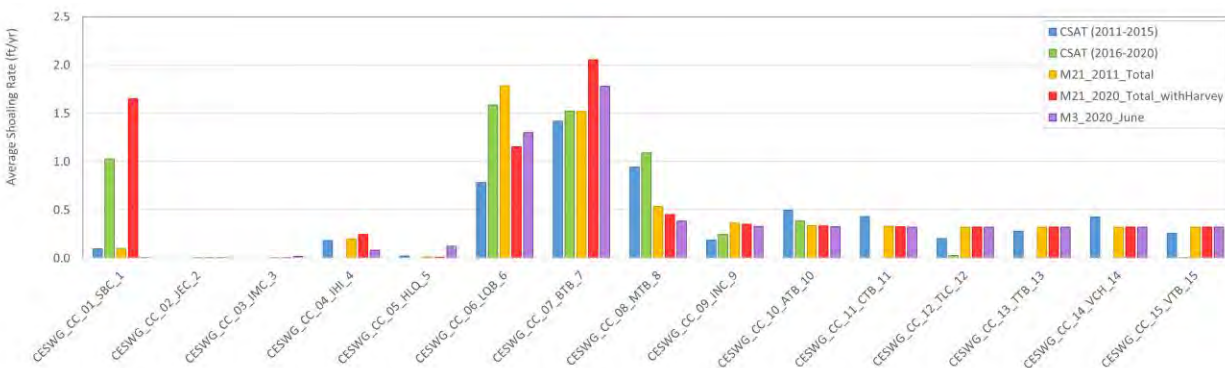


Figure 4.8: Comparison of CSAT shoaling rates and model results (2D and 3D)

## 5. Modeling Assessment of Potential Project Impacts

### 5.1 Model Scenarios

To assess the impact of channel deepening on sedimentation in the channel, two scenarios were considered:

1. In the Future Without Project (FWOP) scenario, the shipping channel was dredged to 54 ft MLLW (-16.6 m, NAVD88). The dredging area includes the expansion of Humble Basin and the terminals (Figure 5.2). The model bathymetry of the FWOP scenario is presented in Figure 5.1a.
2. In the Future With Project (FWP) scenario, extent of the shipping channel from the Gulf of Mexico to the end of the terminals was dredged 75 ft MLLW (-23.0 m, NAVD88) and the remaining channel was dredged to 54 ft MLLW (-16.6 m, NAVD88). The model bathymetry of the FWP scenario is presented in Figure 5.1b. The dredging area includes the expansion of Humble Basin and the terminals (Figure 5.2).

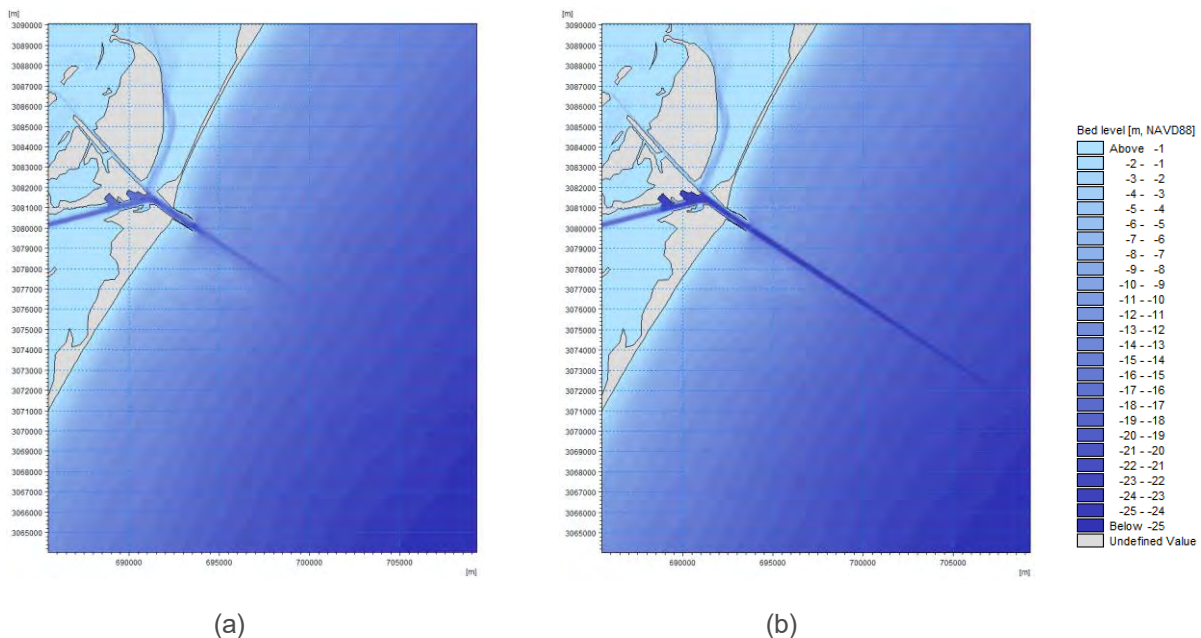


Figure 5.1: Model bathymetry around the jetties for (a) FWOP, and (b) FWP scenarios

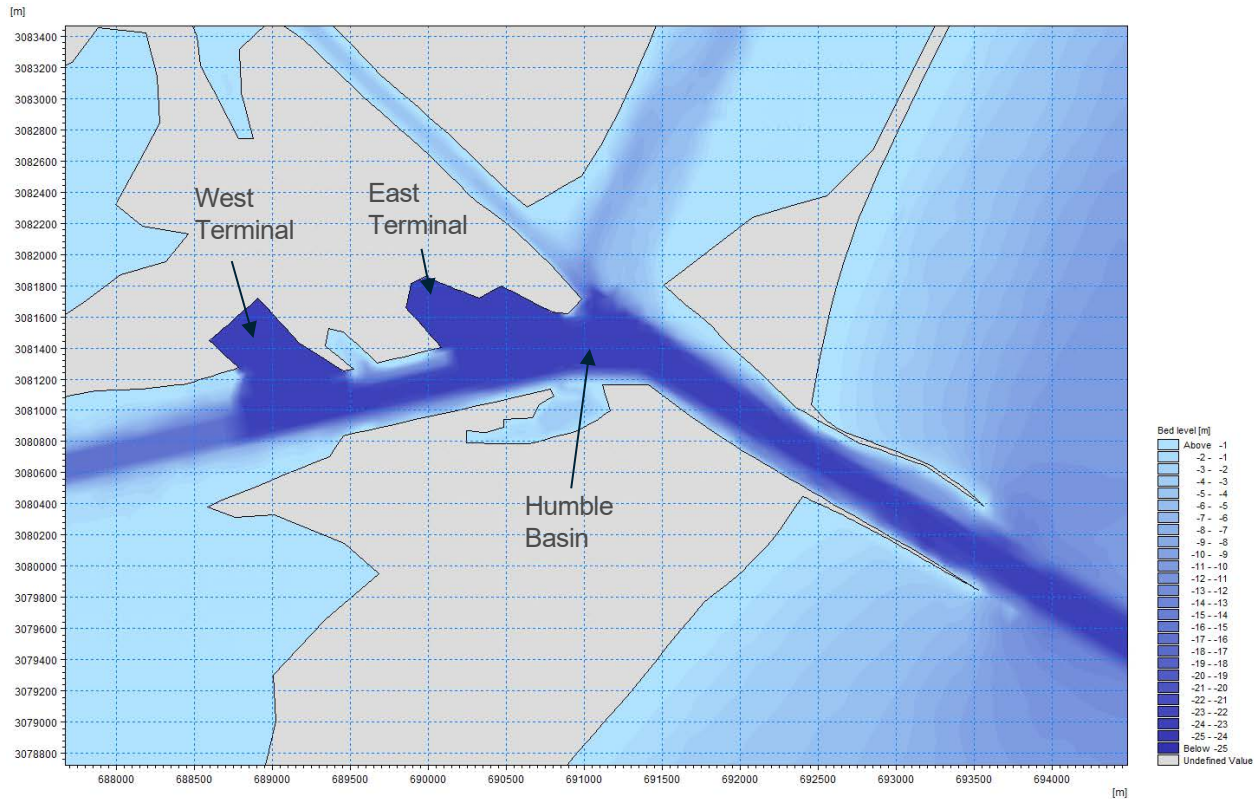
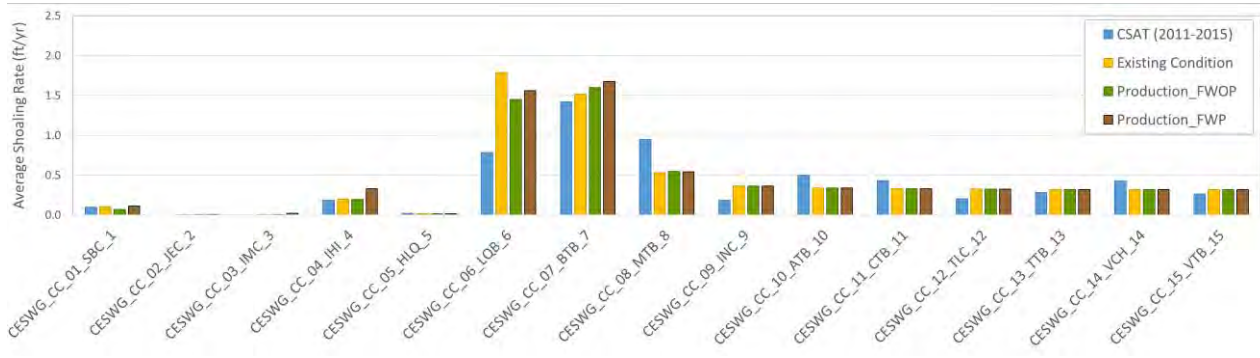


Figure 5.2: Model Bathymetry for FWP scenario showing the terminals

## 5.2 Impact Assessment

### 5.2.1 Shoaling Rates in the Inner Channel

Figure 5.3 shows the average annual shoaling rates from CSAT for the period of 2011-2015 and the 2D model predicted results for the existing, FWOP, and FWP conditions. Between the FWOP and FWP scenarios, the model predicted about 5-10% increase in sedimentation in certain reaches. However, both FWOP and FWP shoaling rates were comparable to the existing condition. Figure 5.4 shows the shoaling rates in different reaches as well as the two terminals present in the FWOP and FWP scenario. Predicted sedimentation rates in Reaches 9 to 15 are based on historic bank erosion rates along the inner harbor shoreline. The model predicted a 5-10% increase in sedimentation under the FWP scenario as a result of deeper channel depths.



**Figure 5.3: Comparison of CSAT shoaling rate (2011-2015) and the 2D model results for existing conditions, FWOP and FWP scenarios**

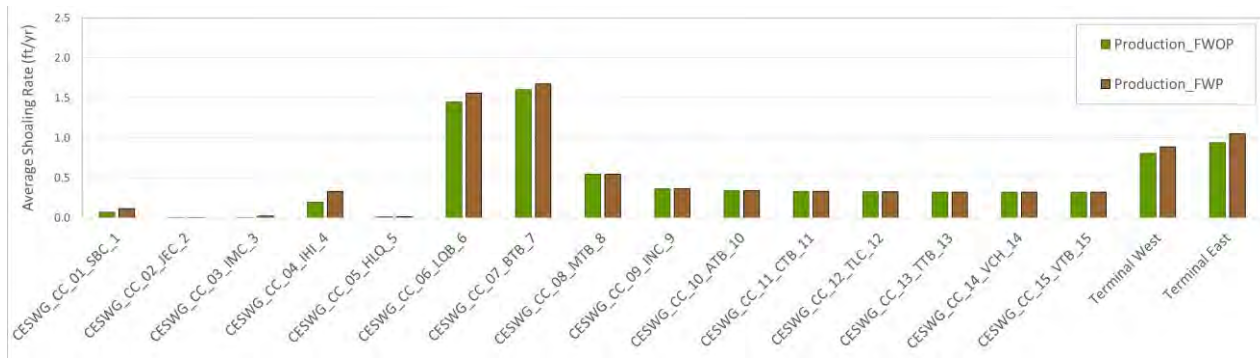


**Figure 5.4: Average annual shoaling rates predicted by the 2D model in the channel including the terminals for FWOP and FWP scenarios**

Figure 5.5 shows the average annual shoaling rates from CSAT for the period of 2011-2015 and the 3D model results for the existing, FWOP, and FWP conditions. The results are in reasonable agreement with the 2D model results. Between the FWOP and FWP scenarios, there was about 5-10% increase in sedimentation in certain reaches but a slight decrease is observed in reach 7 as opposed to an increase seen in the 2D model results. Predicted FWOP and FWP shoaling rates were comparable to the existing condition. Figure 5.6 shows the shoaling rates in the different reaches and the two terminals present in the FWOP and FWP scenario. Overall, both 2D and 3D model results indicate that the project impact on sedimentation rates is limited to less than 10%.

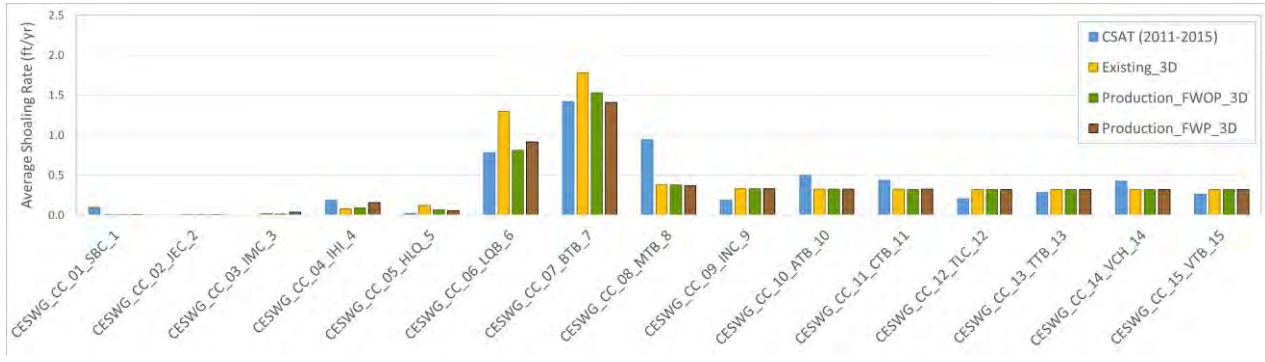


**Figure 5.5: Comparison of CSAT shoaling rate (2011-2015) and the 3D model results for existing conditions, FWOP and FWP scenarios**

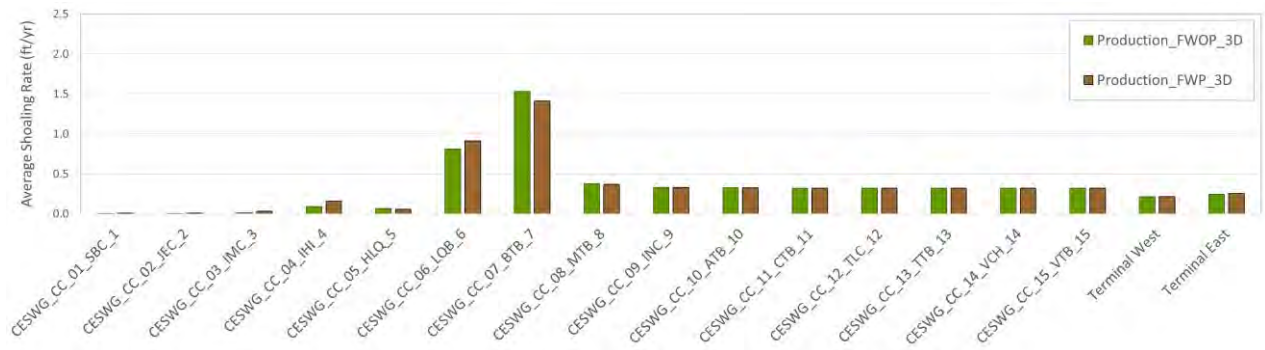


**Figure 5.6: Average annual shoaling rates predicted by the 3D model in the channel including the terminals for FWOP and FWP scenarios**

### 5.2.2 Sedimentation Volumes in the Outer Channel

Sedimentation in the outer channel is dominated by sand transport processes. Predicted sedimentation volumes in the outer channel were calculated for segments 1, 2 and 3 as shown in Figure 5.7. Since the model predicts sedimentation on the channel shoulders, the volume calculation polygon includes both the channel bed and shoulders. Segment 1 is the same longitudinal extent as Reach 1 from the National Channel Network but larger in the transverse direction to include the shoulders. Segment 2 extends to up to the end of the channel for the FWOP scenario and Segment 3 extends to that of the FWP scenario. Model simulations were completed for 2011 and the results were compared.

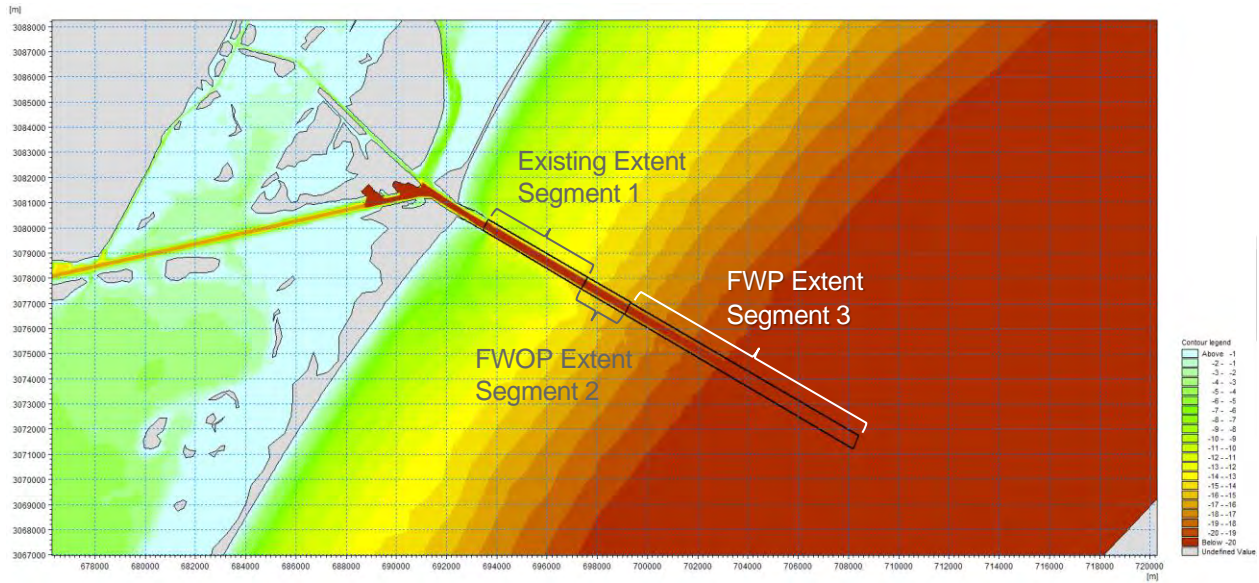


**Figure 5.7: Segments for sediment volume calculation**

The corresponding sedimentation volumes are shown in Table 5.1. For all scenarios, most sedimentation is predicted to occur in Segment 1. Nevertheless, examination of model results indicated that the deeper channel in the FWP scenario further channelizes the ebb flow resulting in increasing sedimentation farther offshore in the channel. Between the existing scenario and FWOP there was ~3000 yd<sup>3</sup> (2294 m<sup>3</sup>) and between the existing scenario and FWP, there was an increase of ~70,000 yd<sup>3</sup> (53,519 m<sup>3</sup>) in Segment 1. In Segment 2, the increase between the existing condition and FWOP scenario is ~11,000 yd<sup>3</sup> (8,410 m<sup>3</sup>) and that between existing and FWP is ~48,000 yd<sup>3</sup> (36,699 m<sup>3</sup>). In Segment 3, the increase between the existing condition and FWOP scenario is ~1,500 yd<sup>3</sup> (1149 m<sup>3</sup>) and that between existing and FWP is ~16,000 yd<sup>3</sup> (12,233 m<sup>3</sup>). In summary, the model predicted that sedimentation in the outer channel increases from approximately 95,000 yd<sup>3</sup>/year (72,633 m<sup>3</sup>/year) for the FWOP to approximately 214,000 yd<sup>3</sup>/year (163,615 m<sup>3</sup>/year) for the FWP scenario, approximately 2.25 times higher. This is primarily due to that fact that the FWP has a deeper and longer channel compared to FWOP.

**Table 5.1: Predicted sedimentation volumes**

Scenario	Sedimentation Volume			
	Segment 1 [yd <sup>3</sup> (m <sup>3</sup> )]	Segment 2 [yd <sup>3</sup> (m <sup>3</sup> )]	Segment 3 [yd <sup>3</sup> (m <sup>3</sup> )]	Total [yd <sup>3</sup> (m <sup>3</sup> )]
Existing	76,000 (58,000)	3,900 (3,000)	100 (77)	80,000 (61,000)
FWOP	78,900 (60,000)	14,300 (11,000)	1,600 (1,200)	94,800 (72,000)
FWP	145,400 (111,000)	52,300 (40,000)	16,300 (12,000)	214,000 (164,000)

## 6. Modeling Assessment of Beach Nourishment, Offshore Berms and Offshore Dredged Material Disposal Area (ODMDS)

---

### 6.1 Model Scenarios

Three FWP scenarios were evaluated to examine the effect of the beach nourishment, offshore berms and ODMDS on channel sedimentation. (Figure 6.1). The ODMDS geometry was obtained from a Delft3D model by Freese & Nichol's. The model runs were done for 2011. The scenarios are as follows:

1. Beach nourishment and offshore berms (fixed bed)
2. Beach nourishment, offshore berms and ODMDS (fixed bed)
3. Beach nourishment, offshore berms and ODMDS (mobile bed)

For the fixed bed scenario, the only available sediment is from the beach nourishment, offshore berms and ODMDS such that their isolated effect can be examined. For the mobile bed scenario, the bed sediment layer is added in addition to the beach nourishment, offshore berms and ODMDS to examine their combined effect.

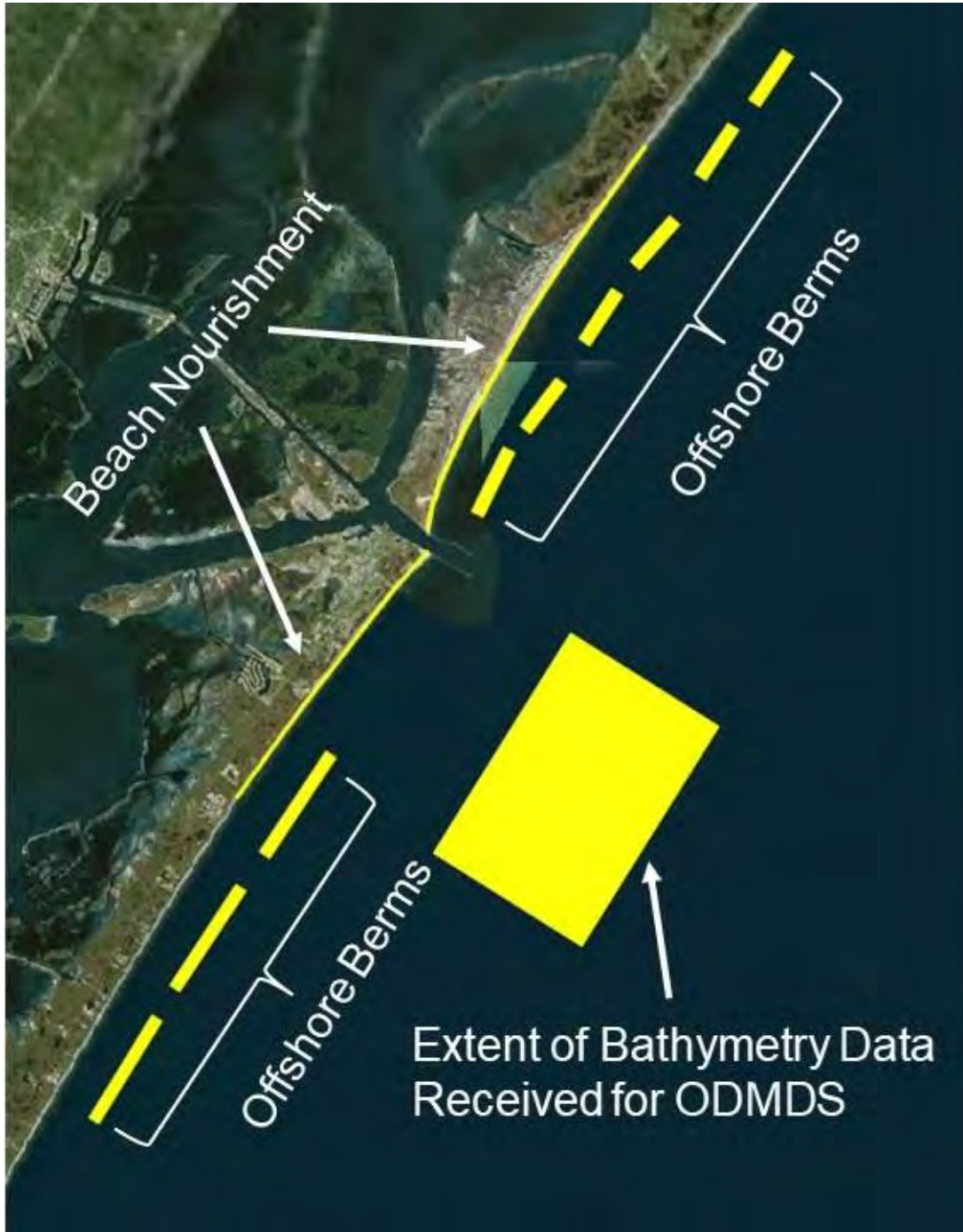


Figure 6.1: Location of the beach nourishment, offshore berms and the extend of data received from Freese and Nichol's for the ODMDS.

## 6.2 Impact Assessment

### 6.2.1 Contribution of Beach Nourishment and Offshore berms to Channel Sedimentation

Simulation results from the beach nourishment and offshore berms over fixed bed are shown in Figure 6.3. The model runs show that little to no sediment from the beach nourishment and offshore berms settled in the channel. The volume of sedimentation in segments 1, 2, and 3 (Figure 5.7) from the model scenario with beach nourishment and offshore berms are shown in Table 6.1. Predicted total sedimentation is less than 600 yd<sup>3</sup> (459 m<sup>3</sup>) suggesting that the beach nourishment and offshore berms make small contributions to channel sedimentation compared to the overall sedimentation.

**Table 6.1: Sedimentation in the channel due to beach nourishment and offshore berms**

Scenario	Sedimentation Volume		
	Segment 1 [yd <sup>3</sup> (m <sup>3</sup> )]	Segment 2 [yd <sup>3</sup> (m <sup>3</sup> )]	Segment 3 [yd <sup>3</sup> (m <sup>3</sup> )]
Beach Nourishment + Offshore berms	480 (367)	180 (138)	0

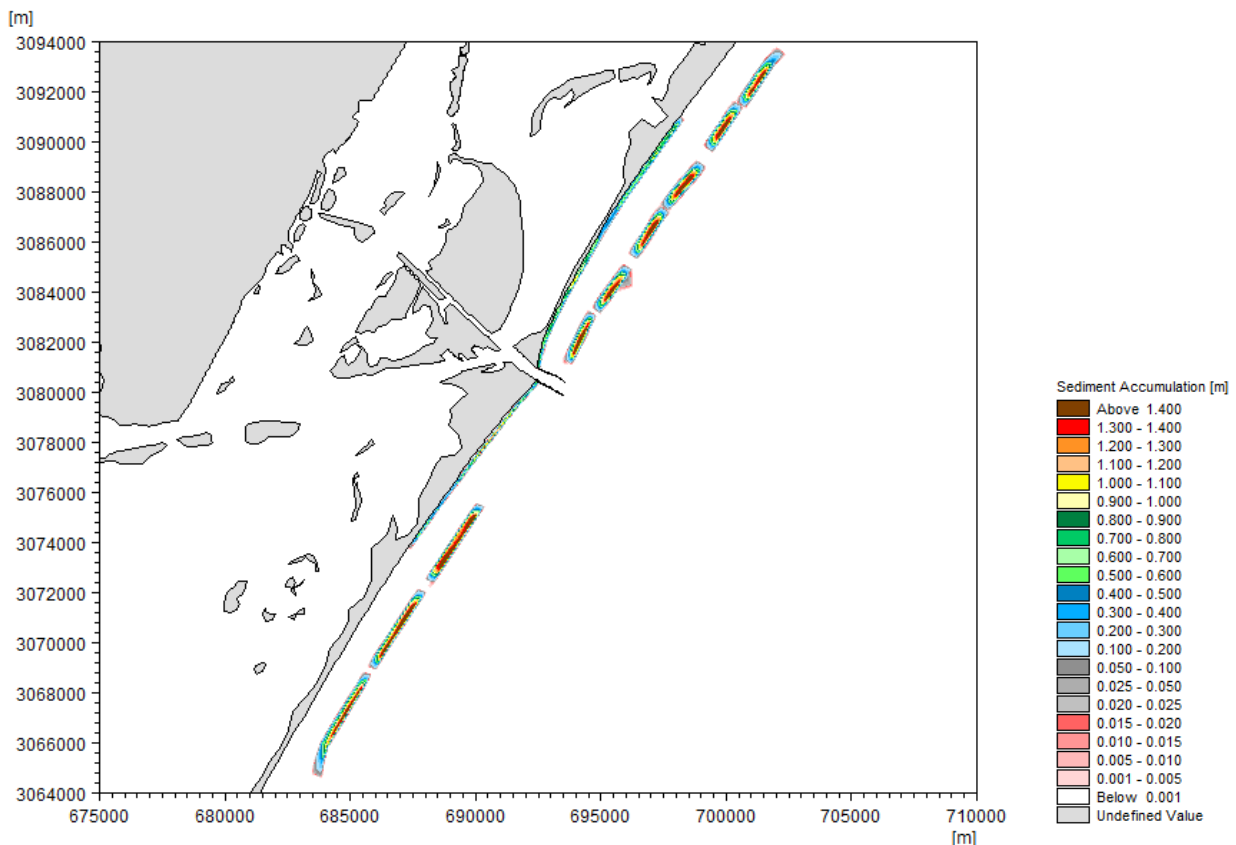


**Figure 6.2: Distribution of settled sediment thickness from the beach nourishment and offshore berms over the fixed bed at the beginning of the model run**

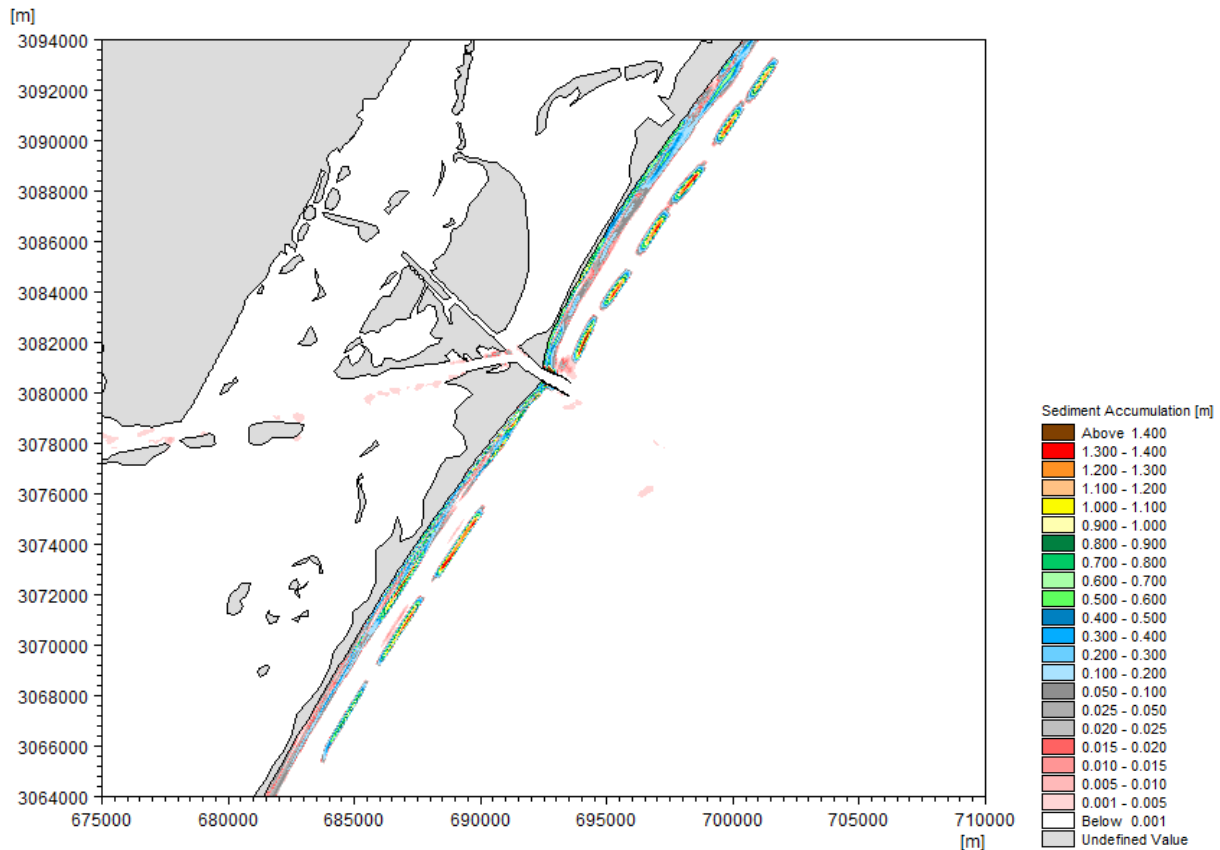


**Figure 6.3: Distribution of settled sediment thickness from the beach nourishment and offshore berms over the fixed bed at the end of the model run**

### 6.2.2 Contribution of the ODMDS Sediment to Channel Sedimentation

Scenarios 1 and 2 described in section 6.1 were used to evaluate the potential contribution from the ODMDS sediment to channel sedimentation. Table 6.2 shows the sedimentation calculated in the segments show in Figure 5.7. The predicted maximum increase in sedimentation due to the ODMDS is approximately 1,200 yd<sup>3</sup> (917 m<sup>3</sup>). The increase in segments 2 and 3 are less than 500 yd<sup>3</sup> (382 m<sup>3</sup>). It is concluded that contribution from the ODMDS sediment to channel sedimentation is small in comparison with the overall sedimentation.

**Table 6.2: Sedimentation in the channel with and without ODMDS**

Scenarios	Sedimentation Volume		
	Segment 1 [yd <sup>3</sup> (m <sup>3</sup> )]	Segment 2 [yd <sup>3</sup> (m <sup>3</sup> )]	Segment 3 [yd <sup>3</sup> (m <sup>3</sup> )]
with ODMDS	1,840 (1407)	870 (665)	900 (688)
without ODMDS	680 (520)	530 (405)	780 (596)

### 6.2.3 Impact of the ODMDS Mound on Channel Sedimentation

Table 6.3 provides predicted sedimentation volumes in the outer channel for four different scenarios including with and without the ODMDS over fixed and mobile beds. Beach nourishment and offshore berms were present in all four scenarios. For the scenarios with fixed bed, the maximum increase in sedimentation occurs in Segment 1 and is less than 1,900 yd<sup>3</sup> (1,453 m<sup>3</sup>). This confirms that the ODMDS direct impact on channel sedimentation is small compared to the overall sedimentation. On the other hand, in the case of mobile bed the increase happens in Segment 2 and is approximately 72,000 yd<sup>3</sup> (55,048 m<sup>3</sup>). Note that Segment 2 is adjacent to the ODMDS mound. The relatively large increase in sedimentation in Segment 2, in the mobile bed run indicates that the ODMDS has an indirect impact on sedimentation through changing the hydrodynamics in the channel as discussed below.

**Table 6.3: Sedimentation in the channel due to the presence of the ODMDS**

Scenario	Sedimentation Volume			
	Segment 1 [yd <sup>3</sup> (m <sup>3</sup> )]	Segment 2 [yd <sup>3</sup> (m <sup>3</sup> )]	Segment 3 [yd <sup>3</sup> (m <sup>3</sup> )]	Total [yd <sup>3</sup> (m <sup>3</sup> )]
w/ ODMDS (Fixed bed)	1,840 (1407)	870 (665)	900 (688)	3,610 (2,760)
w/o ODMDS (Fixed bed)	680 (520)	530 (405)	780 (596)	1,990 (1,522)
w/ ODMDS (Mobile bed)	193,800 (148,000)	124,600 (95,000)	23,900 (18,000)	342,300 (262,000)
w/o ODMDS (Mobile bed)	145,400 (111,000)	52,300 (40,000)	16,300 (12,000)	214,000 (164,000)

To assess the change in hydrodynamics between the scenarios with and without ODMDS, current speeds from 3 points along the channel were extracted (Figure 6.4). Point 1 close to the entrance between the two jetties. Point 2 is further offshore close to the end of the existing channel and Point 3 is in the middle of Segment 2, which is where the highest increase in sedimentation was observed with the ODMDS.

Current roses representing “direction to” for the above 3 points are shown in Figure 6.5, Figure 6.6 and Figure 6.7. At Point1 (Figure 6.5), the flow direction in the run with ODMDS has a higher frequency in the 110 degrees direction and features higher velocities in 110 to 130 degrees directions (i.e., along the channel axis). Although the velocity field at Points 2 and 3 is governed by cross-channel tidal currents, a similar trend as in Point 1 is observed showing stronger along-the-channel velocity component under with-ODMDS conditions.

The presence of the ODMDS adjacent to the channel brings small but important changes to the hydrodynamics of ebb currents creating more channelized flow at a slightly higher velocity that can move more sediment further offshore along the channel. Figure 6.8 shows the comparison of velocity field between with and without the ODMDS mound conditions for an ebb event when the above-mentioned changes in hydrodynamics of the ebb flow is observed. For the scenario without the ODMDS, the velocity plume does not reach as far down the channel. In summary, the model predicted that sedimentation in the outer channel under FWP conditions increases from approximately 214,000 yd<sup>3</sup>/year (164,000 m<sup>3</sup>) in the absence of the ODMDS mound to approximately 342,000 yd<sup>3</sup>/year (262,000 m<sup>3</sup>) (approximately 1.6 times greater) when the ODMDS mound is present.

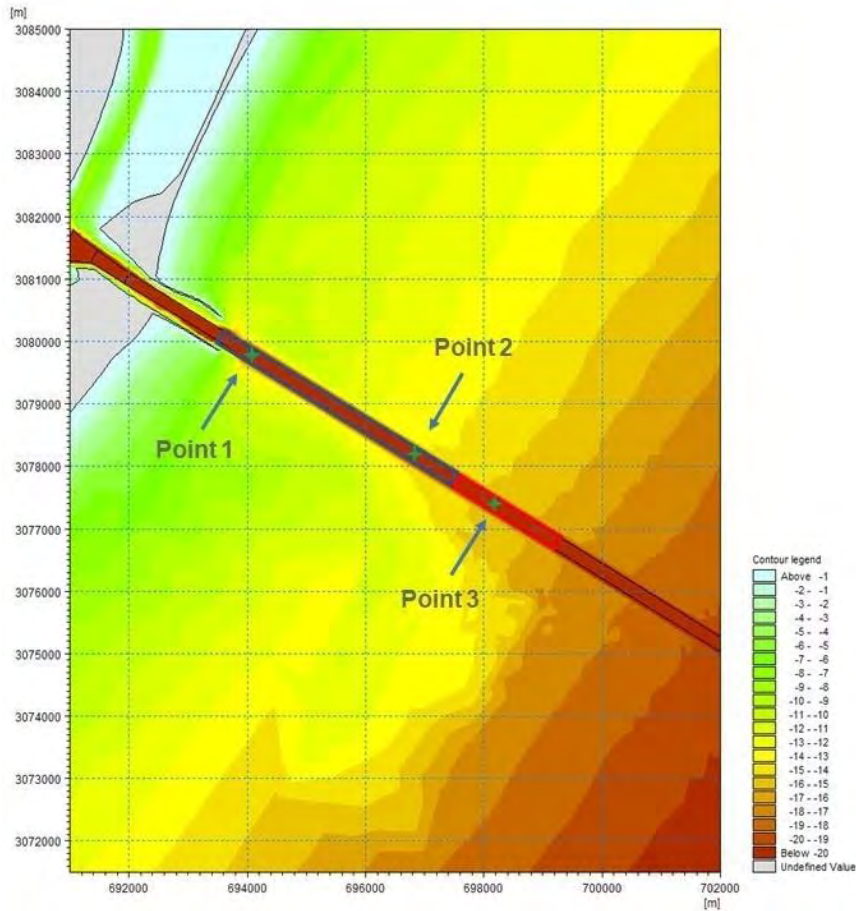


Figure 6.4: Locations used to investigate the change in hydrodynamics due to the ODMS

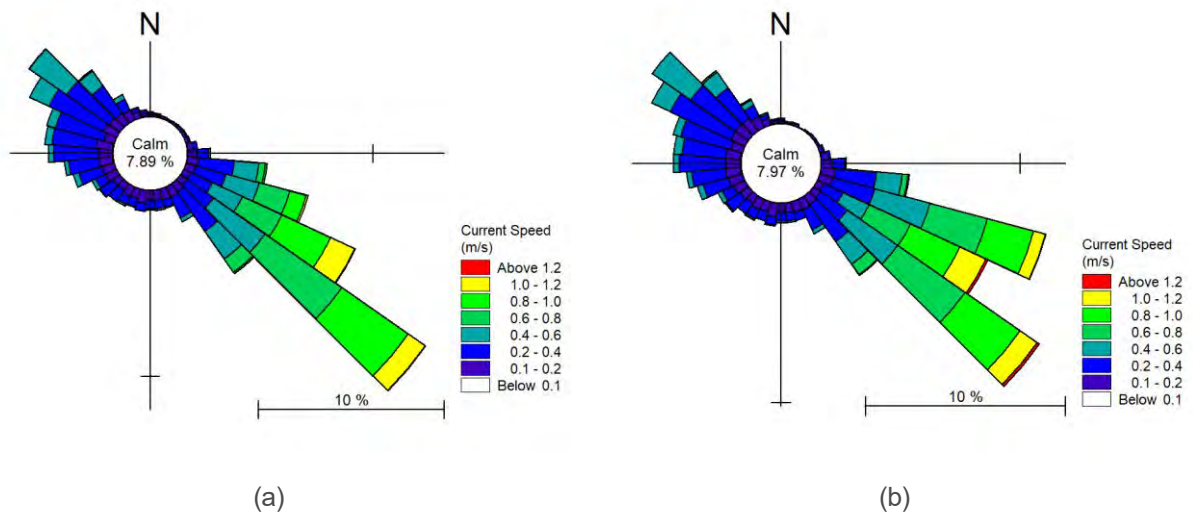


Figure 6.5: Current rose plots at point 1 for scenario (a) without ODMS and (b) with ODMS

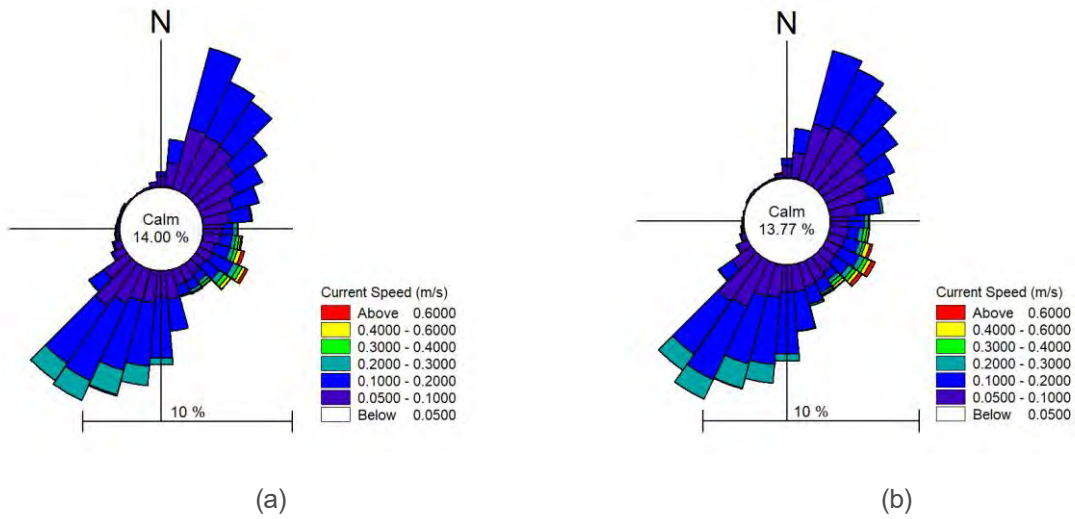


Figure 6.6: Current rose plots at point 2 for scenario (a) without ODMDS and (b) with ODMDS

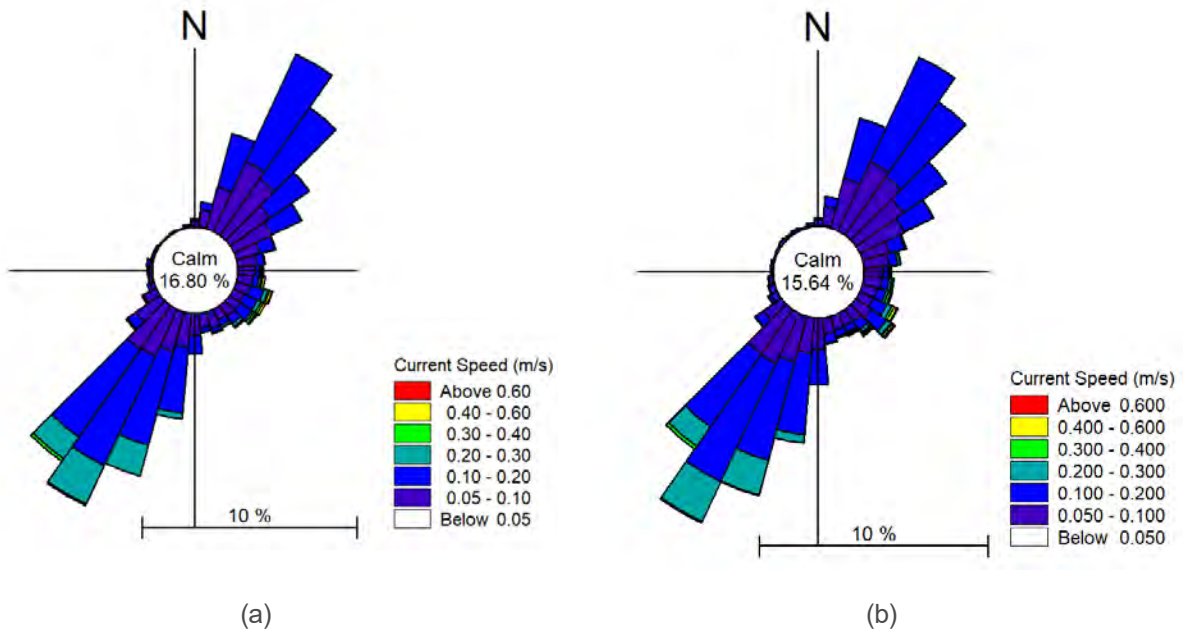
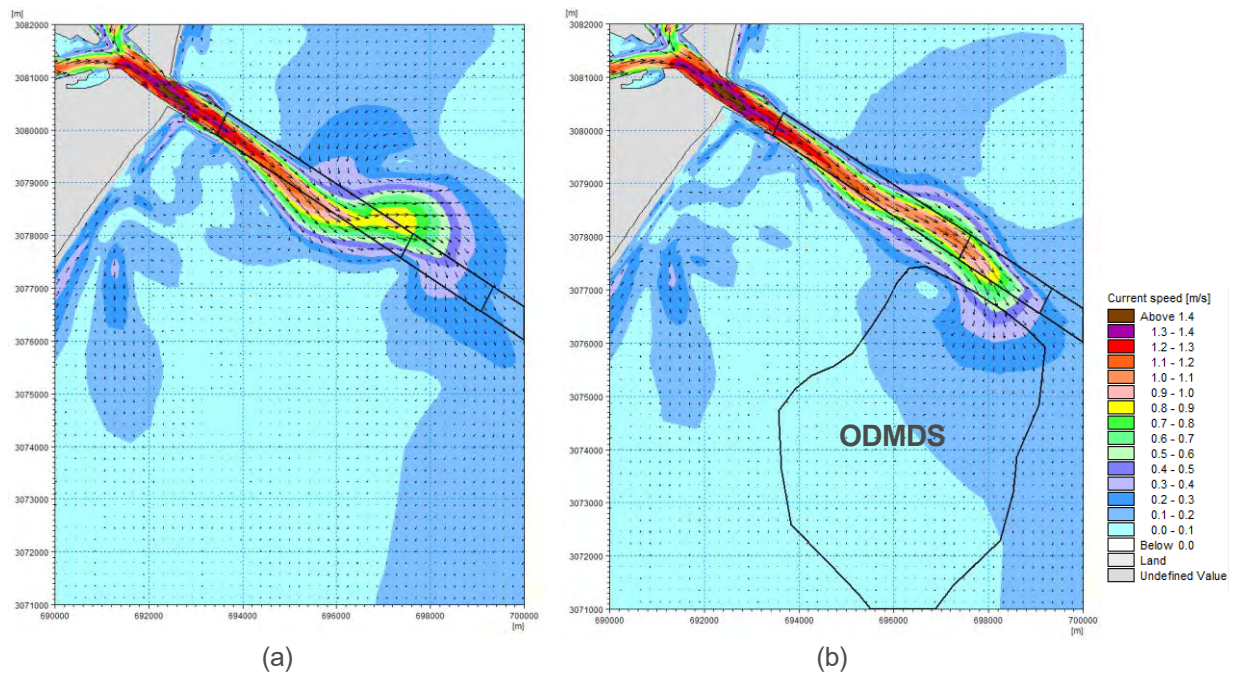


Figure 6.7: Current rose plots at point 3 for scenario (a) without ODMDS and (b) with ODMDS



**Figure 6.8: Velocity field during typical ebb tide for scenario (a) without the ODMDS and (b) with the ODMDS mound**

### 6.2.4 Impact of Hurricanes on Sedimentation in the Outer Channel

The impact of hurricane on channel sedimentation was assessed by conducting one-month model runs using hurricane Harvey. Due to data availability, 2020 HYCOM data was used for the tidal boundaries while the wind and wave conditions were replaced with conditions during Hurricane Harvey (thus providing indicative results). FWP scenarios including beach nourishment, offshore berms and the ODMDS over both fixed and mobile beds were simulated and compared with the existing conditions.

Predicted sedimentation volumes in Segments 1, 2 and 3 are presented in Table 6.4. The fixed bed scenario reflects the sedimentation coming only from the offshore berms, beach nourishment and the ODMDS. Comparing the existing to the FWP mobile bed scenarios, the predicted total sedimentation increased significantly from approximately 675,000 yd<sup>3</sup> (516,000 m<sup>3</sup>) for existing conditions to 1,574,000 yd<sup>3</sup> (1,203,000 m<sup>3</sup>) for FWP conditions, which is about 2.3 times higher similar to the increase under annual wave conditions (Table 5.1). Volumes calculated from the USACE surveys before and after hurricane Harvey indicated that the sedimentation in Segment 1 was approximately 1,000,000 yd<sup>3</sup> (765,000 m<sup>3</sup>). The difference in the model predicted sedimentation (i.e., 675,000 yd<sup>3</sup>) and that from the surveys can be mainly attributed to the fact that the model used 2020 HYCOM currents instead of the 2017 currents due lack of HYCOM data for 2017.

**Table 6.4: Sedimentation in the outer channel due to hurricane**

Scenario	Sedimentation Volume			
	Segment 1 [yd <sup>3</sup> (m <sup>3</sup> )]	Segment 2 [yd <sup>3</sup> (m <sup>3</sup> )]	Segment 3 [yd <sup>3</sup> (m <sup>3</sup> )]	Total [yd <sup>3</sup> (m <sup>3</sup> )]
Existing	610,300 (467,000)	49,000 (37,000)	16,100 (12,000)	610,300 (467,000)
FWP – fixed bed	169,200 (129,000)	52,200 (40,000)	16,100 (12,000)	169,200 (129,000)
FWP – mobile bed	992,800 (759,000)	379,100 (290,000)	201,900 (154,000)	992,800 (759,000)

The above results indicate that individual hurricane events could result in sedimentation volumes in the outer channel that are several times higher than the average annual sedimentation. However, it is noted that Hurricane Harvey was a rare powerful storm that impacted the Texas coastline. The impact of other hurricanes on sedimentation could be significantly different depending on individual hurricane's track and intensity.

Sedimentation in the inner channel was evaluated similarly and the predicted volumes are shown in **Error! Reference source not found.** The location of segments 4, 5 and 6 are shown in Figure 6.9. The extents of these segments are analogous to the reach extents of the National Channel Framework, but the transverse extent is modified to include the shoulders. The predicted sedimentation volumes indicate that the total volume increase between existing conditions and FWP due to Hurricane Harvey is about ~3%. The most increase in sedimentation happens in Segment 4 at ~11%, which is consistent with the results of section 5.2, which predicted an increase of ~10% in shoaling rate. The volume in segment 6 is lower for the FWP condition by ~15%. The eastern portion of segment 6 which is adjacent to the terminals is part of the deeper outer channel which allows higher volume of water coming in from GOM likely resulting in removal of the local sediment.

**Table 6.5: Sedimentation in the inner channel due to hurricane**

Scenarios	Sedimentation Volume			
	Segment 4 [yd <sup>3</sup> (m <sup>3</sup> )]	Segment 5 [yd <sup>3</sup> (m <sup>3</sup> )]	Segment 6 [yd <sup>3</sup> (m <sup>3</sup> )]	Total [yd <sup>3</sup> (m <sup>3</sup> )]
Existing	66,100 (51,000)	470,200 (359,000)	46,400 (35,000)	66,100 (51,000)
FWP – mobile bed	73,400 (56,000)	486,000 (372,000)	39,400 (30,000)	73,400 (56,000)

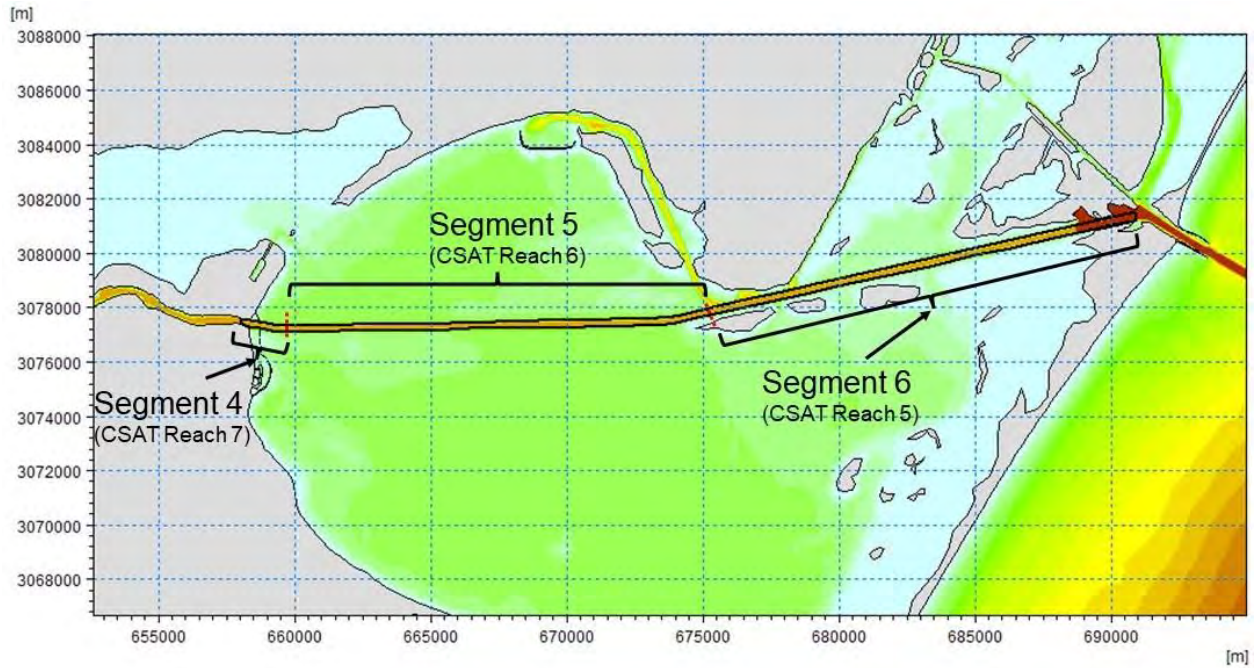


Figure 6.9: Segments for sediment volume calculation in the Corpus Christi Bay

## 7. Stability of Offshore Berms and Beach Nourishment

---

This section assesses the stability of the designed offshore berm and beach nourishment using 1D cross-shore transport numerical models. Waves from the Gulf of Mexico were used as the driving force to determine if the placed sediment will stay in place, move onshore to build the beach (offshore berms), overwash inland (beach nourishment), and/or be lost offshore to deeper waters. Long-term (annual) and short term (storm) wave conditions are applied in the analysis. The potential benefits of the offshore berm to reduced beach erosion was also assessed.

### 7.1 Numerical Models

Two numerical models were used to assess the stability of the offshore berms and beach nourishment: XBeach (<https://oss.deltares.nl/web/xbeach/>) developed by Deltares and CSHORE (<https://usace.contentdm.oclc.org/digital/collection/p266001coll1/id/4558/>) developed by USACE.

XBeach is a numerical model for wave propagation, long waves and mean flow, sediment transport and morphological changes of the nearshore area, beaches, dunes and back barrier during storms. It is a public-domain model that has been developed with major funding from the USACE, Rijkswaterstaat and the EU, supported by a consortium of UNESCO-IHE, Deltares, Delft University of Technology and the University of Miami. It is currently the leading-edge model for simulation of beach and dune erosion under severe storm events.

In this study we have employed the CSHORE model along with XBeach to bring added confidence in the model results as topographic and bathymetric data for calibration is limited. CSHORE is a simple and phase-averaged 1-D nearshore model for predicting hydrodynamics and profile change from depth of closure into the swash zone developed by the USACE.

### 7.2 Beach Profile

The unnourished beach profile was extracted from the Continuously Updated Digital Elevation Model (CUDEM) from San Jose Island as shown in Figure 7.1. The profile extends seaward to an offshore elevation of -65 ft NAVD88. The beach nourishment and offshore berm was added to the profile using placement information sent via CAD files (“BU\_MOD1\_s-ft.dwg” and “Beach\_Dune Fill Features\_s-ft.dwg”) by Freese and Nichols on October 28, 2021.

Figure 7.2 shows the design profile used for the modeling assessment. In the design profile, the offshore berm is placed between the -28 and -31 ft NAVD88 (-8.5 and -9.5 m NAVD88) contours with a berm crest elevation of -25 ft NAV88 (-7.6 m NAVD88). The berm crest width is 900 ft (274 m) on San Jose Island. Side slopes of 1V:24H are used. On Mustang Island, the characteristics of the offshore berm are similar, but the berm crest width is slightly narrower at 800 ft (244 m). On the beach, the nourishment is placed as a dune with crest elevation of 10 ft NAVD88 (3.1 m NAVD88) and width of 75 ft (23 m). Side slopes of 1V:3H are used on the dune. Fronting the dune, an approximately 200 ft (61 m) beach is placed with at an elevation of 6 ft NAVD88 (1.8 m NAVD88). The beach slopes down to the existing profile at a slope of 1V:50H.

Two versions of the design profile were used in the modeling assessment, one that includes the offshore berm and one without the offshore berm in order to determine the potential impact of the offshore berm on the stability of the beach nourishment.

A median ( $D_{50}$ ) sediment size of 0.14 mm was used in both models.

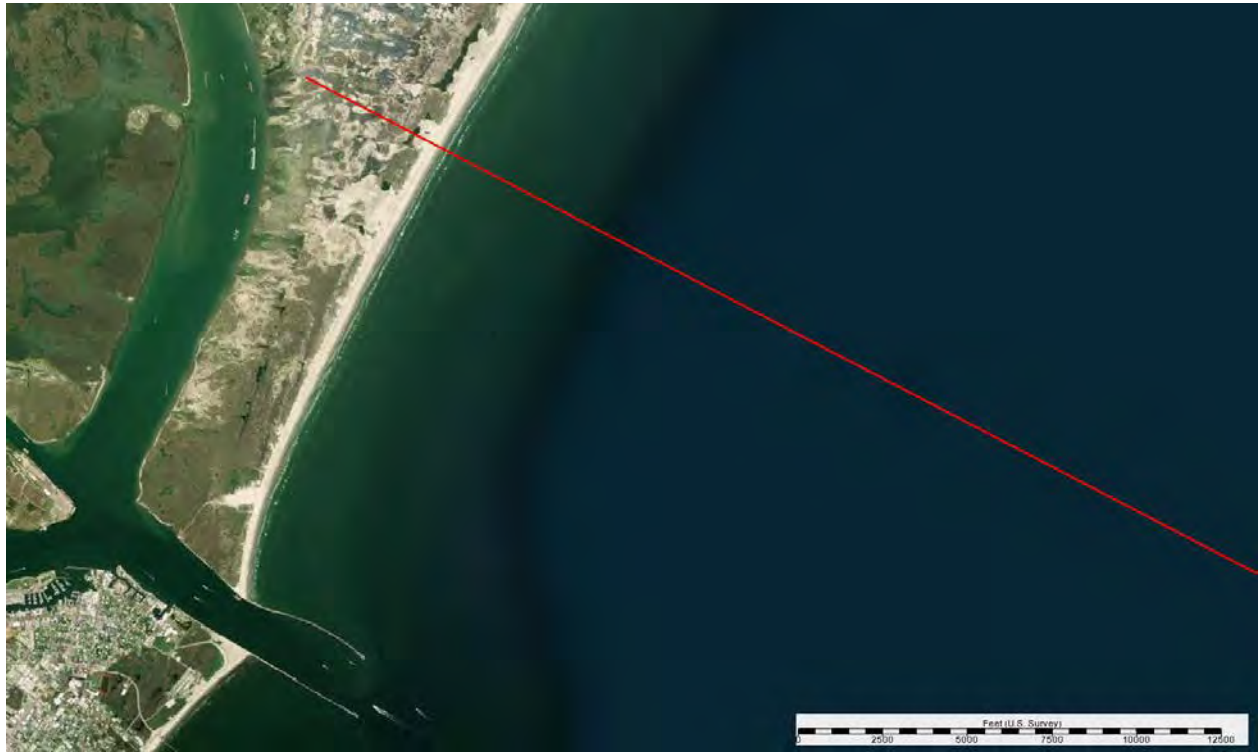


Figure 7.1: Location of design profile

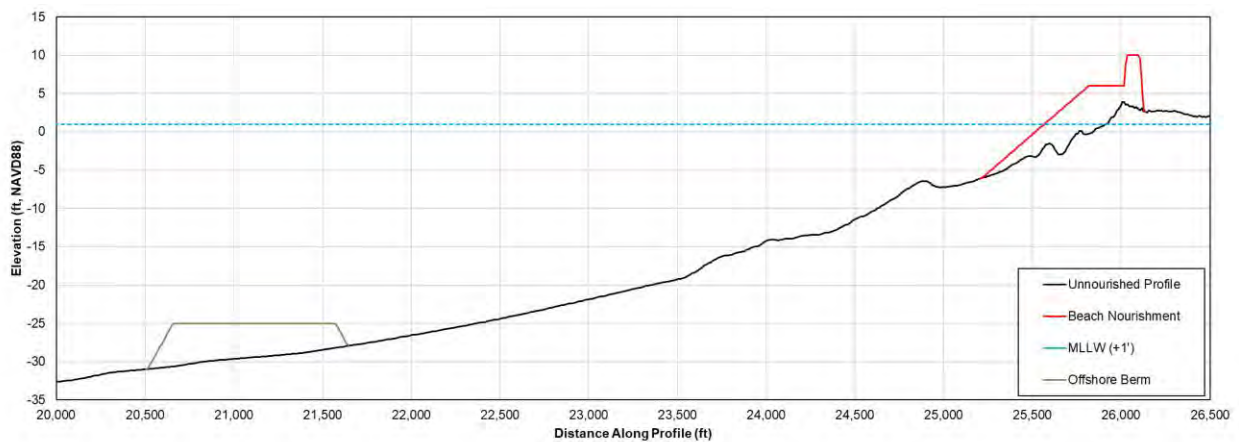
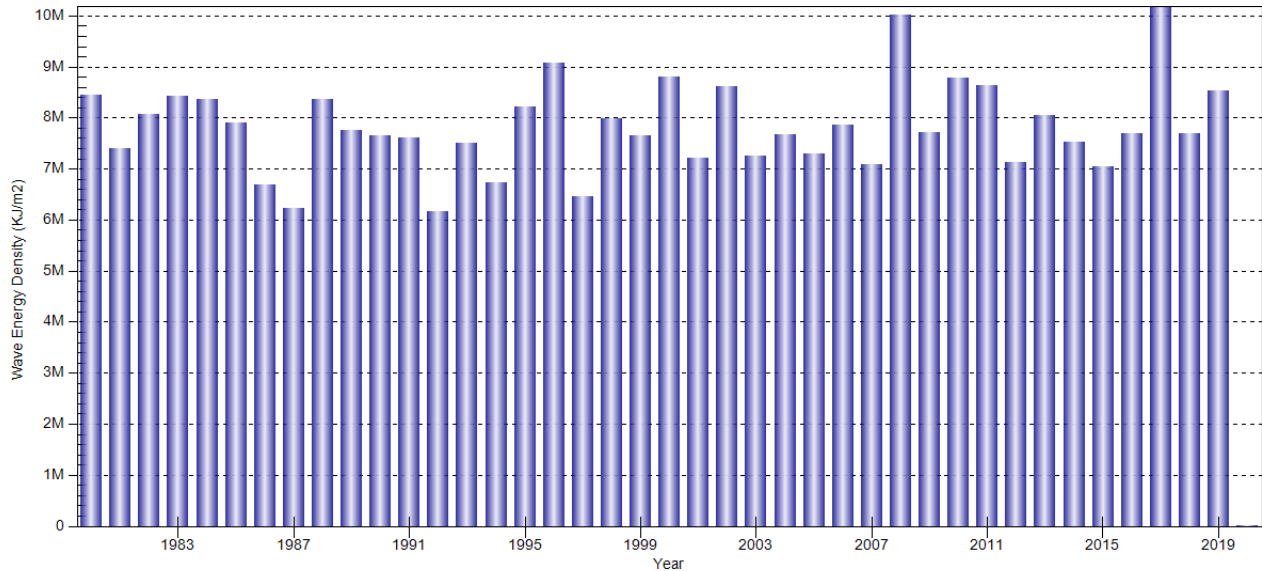


Figure 7.2: Design profile used for the modeling assessment typical on San Jose Island and Mustang Island

### 7.3 Modeling Assessment

#### 7.3.1 Profile Response to Long Term Wave Conditions

Figure 7.3 shows the average annual wave energy density from WIS Station 73040 from 1980 to 2019. The year 2016 was chosen to represent an average wave energy year (approximately 7 million kJ/m<sup>2</sup>) and 2017 was chosen to represent an exceptionally high wave energy year (approximately 11 million kJ/m<sup>2</sup>, partly due to occurrence of Hurricane Harvey in August 2017). Waves from WIS 73032 and water levels from Bob Hall Pier were used as hydrodynamic forcing.



**Figure 7.3: Annual wave energy density from WIS Station 73040 from 1980-2019**

Figure 7.4 and Figure 7.5 show the evolution of the design profile under annual wave conditions in 2016 and 2017, respectively, as predicted by the XBeach and CSHORE models. Results shown in with a solid line include the offshore berm while the dashed-line results do not include the berm. The unnourished profile is shown for reference.

In the 2016 simulation, both XBeach and CSHORE predict erosion and steepening of the nourished beach slope. The eroded material is transported offshore to a depth of -6.5 to -19.5 ft NAVD88 (-2 to -5.9 m NAVD88). The XBeach model predicted more erosion and transported the eroded material farther offshore. In both models, the dune is stable and predicted profile changes with and without the offshore berm are identical, indicating that the offshore berm has little influence on beach stability. Slight erosion on the landward side and accretion on the seaward side of the offshore berm is predicted by XBeach, however the change in berm volume is negligible. CSHORE does not predict any movement of the berm.

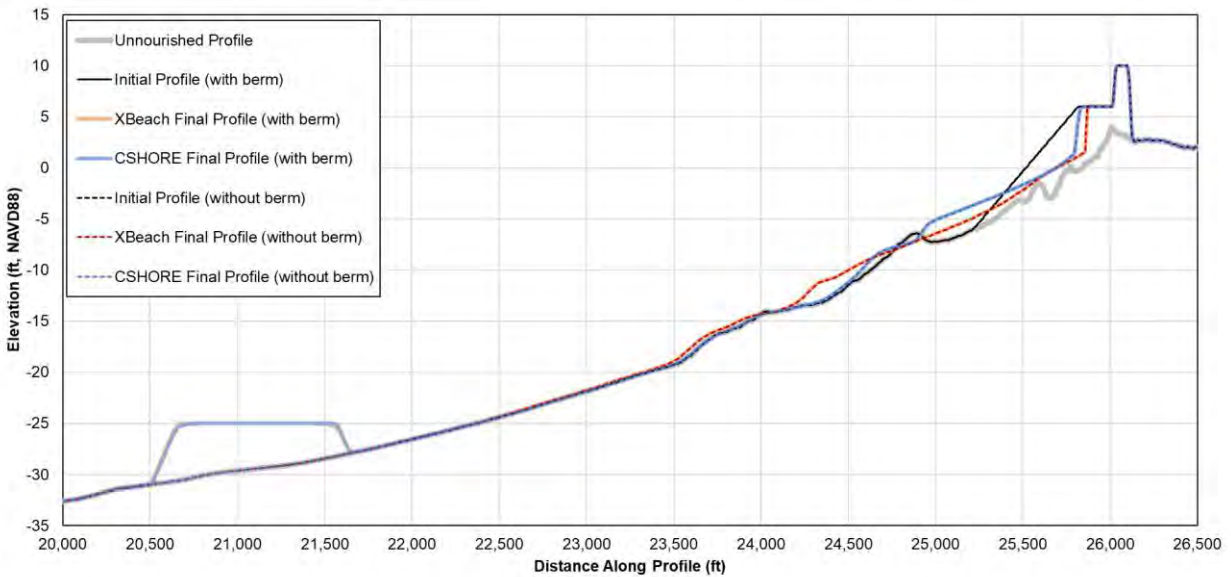


**Figure 7.4: Modeled profile response to 2016 wave conditions from WIS Station 73040**

In 2017, overtopping is predicted by XBeach as a result of Hurricane Harvey (August 2017) and the dune crest elevation is reduced approximately 1.5 ft (0.5 m). The corresponding over-washing deposits the sediment inshore behind the dune. CSHORE does not predict dune crest erosion and the results are similar to the 2016 predictions with a small increase in beach erosion. As in the 2016 simulation, the offshore berm is stable, and the presence of berm does not seem to improve the stability of the nourishment.

Using the USACE Sediment Mobility Tool (<https://navigation.usace.army.mil/SEM/SedimentMobility>), the mean depth of closure in the area was estimated to be 28 ft (8.5 m) with range of 19 to 48 ft (5.8 to 15 m), depending on the method of calculation. As the offshore berm is placed near the limit of the depth of closure or deeper, and as confirmed from the annual runs, it is unlikely that the offshore berm will move substantially at its designed placement depth. Both models predict little to no change in the profile beyond the -19.5 ft NAVD88 (-5.9 m NAVD88) contour.

As most of the beach nourishment is eroded and placed offshore between -6.5 to -19.5 m NAVD88 (-2 to -5.9 m NAVD88), it is expected that the material will move back onshore over time during favorable/accretional wave conditions (see next section). However, beach recovery processes are not well simulated by the XBeach and CSHORE models. To date, simulation of beach recovery has remained a challenge for all profile change models.

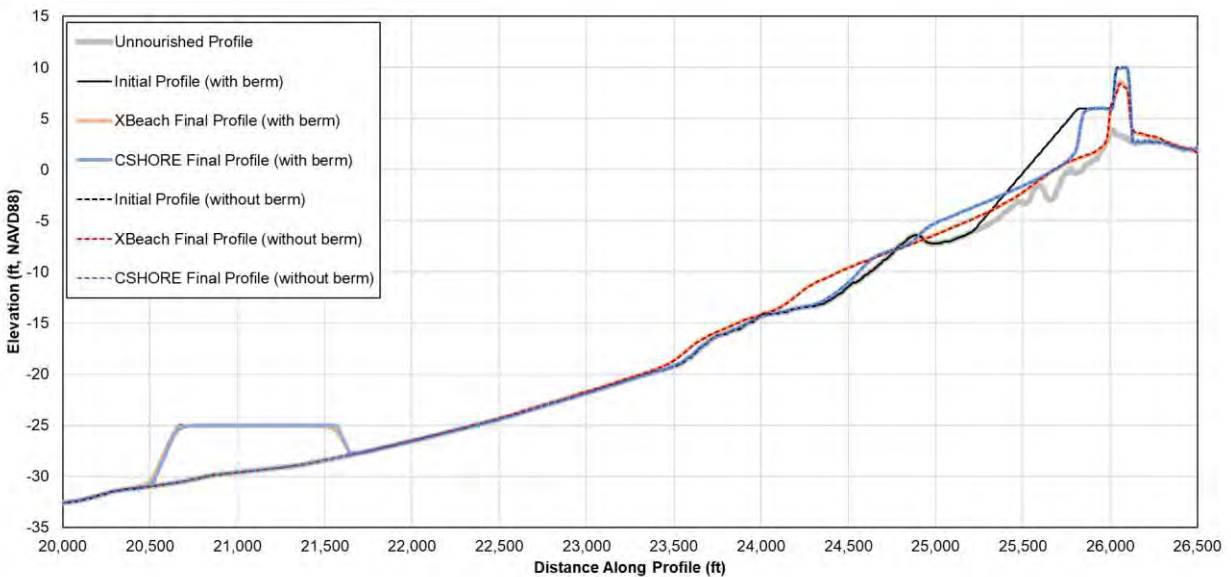


Figure 7.5: Modeled profile response to 2017 wave conditions from WIS Station 73040

### 7.3.2 Short-term Profile Response to Individual Storm Conditions

Table 7.1 summarizes the storms selected to assess the stability of the offshore berms and beach nourishment in response to hurricane events. Hurricane Allen and Hurricane Harvey were chosen as two historically significant storms. Hurricane Hanna and Delta were selected as two storms in recent history that are less extreme but feature characteristics such as higher water level (Hurricane Hanna) and long wave period (Hurricane Delta). Measured waves from the National Data Buoy Center (NDBC) Buoy 42020 were used that provides hourly data at depth of 276 ft (84 m). Compared to the hindcast waves, the buoy waves capture the peaks of the storms more accurately, therefore the buoy waves were used for the storm simulations. Water levels from Bob Hall Pier were used as hydrodynamic forcing for all storms except for Hurricane Allen as the Bob Hall Pier data starts in 1983. Water levels for Hurricane Allen were obtained from an ADCIRC model of Hurricane Allen (Legacy USACE Texas Study, Save Point 28) obtained from the Coastal Hazard System (<https://chs.ercd.dren.mil/Study>).

Table 7.1: Storm conditions for offshore berm and beach nourishment stability assessment

Storm	Simulation Period	Maximum Values during Storm		
		Peak Significant Wave Height ( $H_{m0}$ , ft)	Peak Wave Period ( $T_p$ , s)	Peak Water Level at Bob Hall Pier (ft, NAVD88)
Hurricane Allen	1980/8/8 0:00 to 1980/8/12 0:00	22.7	14.7	5.6**
Hurricane Harvey	2017/8/24 0:00 to 2017/8/26 12:00	24.1	13.8	3.9
Hurricane Hanna	2020/7/25 0:00 to 2020/7/27 0:00	22.8	10.8	6.4

Storm	Simulation Period	Maximum Values during Storm		
		Peak Significant Wave Height ( $H_{m0}$ , ft)	Peak Wave Period ( $T_p$ , s)	Peak Water Level at Bob Hall Pier (ft, NAVD88)
Hurricane Delta	2020/10/8 12:00 to 2020/10/10 12:00	15.1	14.8	3.8

\*\* Water levels for Hurricane Allen were obtained from an ADCIRC model of Hurricane Allen (Legacy USACE Texas Study, Save Point 28) obtained from the Coastal Hazard System

Figure 7.6 and Figure 7.7 show the evolution of the design profile during Hurricane Allen and Hurricane Harvey, respectively. These storms were particularly strong with large wave heights, periods, and long storm durations. In both storms, XBeach predicts overtopping and erosion of the entire dune, from 10 ft NAVD88 (3.1 m NAVD88) to an elevation of 1.5 ft NAVD88 (0.5 m NAVD88) after Hurricane Allen and 3 ft NAVD88 (0.9 m NAVD88) after Hurricane Harvey. In both simulations, the offshore berm was not impacted and is stable. In both cases, CSHORE does not predict significant dune erosion.

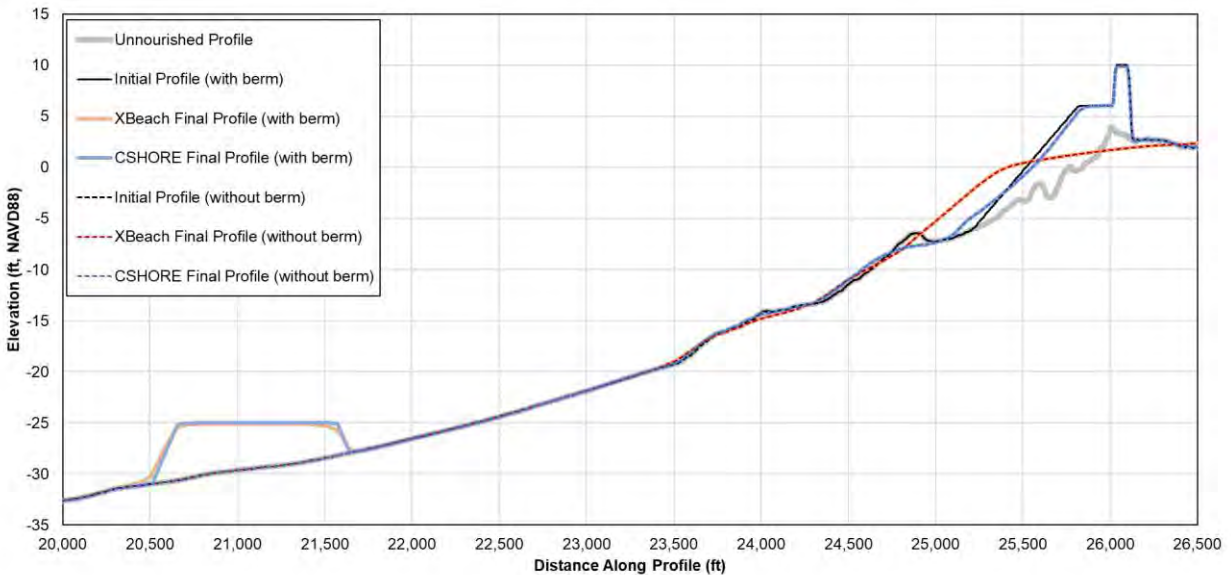
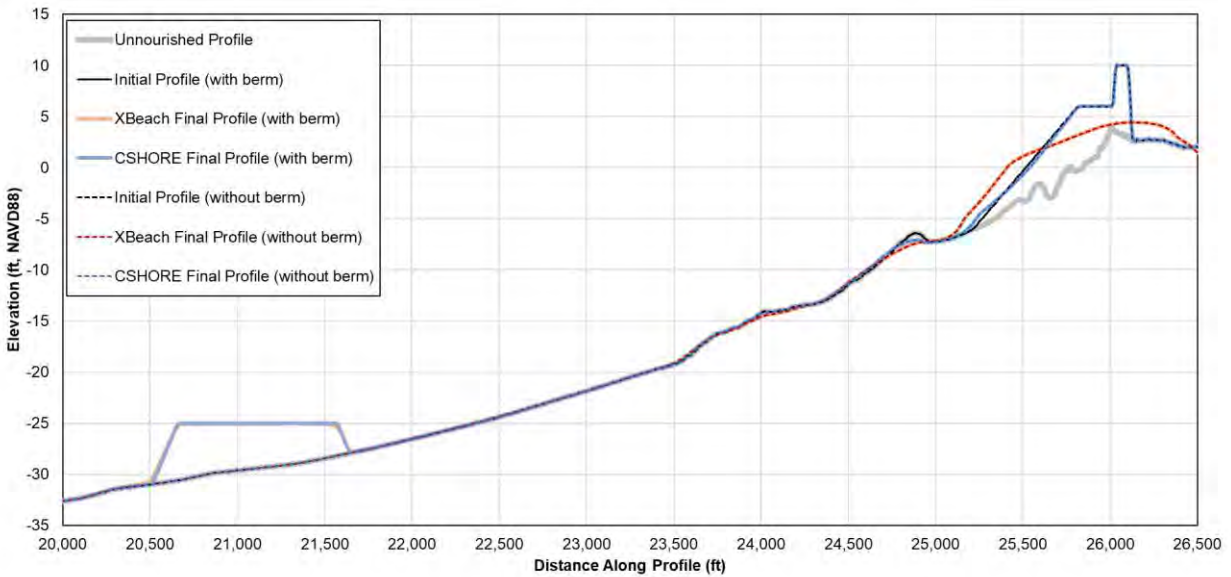


Figure 7.6: Modeled profile response to Hurricane Allen



**Figure 7.7: Modeled profile response to Hurricane Harvey**

To support the beach erosion predicted by XBeach during Hurricane Harvey, dune crest elevation was obtained across the transect shown in Figure 7.8 from a 2016 LiDAR survey (pre-Hurricane Harvey) and 2018 USACE LiDAR survey (post-Hurricane Harvey). The satellite image in Figure 7.8 (from July 6, 2020) and Figure 7.9 (from August 28, 2017) show post-Hurricane Harvey overwash fans behind the beach approximately 3 miles (5 km) northeast from Aransas Pass.

Figure 7.10 shows that pre-Hurricane Harvey, the dune crest was generally above 9 ft NAVD88 (2.7 m NAVD88), up to approximately 14 ft NAVD88 (4.3 m NAVD88). After Hurricane Harvey, breached areas have elevations as low as -3 ft NAVD88 (-0.9 m NAVD88). These surveyed elevations support predictions from XBeach during Hurricane Harvey where the dune crest elevation is lowered from 10 to 3 ft NAVD88 (3.1 to 0.9 m NAVD88). Both Figure 7.9 and Figure 7.10 indicate that the amount of erosion varied along the shoreline which can be influenced by the local profile morphology and particularly by the pre-hurricane dune crest elevation, presence of vegetation, and variations in beach sediment composition that were not included in the simulations.



Figure 7.8: Transect location (pink) across the dune crest (satellite image dated July 6, 2020)



Figure 7.9: Satellite image from August 28, 2017 (post-Hurricane Harvey) from Google Earth

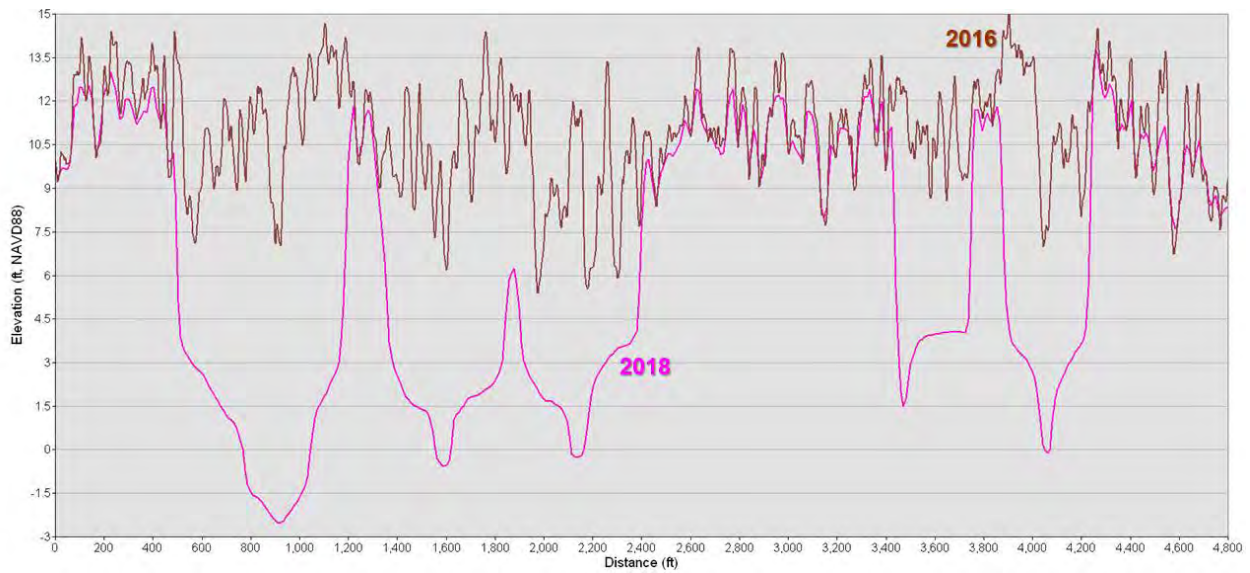


Figure 7.10: Pre- (2016) and post-Hurricane Harvey (2018) dune crest elevations

Figure 7.11 and Figure 7.12 show the evolution of the design profile during Hurricane Hanna and Hurricane Delta. These storms were not as strong as Hurricane Allen and Hurricane Harvey and had lower wave heights and/or periods. During Hurricane Hanna, XBeach predicts beach erosion with sediment moving to the lower part of the beach between 0 to -6.5 ft NAVD88 (0 to -2 m NAVD88). CSHORE does not predict significant erosion during Hurricane Hanna. Both models predict that the offshore berm is stable and unimpacted during the storm and that the berm does not improve beach stability.

During Hurricane Delta, a difference is observed in the XBeach predicted profiles with and without the offshore berm. The berm provides protection to the beach under the waves with long periods and relatively low surge. Waves with longer wave periods have a deeper wave base (maximum depth at which a wave causes significant water motion) and can be impacted by morphological features in deeper water, like the offshore berm. In larger storm events with long wave periods like Hurricane Allen, the waves and surge are large enough that the presence of the berm is not significant. Neither CSHORE nor XBeach predict any significant change in the offshore berm morphology.

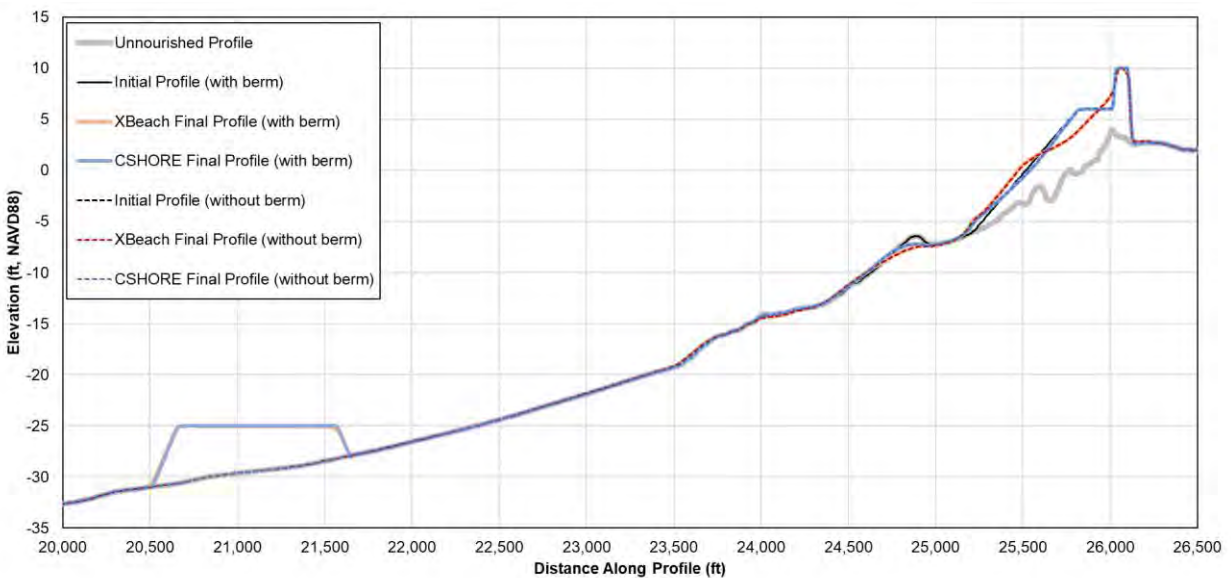


Figure 7.11: Modeled profile response to Hurricane Hanna

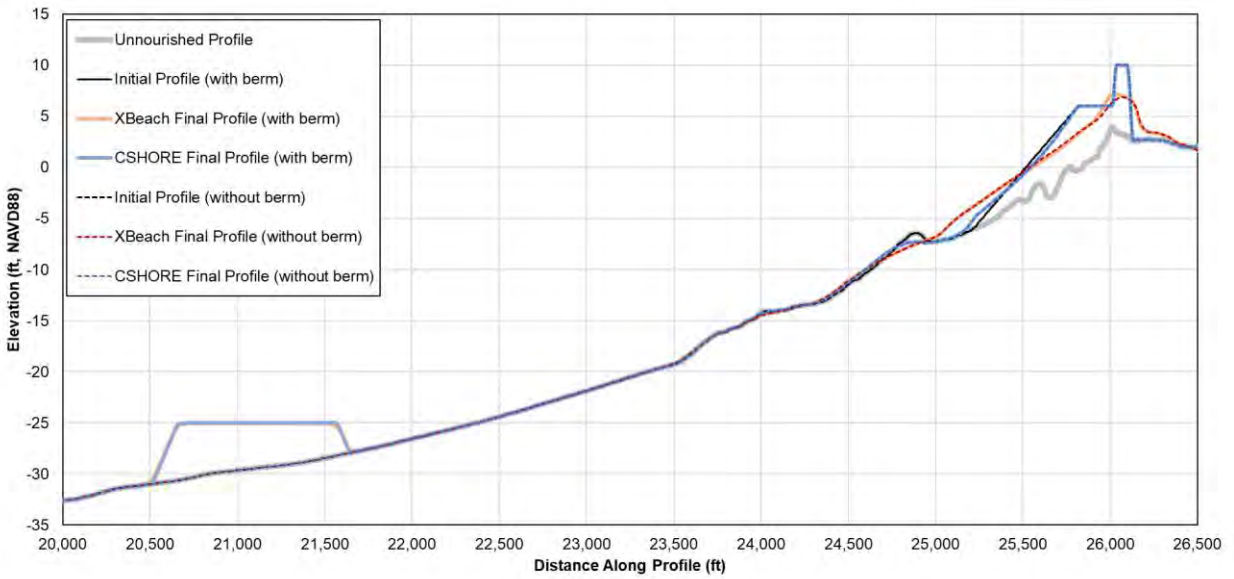


Figure 7.12: Modeled profile response to Hurricane Delta

## 8. Fate of Beach Nourishment

---

The fate of the placed beach nourishment was assessed using a sediment budget model developed by Baird. Cross-shore and longshore transport processes were incorporated in the model using XBeach (cross-shore) and Baird's COSMOS model (longshore) (Southgate and Nairn, 1993; Nairn and Southgate, 1993). The potential channel infilling volumes and the stability of the offshore berms were also assessed. The development of the model, calibration, and results are discussed in the follow section.

### 8.1 Development and Setup of the Sediment Budget Model

#### 8.1.1 Representative Profiles and Model Domain

Four representative profiles are used to represent the model domain:

- Nourished profile with offshore berm
- Unnourished profile with offshore berm
- Nourished profile without offshore berm
- Unnourished profile without offshore berm (existing profile)

While the actual profiles along the domain can vary (i.e., between areas with and without offshore berms), these four profiles are used in combinations to approximate defining features of each area of the model domain. These approximations allow the sediment budget model to execute quickly as cross-shore and longshore transport rates are pre-computed for four profiles only. Figure 8.1 shows the cross-shore calculation grid for the sediment budget model. The cross-shore cells are numbered from 1 to 6 starting from the offshore moving onshore:

1. Offshore portion of the profile extending from the -65 ft NAVD88 (-20 m NAVD88) contour to approximately -35 ft NAVD88 (-11 m NAVD88); this area is assumed to be beyond the depth of closure and has minimal changes in elevation over time
2. Offshore area between -35 and -25 ft NAVD88 (-11 and -7.6 m NAVD88) where the offshore berm may be placed in profiles where the offshore berm exists
3. Nearshore area between -25 and -15 ft NAVD88 (-7.6 and -4.6 m NAVD88)
4. Nearshore area between -15 and -7 ft NAVD88 (-4.6 and -2.1 m NAVD88), toe of beach nourishment in profiles where beach nourishment exists
5. Beach area from -7 ft NAVD88 (-2.1 m NAVD88), toe of beach nourishment in profiles where beach nourishment exists to the backside of the dune
6. Backdune area where overwashed sediment may be deposited

A median ( $D_{50}$ ) sediment size of 0.14 mm was used in the model for both existing and placed sediment.

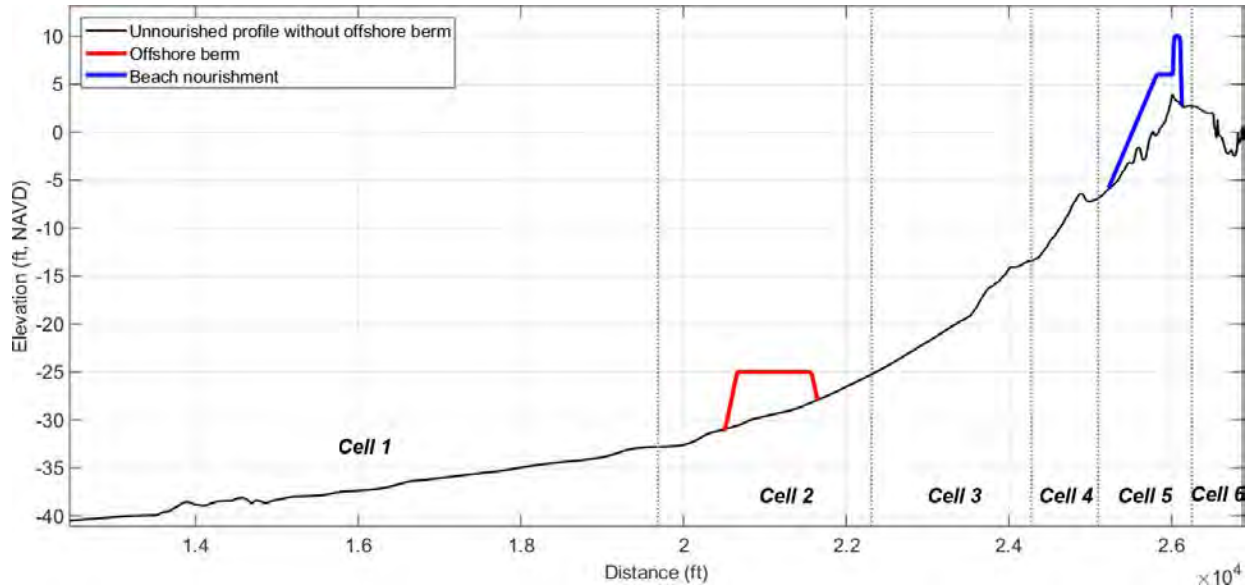


**Figure 8.1: Cross-shore sections of the representative beach profile; profile with beach nourishment and offshore berm shown**

In the alongshore direction, the sediment budget model is comprised of two separate domains: the Mustang Island domain extending 11 miles (18 km) southwest from the Aransas Pass south jetty and the San Jose Island domain which extends nine miles (15 km) northeast of the north jetty, as shown in Figure 8.2. The Mustang Island domain is comprised of 29 cells in the alongshore and six (as described above) cells in the cross-shore direction. The San Jose Island domain is comprised of 26 cells in the alongshore direction and 6 cells in the cross-shore direction.

For this modeling assessment, it is assumed that there is no exchange of sediment between the two model domains. In other words, the sediment budget model does not allow sediment to pass through the north boundary on the Mustang Island domain to the south boundary on the San Jose Island domain (i.e., boundaries adjacent to the navigation channel). Because of this assumption, the sediment volume accumulating in the first cells (offshore cell) along the north and south boundary of the Mustang Island and San Jose Island domain, respectively, are assumed to be trapped by the navigation channel. This assumption is consistent with a deep navigation channel and the corresponding predicted volume roughly represents the potential channel infilling volume under FWP conditions. However, this process was more accurately modeled by the assessment of channel sedimentation which was discussed in Section 6.2.

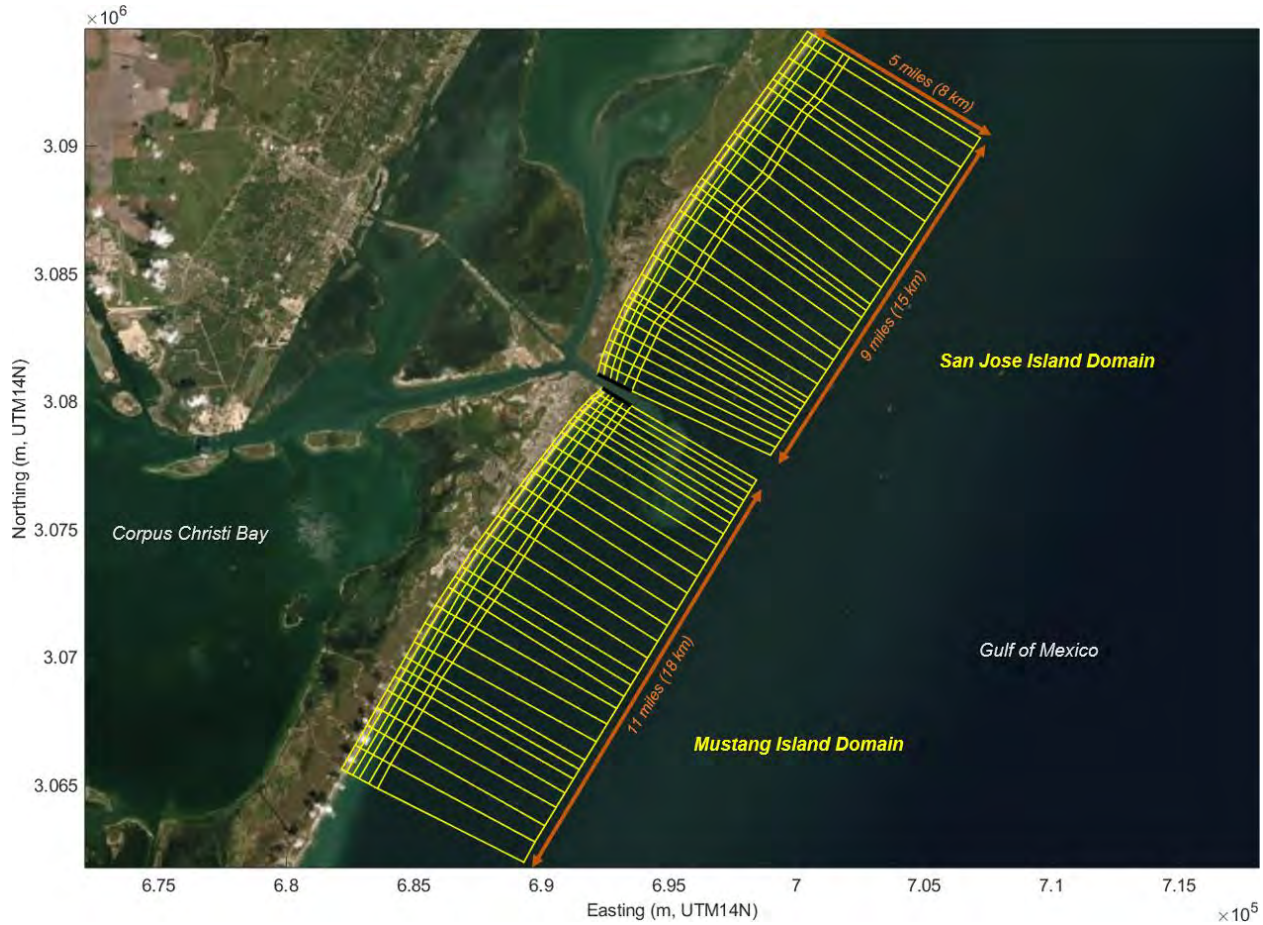


**Figure 8.2: Sediment budget model domains**

### 8.1.2 Model Equations

The sediment budget model sign convention for sediment transport is positive for northeastward transport and negative for southwestward transport. The variables  $i$  and  $j$  specify the cell numbering in the alongshore direction (from west to east) and cross-shore direction (offshore to onshore), respectively. The timestep,  $t$ , is measured in hours. The cell volumes, in cubic yards, are in reference to the unnourished profile (i.e., existing conditions). For example, beach nourishment is specified by a positive cell volume and may decrease over time, indicating gradual erosion (loss of the nourishment volume). The cell volume can become negative, indicating that the cell has lost all the initial nourishment volume and is now eroding sediment on the existing beach. The sediment budget model runs in MATLAB.

The sediment model calculations follow the sequence of time steps in the input wave time series from WIS Station 73040. At each timestep, the cell volume,  $V(t)_{ij}$ , is calculated based on changes due to cross-shore transport,  $C(t)_{ij}$ , and longshore sediment transport gradient,  $\Delta L(t)_{ij}$ :

$$V(t)_{ij} = V(t - 1)_{ij} + C(t)_{ij} - \Delta L(t)_{ij}$$

Note that  $V(0)_{ij}$  is equal to the initial beach volume.

The volume change due to cross-shore transport,  $C(t)_{ij}$ , is obtained for the wave condition at each timestep using the matrix of XBeach profile model results through an interpolation function or through the onshore transport algorithm, as described in Section 8.1.3, for each of the four representative profiles. This rate is then weighted based on the portion of sediment available in Cell 5 (on the beach) in the previous timestep,  $P(t)_i$ :

$$P(t)_i = V(t-1)_{i5} / V_{i5}^{max} \text{ when } V(t-1)_{i5} \geq 0$$

$$P(t)_i = V(t-1)_{i5} / V_{i5}^{min} \text{ when } V(t-1)_{i5} < 0$$

When  $V(t-1)_{i5}$  is positive,  $P(t)_i$  represents volume in the cell divided by the fully nourished cell volume,  $V_{i5}^{max}$ , and the  $C(t)_{ij}$  is calculated by:

$$C(t)_{ij} = w_{ij} \times CSF \times [(1 - P(t)_i) \times C(t)_{ij}^u + P(t)_i \times C(t)_{ij}^n]$$

Where  $CSF$  is the cross-shore scaling factor,  $C(t)_{ij}^u$  is the volume change for the unnourished profile (yd<sup>3</sup>/ft),  $C(t)_{ij}^n$  is the volume change for the nourished profile (yd<sup>3</sup>/ft),  $w_{ij}$  is the cell width (ft, alongshore). Depending on the features of the profile, the values of  $C(t)_{ij}^u$  and  $C(t)_{ij}^n$  may be for the profile with or without an offshore berm.

When  $V(t-1)_{i5}$  is negative,  $P(t)_i$  represents volume in the cell divided by the minimum cell volume (negative),  $V_{i5}^{min}$ , and  $C(t)_{ij}$  is calculated by:

$$C(t)_{ij} = w_{ij} \times CSF \times [(1 - P(t)_i) \times C(t)_{ij}^u]$$

In this situation, it is assumed that a cell without any volume to erode has a volume change of 0.

The longshore sand transport gradient,  $\Delta L(t)_{ij}$ , at each timestep is calculated in a similar way to the cross-shore transport. The longshore transport rate,  $L(t)_{ij}$ , is obtained for the wave condition at each timestep using the matrix of COSMOS longshore transport model results through an interpolation function, as described in Section 8.1.4, for each of the four representative profiles:

$$L(t)_{ij} = LSF(t)_{ij} \times [(1 - P(t)_i) \times L(t)_{ij}^u + P(t)_i \times L(t)_{ij}^n]$$

Where  $LSF(t)_{ij}$  is the longshore scaling factor,  $L(t)_{ij}^u$  is the longshore transport rate for the unnourished profile (m<sup>3</sup>), and  $L(t)_{ij}^n$  is the volume change for the nourished profile (m<sup>3</sup>). Depending on the features of the profile, the values of  $L(t)_{ij}^u$  and  $L(t)_{ij}^n$  may be for the profile with or without an offshore berm.

The average longshore transport of adjacent cells is calculated to estimate the transport at each cell boundary. The gradient in longshore transport is calculated by subtracting the east boundary from the west boundary, therefore a positive gradient indicates that the cell is losing volume (eroding) and negative number means the cell is gaining volume (accreting):

$$\Delta L(t)_{ij} = \left[ \left( \frac{L(t)_{i+1j} + L(t)_{ij}}{2} \right) - \left( \frac{L(t)_{ij} + L(t)_{i-1j}}{2} \right) \right]$$

At the jetty boundary, the longshore transport rate is set to 0 to not allow sediment to pass through and for a fillet beach to develop. For a jetty on the east side of a cell (Mustang Island):

$$\Delta L(t)_{ij} = \left[ 0 - \left( \frac{L(t)_{ij} + L(t)_{i-1j}}{2} \right) \right]$$

For a jetty on the west side of a cell (San Jose Island):

$$\Delta L(t)_{ij} = \left[ \left( \frac{L(t)_{i+1j} + L(t)_{ij}}{2} \right) - 0 \right]$$

At the west boundary in the Mustang Island domain, the longshore transport west of the first cell,  $L(t)_{i-1j}$ , is equal to the first cell,  $L(t)_{ij}$ :

$$\Delta L(t)_{ij} = \left[ \left( \frac{L(t)_{i+1j} + L(t)_{ij}}{2} \right) - L(t)_{ij} \right]$$

Similarly, in the San Jose Island domain at the east boundary,  $L(t)_{i+1j} = L(t)_{ij}$ :

$$\Delta L(t)_{ij} = \left[ L(t)_{ij} - \left( \frac{L(t)_{ij} + L(t)_{i-1j}}{2} \right) \right]$$

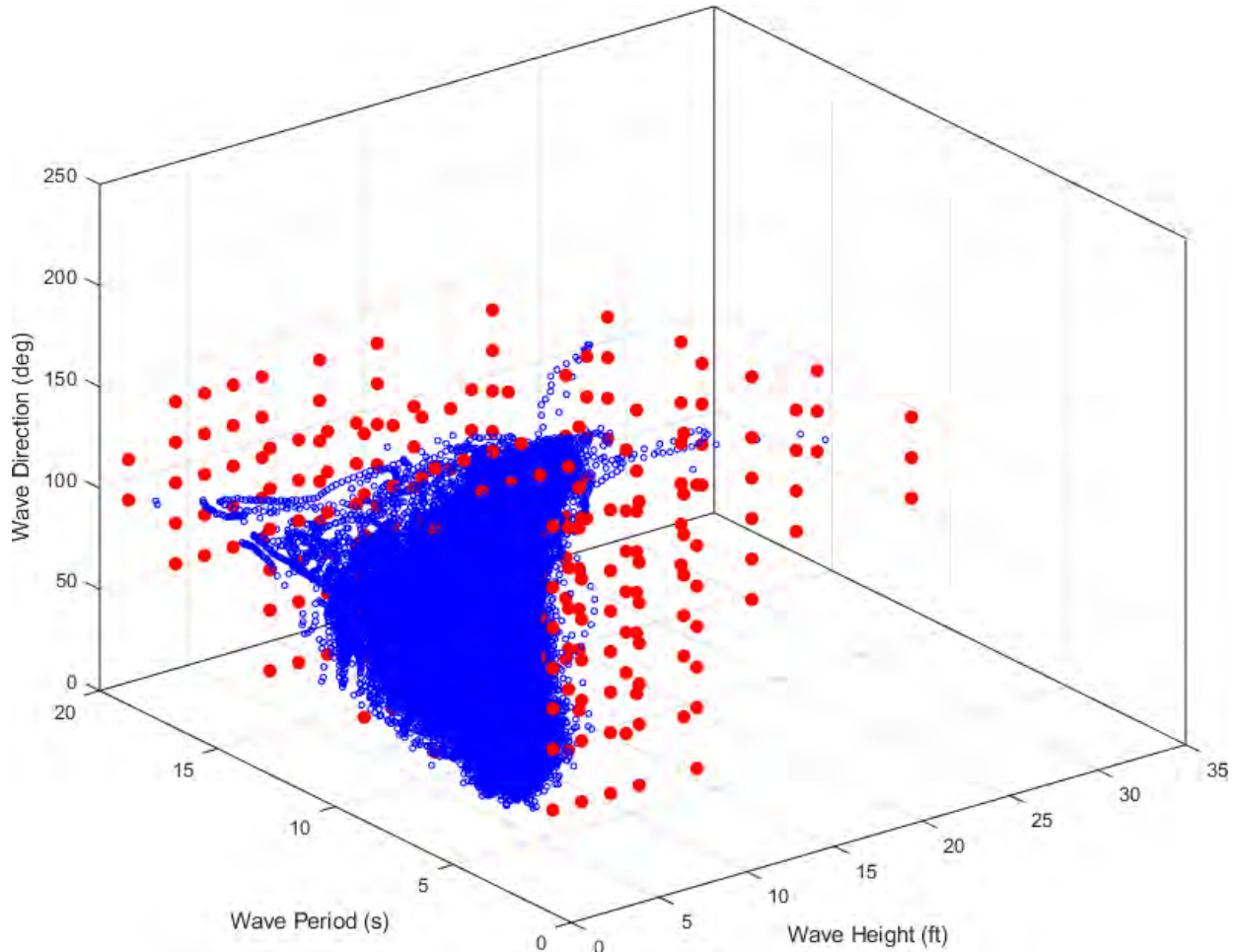
Maximum and minimum cell volumes are also specified in the sediment budget model. Minimum volumes prevent erosion of the profile beyond the historic low elevation (approximately 3 ft NAVD88 or 0.9 m NAVD88 based on dune crest surveys post Hurricane Harvey) while maximum volumes are set to prevent excessive accretion in cells. For example, in the cells adjacent to the jetties, when the maximum volume is reached, the excess material will move offshore until the maximums are no longer exceeded. This process simulates the process in which the sediment will move offshore along the jetty by rip currents.

### 8.1.3 Cross Shore Transport

#### 8.1.3.1 Beach Erosion (Offshore Transport)

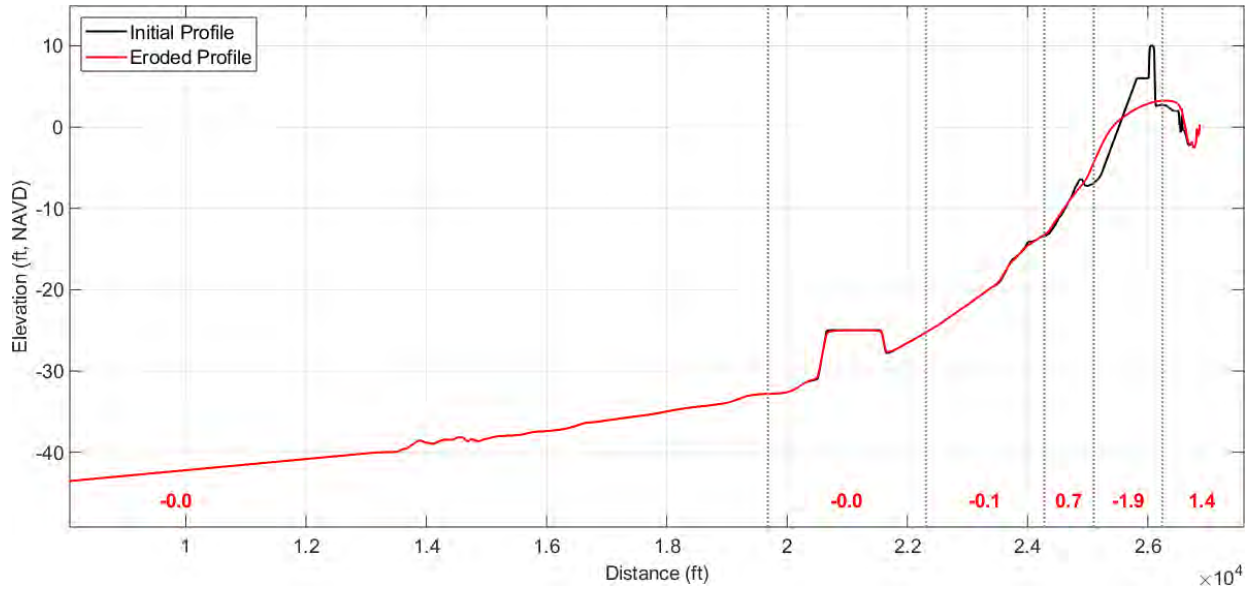
The XBeach model, introduced in Section 0, was used to determine the cross-shore volume change for each representative profile due to erosion. The 1D cross-shore model returns the profile change corresponding to a wave (wave height, period, and direction) and water level condition.

In total, 269 wave conditions (nine wave heights, seven wave periods, and seven wave directions) with three water levels were simulated for the four representative profiles resulting in a total of  $269 \times 3 \times 4 = 3,228$  individual XBeach model runs. Figure 8.3 shows the 269 wave conditions each represented by the red points. The blue points represent all wave conditions measured at WIS Station 73040 from 1980 to 2019. The red points form a matrix of conditions from which any wave condition can be interpolated. The XBeach model results were post-processed to determine an erosion/accretion rate ( $\text{yd}^3/\text{ft}/\text{hr}$ ) for each of the 6 profile cells and saved to a MATLAB MAT-file. The resulting matrix of XBeach results is interpolated to find the corresponding erosion/accretion volume for each time step in the simulation period wave and water level timeseries.



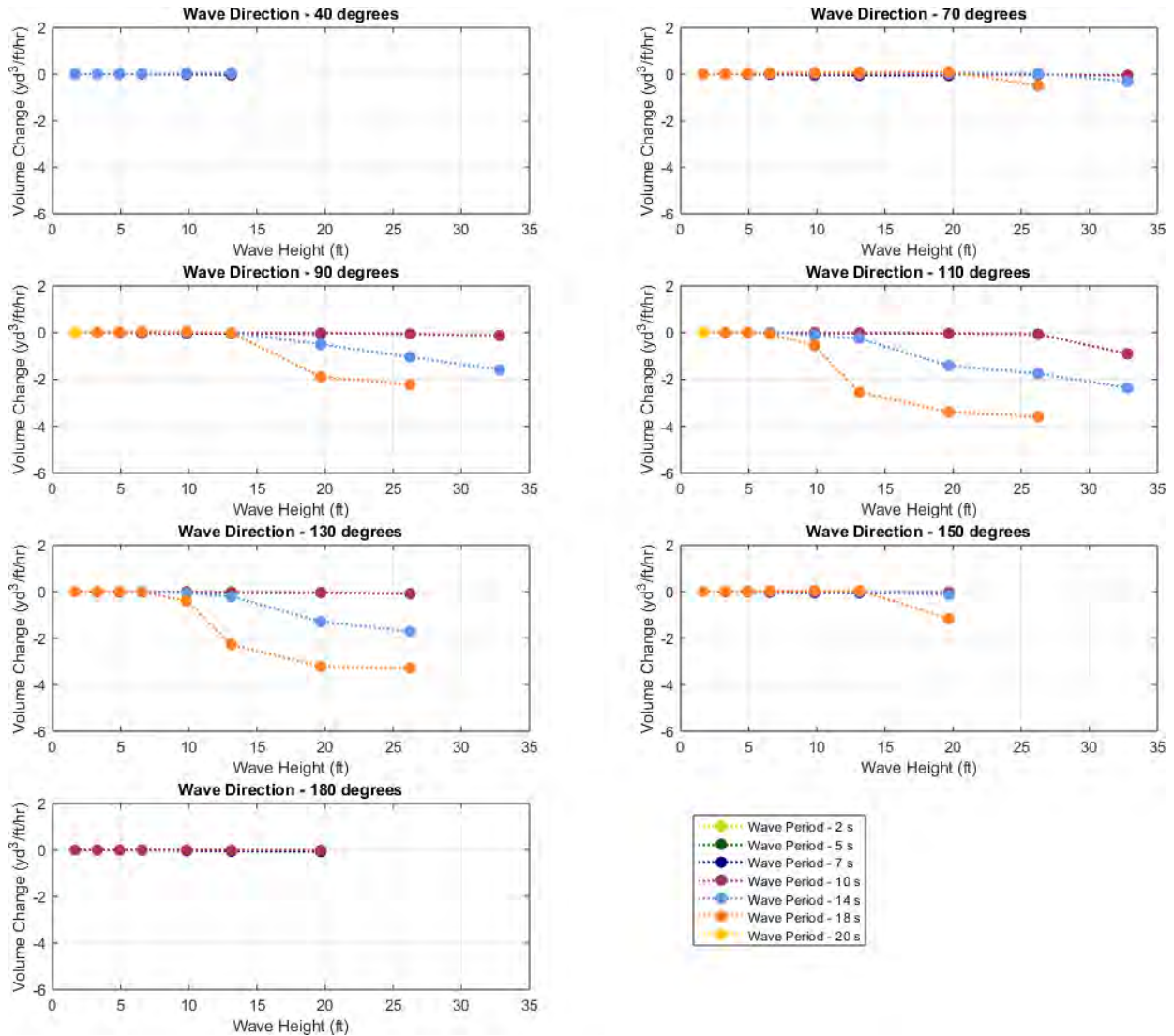
**Figure 8.3: Matrix of XBeach wave conditions (red points) and all wave conditions measured at WIS Station 73040 from 1980 to 2019 (blue points)**

Figure 8.4 shows an example of the summarized data from a single XBeach run {3.2 ft NAVD88 (1 m NAVD88) water level, 26.2 ft (8 m) wave height, 10 s wave period, 90-degree wave direction}. The results show a loss of 1.9 yd<sup>3</sup>/ft/hr (4.7 m<sup>3</sup>/m/hr) over the beach nourishment cell (Cell 5) after one hour of the above wave attack. The sediment lost from the nourishment area is deposited in the backdune (Cell 6; 1.4 yd<sup>3</sup>/ft/hr or 3.4 m<sup>3</sup>/m/hr) and moved offshore to Cell 4 (0.7 yd<sup>3</sup>/ft/hr or 1.7 m<sup>3</sup>/m/hr). Minor erosion is predicted for Cell 2 and 3. No changes are predicted for the offshore cell (Cell 1).



**Figure 8.4: Example of XBeach results for one wave condition {3.2 ft NAVD88 (1 m NAVD88) water level, 26.2 ft (8 m) wave height, 10 s wave period, 90-degree wave direction} and summarized cross-shore volume change rates (in yd<sup>3</sup>/ft/hr)**

Figure 8.5 summarizes the cross-shore volume change rates for all wave conditions at Cell 5 (nourished beach) with a water level of 3.2 ft NAVD88 (1 m NAVD88). The figure shows that little to no cross-shore change is predicted over the beach when wave direction is less than 40 degrees or larger than 180 degrees. When waves approach the shore more directly in the 110 and 130-degree wave conditions, greater wave heights and longer periods result in more erosion, up to approximately 4 yd<sup>3</sup>/ft/hr (9 m<sup>3</sup>/m/hr).



**Figure 8.5: Summary of cross-shore volume change over Cell 5 (nourished beach with offshore berm) under all wave conditions with a water level of 3.2 ft NAVD88 (1 m NAVD88)**

### 8.1.3.2 Beach Recovery (Onshore Transport)

As mentioned in Section 7.3.1, the XBeach model does not simulate onshore sediment movement and the corresponding beach recovery. Onshore sediment movement typically occurs when waves have relatively smaller heights and longer wave periods (or wave lengths). These waves are gently sloped and tend to deposit sediment on the beach. Sunamura and Horikawa (1974) developed the criterion,  $C_s$ , as a function of wave steepness, beach slope, and sediment size to determine if the beach will erode or accrete under a particular wave condition:

$$C_s = (H_0/L_0)(\tan\beta)^{0.27}(L_0/d)^{0.67}$$

where  $H_0$  is the deepwater wave height,  $L_0$  is the deepwater wavelength,  $\tan\beta$  is the bottom slope, and  $d$  is the sediment grain size.

When  $C_s$  is less than the critical  $C_s$  value ( $C_{s_{crit}}$ ), the beach is likely to accrete (onshore movement). The value of  $C_{s_{crit}}$  is approximately 18 for natural beaches but can vary for different beach environments. In the present sediment budget model, the value of  $C_{s_{crit}}$  is used as a calibration factor.

The model calculates the  $C_s$  value for each timestep. If the  $C_s$  value is greater than the critical value, the cross-shore volume changes predicted by XBeach (previous section) is used. If the  $C_s$  value is less than the critical value and the wave height is greater than a certain threshold (to limit movement during very calm periods), onshore movement is allowed. Onshore movement is applied by removing a portion of the accumulated sediment in Cell 2 and 3 ( $V_o$ ) and distributing the sediment back to Cells 4 and 5. The portion that is removed and the subsequent redistribution is tuned during calibration. A schematic of the application of onshore movement process is shown in Figure 8.6.

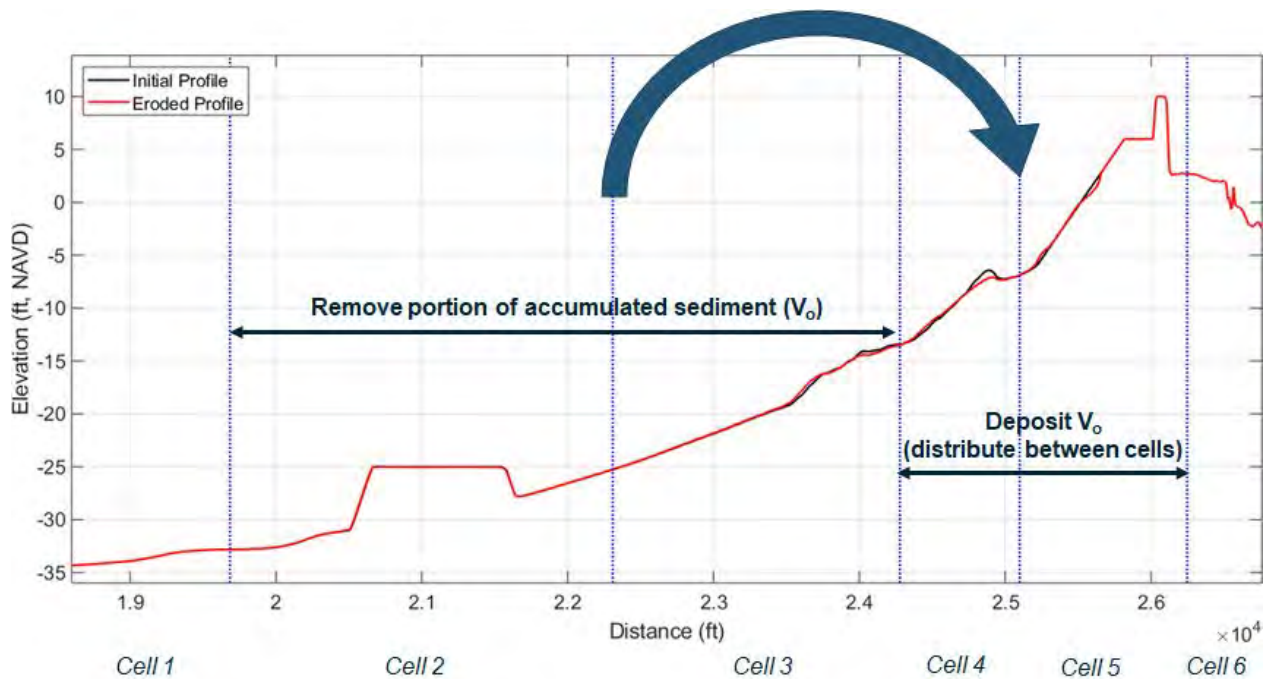


**Figure 8.6: Schematic of onshore sediment movement process applied in the sediment budget model**

### 8.1.4 Longshore Transport

Longshore transport gradient is defined as variation in longshore transport rate in the alongshore direction that can create a positive or negative imbalance in the sediment budget resulting in accretion or erosion, respectively. Longshore transport rates are determined using the COSMOS model. COSMOS is a processes-based numerical model that estimates wave transformation, wave-induced currents, and sediment transport across a user-specified nearshore profile. The model can be run for a single wave and water level condition or for a long sequence of wave and water level conditions at specified time increments. COSMOS has been extensively used and verified by Baird in numerous projects around the world.

Figure 8.7 shows the potential longshore transport rates for a nourished profile with offshore berm from 1980 to 2019 using waves from WIS Station 73040. Positive numbers indicate transport towards the northeast. Over the 40-year period, the net transport is towards the northeast on average. Years where the transport is towards the southwest coincide with significant hurricanes where the counterclockwise winds generate easterly

waves that move nearshore sediment towards the west. Significant hurricanes included in this 40-year period are Hurricane Allen (1980), Hurricane Gilbert (1988), Hurricane Katrina (2005), Hurricane Ike (2008), and Hurricane Harvey (2017).

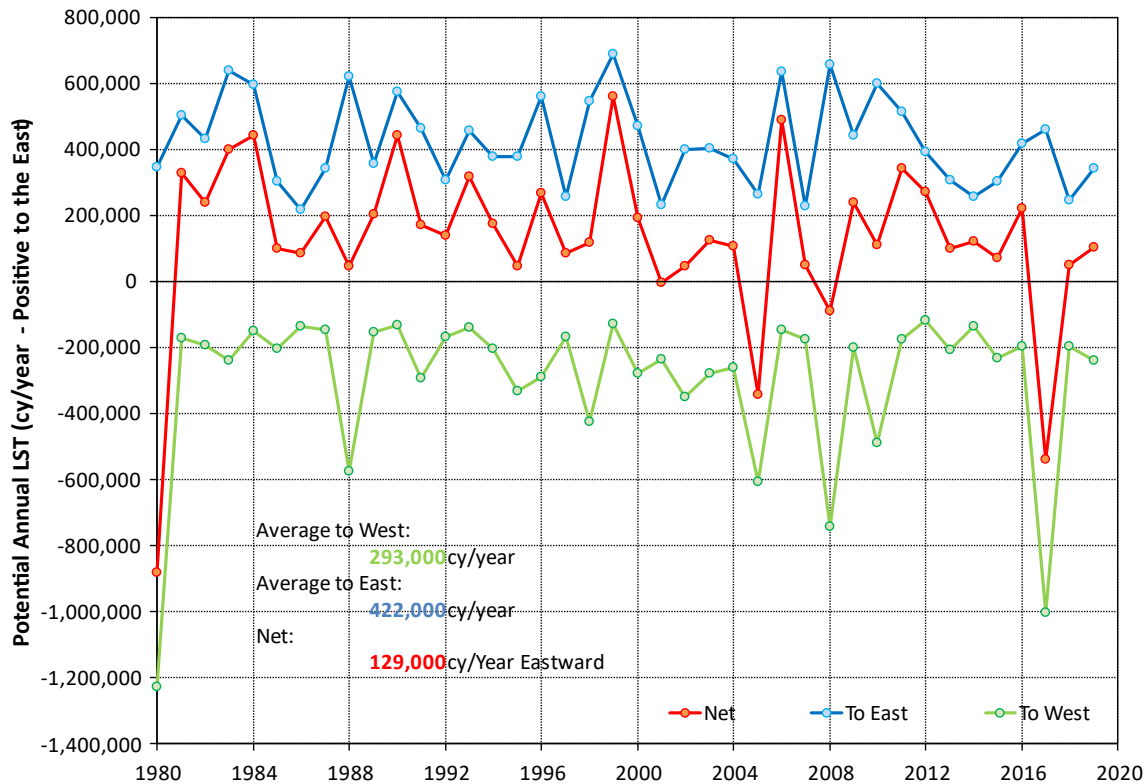


**Figure 8.7: Potential annual longshore transport rates from 1980 to 2019 for a nourished profile with offshore berm**

Similar to the cross-shore volume change modeling completed with the XBeach model, a total of 269 wave conditions (nine wave heights, seven wave periods, and seven wave directions) with three water levels were run for the four representative profiles in COSMOS (3,228 individual model runs). The COSMOS model results were post-processed to determine a longshore transport rate (yd<sup>3</sup>/hr) for each of the 6 profile cells. The matrix of COSMOS results is interpolated to find the corresponding longshore transport rate at each time step in the input wave and water level timeseries. Alongshore transport rates are highest in the nearshore area between the -20 and -5 ft NAVD88 (-6 and -2 m NAVD88) contours (Cells 3 and 4) and decrease towards the onshore and offshore directions.

Figure 8.8 summarizes the longshore transport rates for all wave conditions at Cell 5 (nourished beach) with a water level of 3.2 ft NAVD88 (1 m NAVD88). The figure shows that longshore transport is towards the west (negative) when wave directions are less than 110 degrees. Longshore transport rates are higher when wave heights are greater and wave periods are longer.

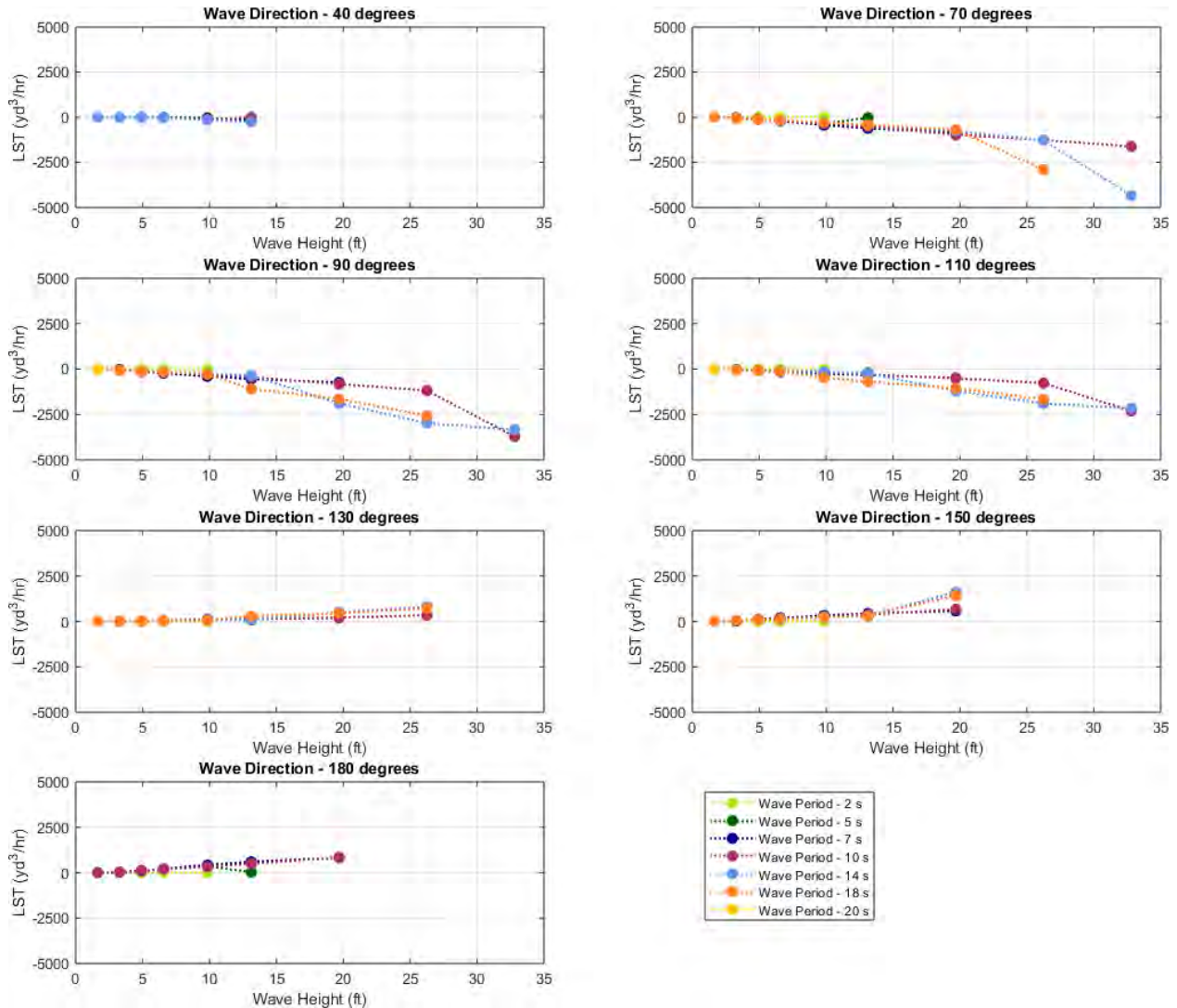


**Figure 8.8: Summary of potential longshore transport rates at Cell 5 (nourished beach with offshore berm) under all wave conditions with a water level of 3.2 ft NAVD88 (1 m NAVD88)**

### 8.1.5 Scaling Factors

A cross shore scaling factor (*CSF*) can be specified in the sediment budget model as a calibration parameter. The cross-shore factor is constant throughout the domain and does not change over time.

The long shore scaling factor (abbreviated as LSF;  $LSF(t)_{ij}$  in model equations) varies with time and space, depending on the wave condition. Figure 8.9 shows the distribution of LSF for an eastward wave. As the wave approaches the north jetty, the wave diffracts around the tip, creating a counterclockwise circulation that moves sediment towards the west. This is reflected in the LSF distribution where the LSF is negative and small (approximately -0.05) in the shadow zone of the north jetty. The negative LSF, multiplied by the positive longshore transport rate (as overall transport is towards the east), changes the transport direction to

negative/westward to capture littoral processes behind the north jetty. The more oblique the wave, the larger the shadow zone.

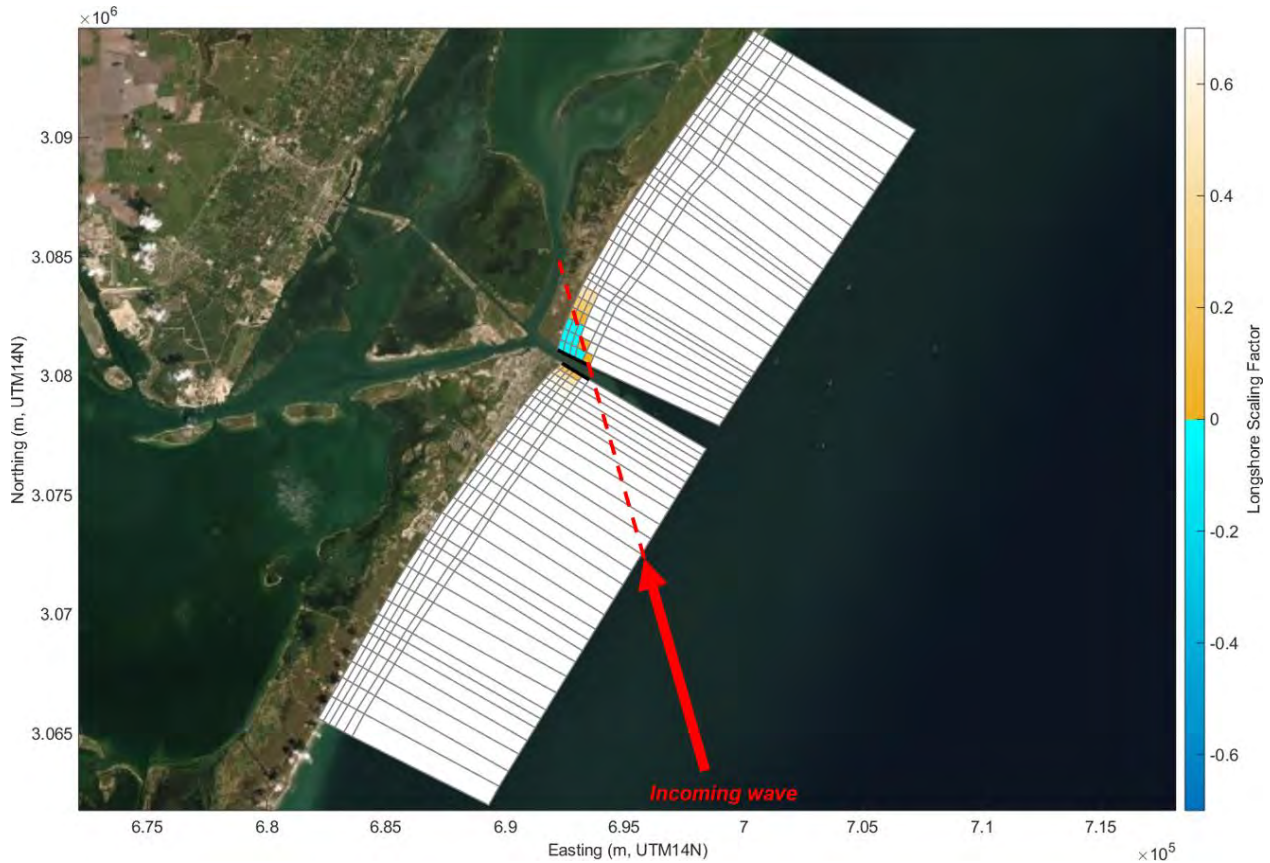


**Figure 8.9: Longshore scaling factors for incoming wave from the south (164 degrees from north)**

## 8.2 Model Calibration

The shoreline along the Mustang Island and San Jose Island domains are relatively stable. The shoreline change analysis from the University of Texas at Austin Bureau of Economic Geology estimated  $\pm 2$  ft/yr ( $\pm 0.6$  m/yr) of shoreline change from 1950-2019 (Paine et al., 2021).

Because of the lack of definitive accretion/erosion trends to calibrate the model against, the objective of the sediment budget model calibration was to simulate a long-term FWOP (unnourished, no offshore berms) scenario that would produce relatively small changes along the shoreline cells. Calibration of the model primarily focused on the San Jose Island domain and the calibrated parameters were extended to the Mustang Island domain for validation. The 1992-2002 period was chosen for calibration as it is a calmer period with no major hurricanes with an overall net easterly alongshore transport.

Figure 8.10 shows the sediment budget model results for the calibration period. The colored cells in the figure show the change in sediment thickness relative to the initial FWOP seabed elevation at the end of the modeling period. To create the plot, the cell volume is divided by the cell area to represent average thickness. Cells with warm colors (positive thickness) represent volume gain above the FWOP elevation. Cool colors (negative thickness) indicates that volume has been lost/eroded below the FWOP seabed elevation. The

figure is intended to visualize the trends in the domain only and the value of the thickness should not be taken literally.

Figure 8.10 shows that erosion generally occurs on the beach and in the nearshore area while sediment is overwashed to the back dune area. Cells along the shoreline (Cell 5) generally lose 1 yd<sup>3</sup>/ft/yr (3 m<sup>3</sup>/m/yr). This loss rate corresponds to a lateral shift of approximately 1 ft/year of the FWOP profile, measured between the depth of closure and the top of the dune, which is within the range reported by Paine et al., 2021. Most of the lost sediment is redistributed across the domain through overwashing to the back dune area and also moved offshore. Sediment that is moved offshore may be transported to the channel area, where it is assumed to be trapped by the deep navigation channel.

In the Mustang Island domain, 267k yd<sup>3</sup>/yr (204 m<sup>3</sup>/yr) enters (i.e., moves eastward to) the domain from the west boundary and 155k yd<sup>3</sup>/yr (119 m<sup>3</sup>/yr) exits (i.e., moves westward out of the domain) for a net exchange of 112k yd<sup>3</sup>/yr (86 m<sup>3</sup>/yr) to the east (into the domain). The volume exiting the domain on the east boundary (potential channel infilling) is 165k yd<sup>3</sup>/yr (126 m<sup>3</sup>/yr). The total volume change in the domain is 53k yd<sup>3</sup>/yr (41 m<sup>3</sup>/yr) representing net erosion. Similarly, on San Jose Island, the sediment budget is balanced: 52k yd<sup>3</sup>/yr (40 m<sup>3</sup>/yr) leaves the domain from the east boundary while 25k yd<sup>3</sup>/yr (19 m<sup>3</sup>/yr) leaves the domain from the west boundary and is balanced by 77k yd<sup>3</sup>/yr (59 m<sup>3</sup>/yr) of net erosion within the domain. As the net longshore transport is towards the east during the calibration period, potential channel infilling volumes are greater from the Mustang Island domain. The predicted total potential channel infilling volume from both domains is 190k yd<sup>3</sup>/yr (146 m<sup>3</sup>/yr).

Table 8.1 summarizes final parameters and values used for the calibrated sediment budget model.

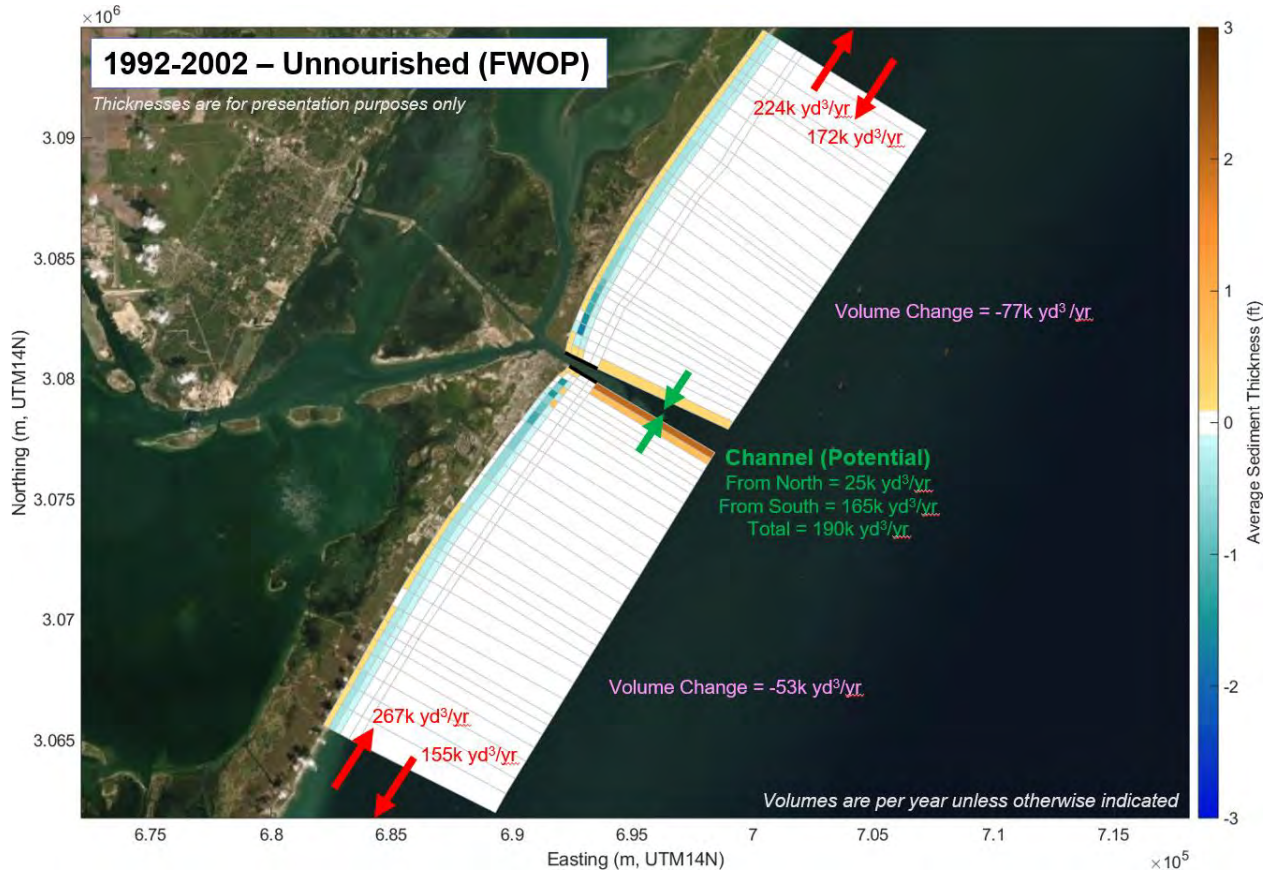


Figure 8.10: Sediment budget model results for the 1992-2002 calibration period (FWOP, average thicknesses shown are for presentation purposes only and should not be taken literally)

Table 8.1: Sediment budget model parameters

Parameter	Value
CSF	0.5
LSF (max)	0.7
$C_{scrit}$	40
Minimum wave height threshold for onshore movement	0.8 ft (0.25 m)
Accumulated sediment relocated during onshore transport	2.5%
Distribution of placed sediment during onshore transport	25% in Cell 4 and 75% in Cell 5

### 8.3 Beach Nourishment Assessment Runs

Three modeling periods were used for the beach nourishment assessment runs:

- 2011 – one year run with net eastward longshore transport (same period as the 2D model runs)

- 1992 to 2002 – eleven-year run with no major hurricane events (net eastward longshore transport)
- 2000 to 2019 – 20-year run that includes several significant hurricanes (Hurricane Katrina, Hurricane Ike, and Hurricane Harvey) that can move sediment back towards the west

Figure 8.11 shows the cells where the beach nourishment and offshore berms were placed (i.e., volume added) to represent the FWP scenario. The orange cells indicate beach nourishment while the green cells indicate the offshore berms. According to the CAD file “Beach\_Dune Fill Features\_s-ft\_dwg” by Freese and Nichols sent via email on October 28, 2021, approximately 2.0 million yd<sup>3</sup> (1.5 million m<sup>3</sup>) and 4.0 million yd<sup>3</sup> (3.1 million m<sup>3</sup>) of beach nourishment is to be placed on Mustang Island and San Jose Island, respectively, in the FWP scenario. Three offshore berms are placed on Mustang Island with a total volume of 4.3 million yd<sup>3</sup> (3.3 million m<sup>3</sup>) and six berms are placed on San Jose Island totaling 5.1 million yd<sup>3</sup> (3.9 million m<sup>3</sup>).

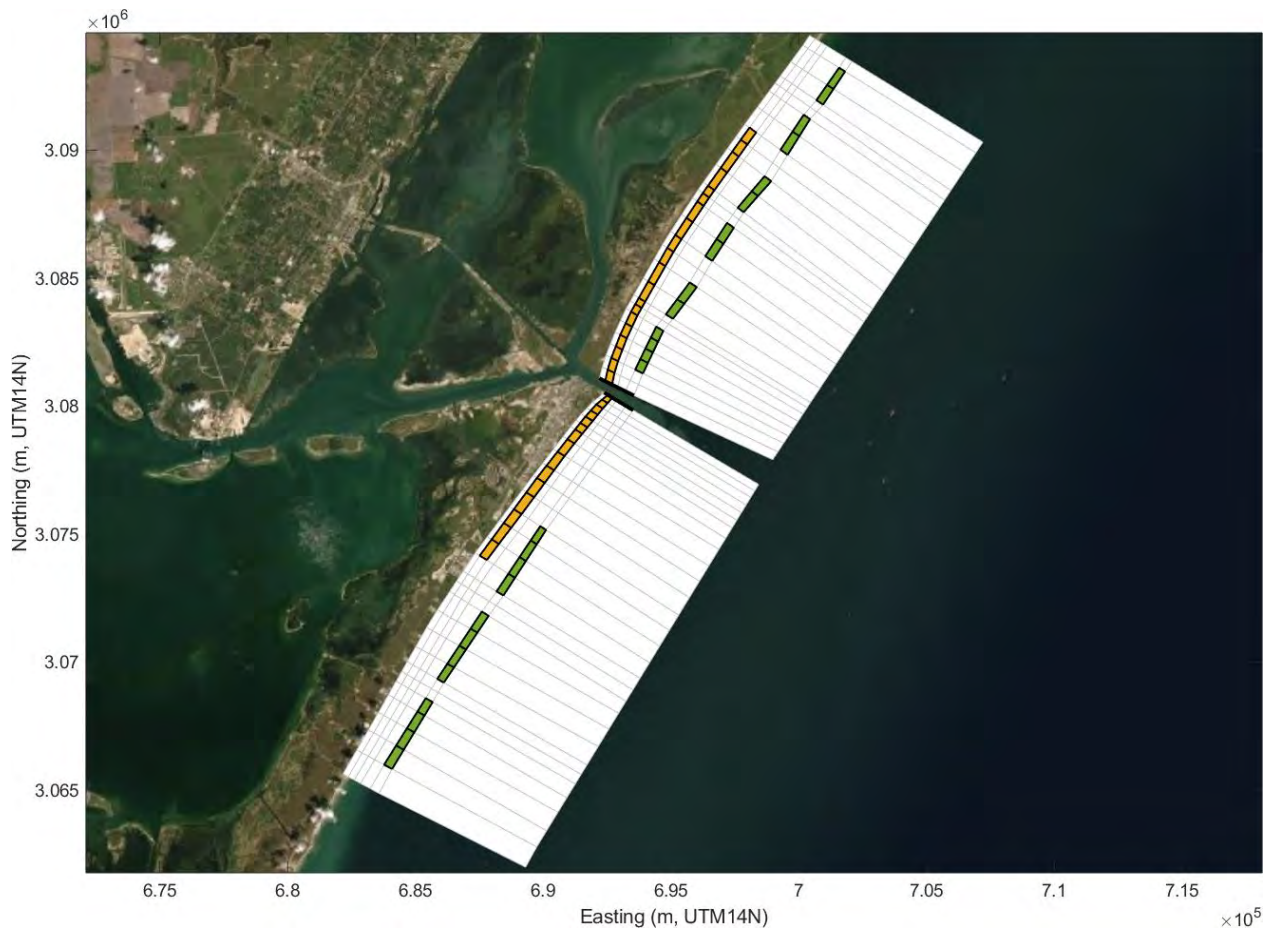


**Figure 8.11: Beach nourishment (orange) and offshore berm (green) placement cells within the Mustang Island and San Jose Island domains**

Figure 8.12 summarizes the sediment budget model run results for the FWP conditions for the 2011 model period. During 2011, the Mustang Island domain gains sediment in the nourishment footprint area due to the filling of the fillet beach on the west side of the jetty as the sediment is transported east. In the San Jose Island domain, 65k yd<sup>3</sup> (50k m<sup>3</sup>; 3% of the total placed volume) of beach nourishment is lost from the nourishment footprint. The total potential channel infilling volume from both domains is 179k yd<sup>3</sup>/yr (138 m<sup>3</sup>/yr) which is in

reasonable agreement with MIKE21 prediction (Table 5.1) for the FWP (i.e., deepened channel) conditions in 2011.

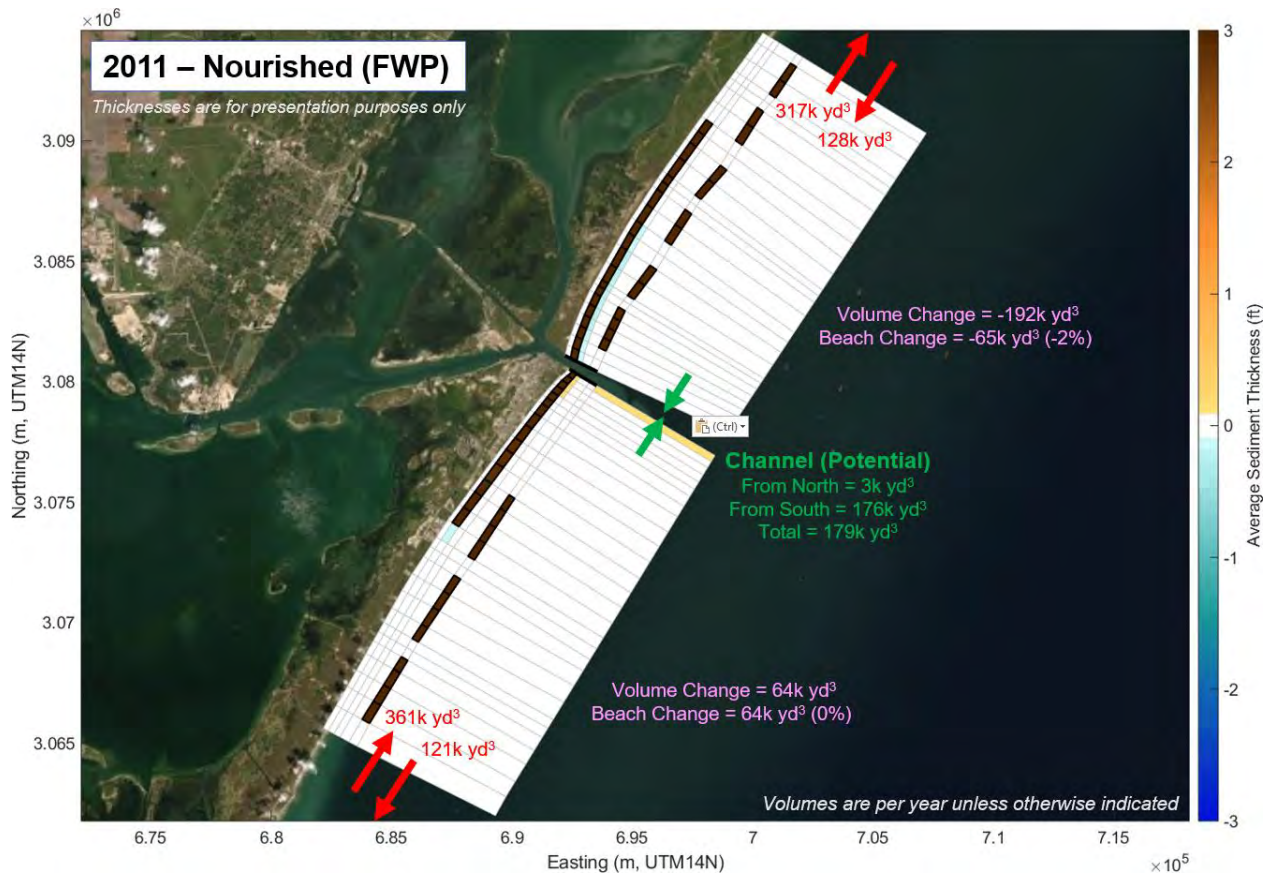


**Figure 8.12: Sediment budget model results for 2011 (FWP, thicknesses shown are for presentation purposes only and should not be taken literally)**

Figure 8.13 and Figure 8.15 summarize the sediment budget model run results for the FWP conditions for the 1992-2002 simulation period. In the 1992-2002 period, 321k yd<sup>3</sup> (245k m<sup>3</sup>) of sediment is lost from the Mustang Island domain nourishment footprint (16% of the total placed volume) while 34k yd<sup>3</sup> (26k m<sup>3</sup>) is gained in the San Jose Island domain nourishment footprint. During this period, the sediment has filled out the Mustang Island fillet beach and sediment is being transported along the jetty offshore towards the channel, similar to the FWOP conditions. The larger footprint of the beach nourishment on San Jose Island allows the sediment to move back and forth (i.e., northeastward or southwestward) along the nourishment footprint while staying within (and moving back into) the nourishment footprint over time. While the beach nourishment volume of the Mustang Island domain generally goes down over time, the San Jose Island domain volume cycles positive and negative as the sediment has a larger footprint to stay within. The nourishment along San Jose Island is also fronted by offshore berms to a greater extent than the Mustang Island nourishment, adding additional stability to the beach.

The predicted total potential channel infilling volume from both domains is 180k yd<sup>3</sup>/yr (138 m<sup>3</sup>/yr). This is similar to the predicted volume under the FWOP conditions (190k yd<sup>3</sup>/yr, Figure 8.10) and indicates that the impact of beach nourishment and offshore berms on channel sedimentation is small.

While the beach nourishment volume in the San Jose Island domain stays relatively constant over the modeling period, the distribution of sediment changes over time. At the end of the 1992-2002 period, an area of localized erosion approximately 1000 ft (300 m) in length located approximately 1000 ft (300 m) northeast of the north jetty in the San Jose Island domain. This area is where the diffracted waves change directions (e.g., the northeastward waves reverse direction and advance towards the southwest) and localized erosion occurs. A similar area is seen on the Mustang Island domain. These areas lose sediment faster than others within the nourishment footprint.

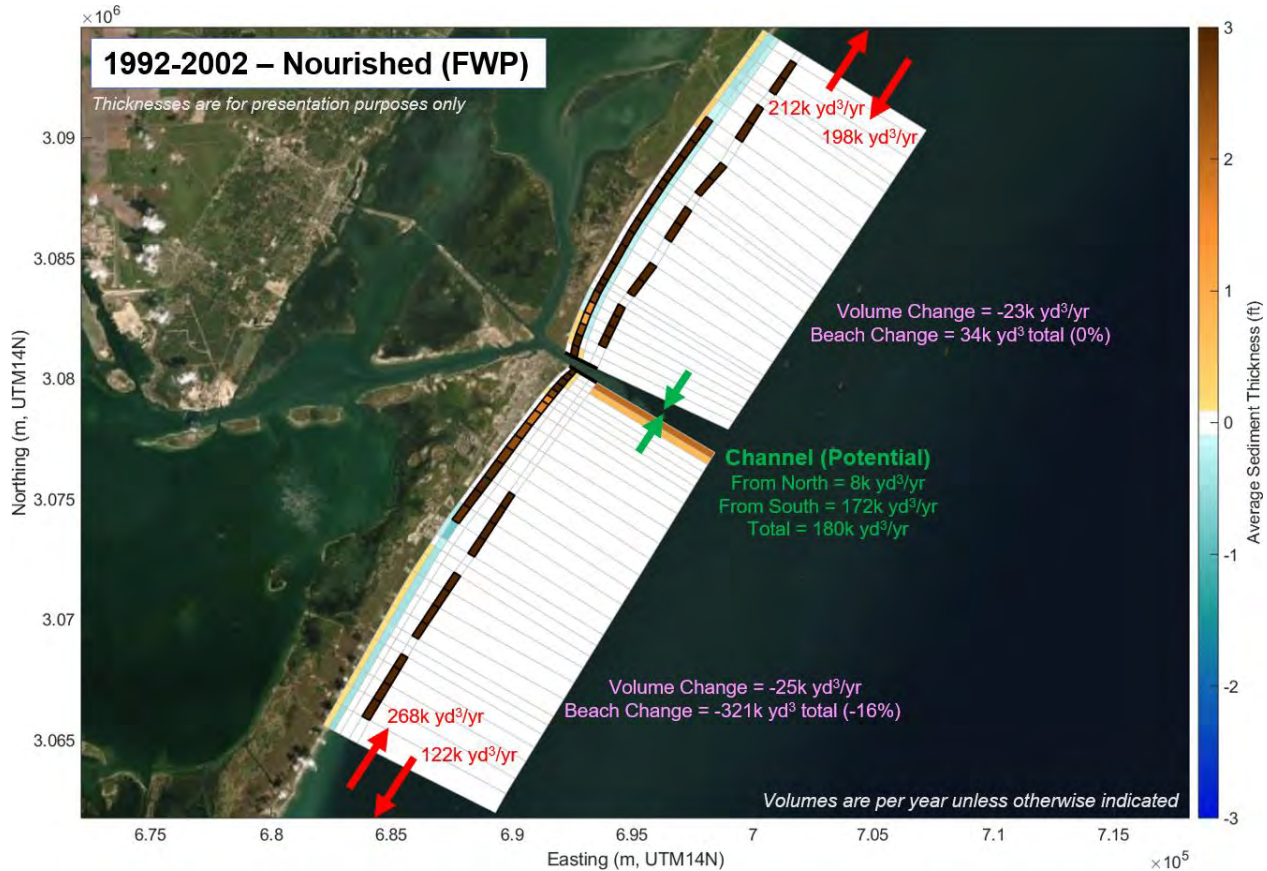


**Figure 8.13: Sediment budget model results for the 1992-2002 model period (FWP, thicknesses shown are for presentation purposes only and should not be taken literally)**

The 2000-2019 simulation period results are shown in Figure 8.14 and Figure 8.16. The northeastward and southwestward volumes at the northeast and southwest boundaries of the San Jose Island and Mustang Island domain boundaries are more balanced in the 2000-2019 run as the hurricanes transport more sediment to the southwest, offsetting the typical northeastward transport. By the end of the 2019-2019 modeling period, all the nourishment volume placed at Mustang Island has been eroded while 40% (1,613k yd³ or 1,233k m³) is eroded from San Jose Island. The larger volume of beach nourishment, longer nourishment length, and presence of offshore berms help to extend the longevity of nourishment at San Jose Island. The volume of sediment entering the channel from the San Jose Island domain is increased during this period as the hurricanes push sediment to the southwest. As with the 1992-2002 period, there are also areas of localized erosion north and south of the San Jose Island and Mustang Island fillet beaches.

In all modeling periods, the offshore berms are predicted to be stable. The impact of placement of beach nourishment and offshore berms on channel sedimentation was predicted to be small.

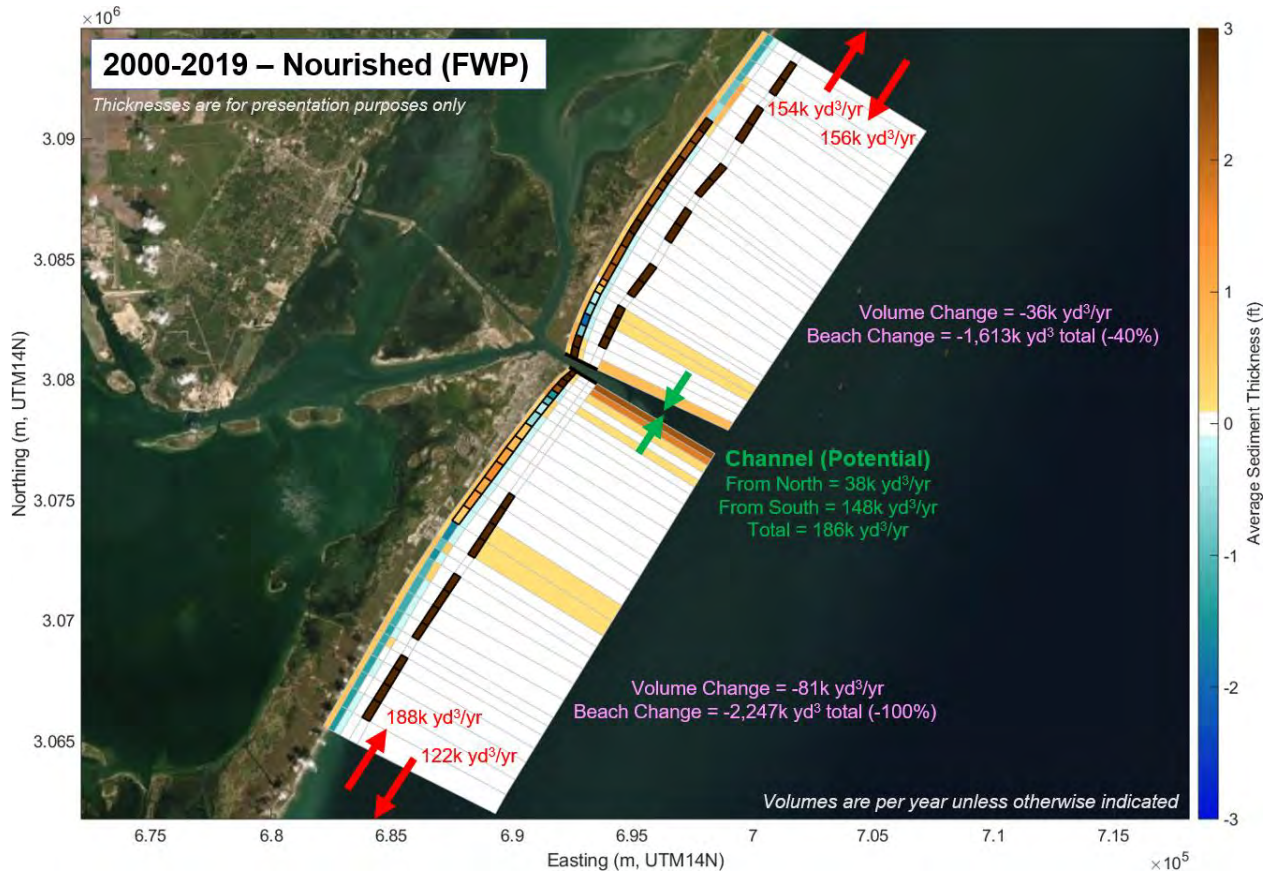
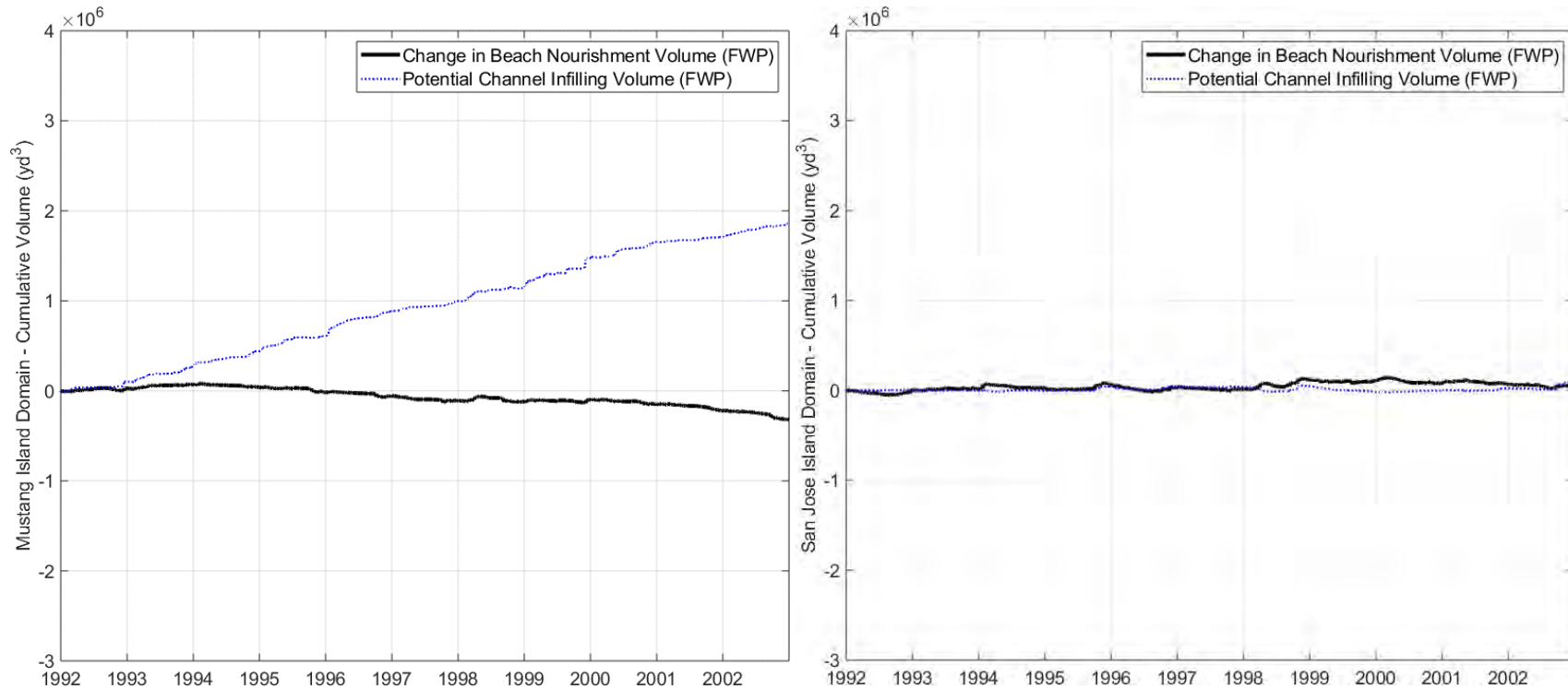
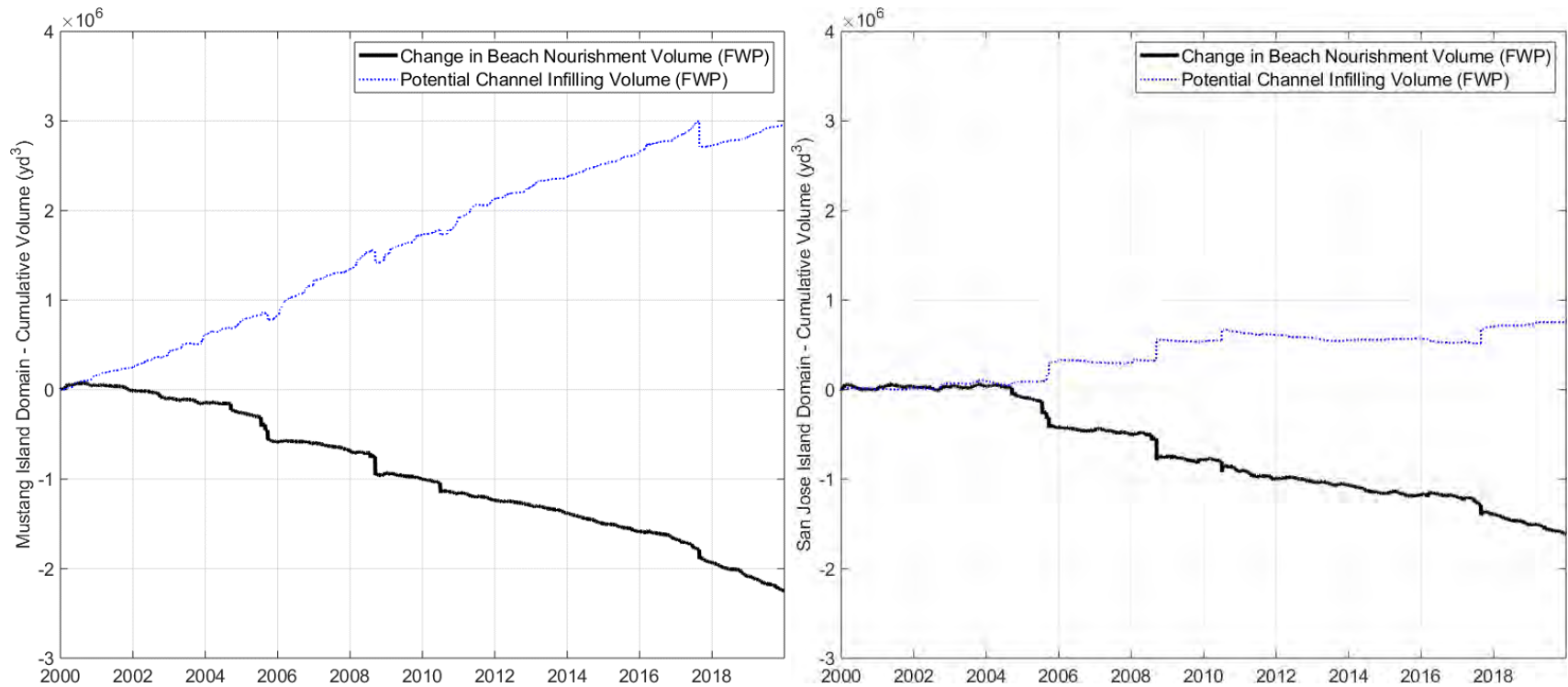


Figure 8.14: Sediment budget model results for the 2000-2019 model period (FWP, thicknesses shown are for presentation purposes only and should not be taken literally)



**Figure 8.15: Change in beach nourishment volume and potential channel infilling volumes for the Mustang Island (left) and San Jose Island (right) domains for the period from 1992-2002**



**Figure 8.16: Change in beach nourishment volume and potential channel infilling volumes for the Mustang Island (left) and San Jose Island (right) domains for the period from 2000-2019**

## 9. Conclusions

---

The impacts of the Future With Project (FWP) scenario on channel sedimentation are summarized below:

- Predicted FWOP and FWP shoaling rates for the inner channel were comparable to the existing condition. Overall, both 2D and 3D model results indicate that the project impact on sedimentation rates is limited to less than 10%.
- The model predicted that sedimentation in the outer channel increases from approximately 95,000 yd<sup>3</sup>/year (73,000 m<sup>3</sup>/year) for the FWOP to approximately 214,000 yd<sup>3</sup>/year (164,000 m<sup>3</sup>/year) for the FWP scenario, approximately 2.25 times higher. This is primarily due to that fact that the FWP has a deeper and longer channel compared to FWOP.
- The beach nourishment and offshore berms make small contributions to channel sedimentation with less than 600 yd<sup>3</sup> (459 m<sup>3</sup>) of total sedimentation per year as predicted by the 2D model.
- The model predicted that sedimentation in the outer channel under FWP conditions increases from approximately 214,000 yd<sup>3</sup>/year (164,000 m<sup>3</sup>/year) in the absence of the ODMDS mound to approximately 342,000 yd<sup>3</sup>/year (262,000 m<sup>3</sup>) (approximately 1.6 times greater) when the ODMDS mound is present.
- Individual hurricane events could result in sedimentation volumes in the outer channel that are several times higher than the average annual sedimentation. In contrast, the impact of hurricane on the inner channel is small.

The modeling assessment of the cross-shore profile response to long term wave conditions and short-term storm conditions found that:

- No significant movement of the offshore berm is expected
- The offshore berm is placed beyond the mean depth of closure, and it is unlikely that significant sediment movement will occur at the designed placement depth
- XBeach predicts overtopping of the dune during severe storms (e.g., Hurricane Allen and Hurricane Harvey)
- XBeach storm response predictions were validated using pre- and post-Hurricane Harvey imagery and surveys
- The offshore berm is not expected to provide significant shore protection, except in smaller storms with longer wave periods
- The true extent of beach erosion varies along the shoreline and is influenced by local profile morphology including the dune crest height among other factors which are not reflected in a one-dimensional model

The modeling assessment of the fate of beach nourishment found that:

- In the Mustang Island domain, the average nourishment loss rate is approximately 29k to 112k yd<sup>3</sup> (22k to 86k m<sup>3</sup>) per year (1 to 5% of the total volume per year); the lost sediment is generally transported to the northeast where it moves along the jetty and offshore towards the channel
- In the San Jose Island domain, the average nourishment erosion rate is approximately 0 to 80k yd<sup>3</sup> (0 to 62k m<sup>3</sup>) per year (0 to 2% of the total volume per year); the lost sediment is generally redistributed over the model
- The larger footprint of the beach nourishment on San Jose Island allows the sediment to move back and forth along the nourishment footprint while staying within (and moving back into) the nourishment footprint over time

- The nourishment along San Jose Island is also fronted by offshore berms to a greater extent than the Mustang Island nourishment, adding additional stability to the beach
- Areas between 1,000 to 2,000 ft (300 to 600 m) north and south from the jetty in both the Mustang Island and San Jose Island domain are expected to lose sediment earlier
- The impact of beach nourishment on channel sedimentation is expected to be small
- The offshore berms are expected to remain stable over time

## 10. References

---

Nairn, R.B. and Southgate, H.N. (1993). Deterministic Profile Modelling of Nearshore Processes. Part II. Sediment Transport and Beach Profile Development. *Coastal Engineering*, 19. pp. 57-96.

Paine, J. G., Caudle, T., and Andrews, J. R., 2021, Shoreline movement and beach and dune volumetrics along the Texas Gulf Coast, 1930s to 2019: The University of Texas at Austin, Bureau of Economic Geology, final report prepared for the General Land Office under contract no. 16-201-000, 101 p.

Southgate, H.N. and Nairn, R.B. (1993). Deterministic Profile Modelling of Nearshore Processes. Part I. Waves and Currents. *Coastal Engineering*, 19. pp. 27-56.

Sunamura, T., & Horikawa, K. (1974). TWO-DIMENSIONAL BEACH TRANSFORMATION DUE TO WAVES. *Coastal Engineering Proceedings*, 1(14), 53. <https://doi.org/10.9753/icce.v14.53>

(HYCOM). Retrieved from HYbrid Coordinate Ocean Model (HYCOM). <https://www.hycom.org/>

Texas General Land Office. (2021, June). Texas Sediment Geodatabase. Retrieved from Texas Sediment Geodatabase: <https://cgis.glo.texas.gov/txsed/index.html>

USACE. (2017, March 15). U.S. Army Corps of Engineers Geospatial. Retrieved June 2021, from U.S. Army Corps of Engineers Geospatial: [https://geospatial-usace.opendata.arcgis.com/datasets/9227967a2748410983352b501c0c7b39\\_2/explore?location=26.149814%2C-96.223736%2C9.51](https://geospatial-usace.opendata.arcgis.com/datasets/9227967a2748410983352b501c0c7b39_2/explore?location=26.149814%2C-96.223736%2C9.51)